Oscillating plasmas: from strong nonideality to fusion temperatures. Experiment and PiC simulations.

Yu.K.Kurilenkov[1], V.P.Tarakanov[1], S.Yu.Gus'kov[1,2], A.V.Oginov[1,2]

[1]Joint Institute for High Temperatures RAS Moscow Russia.
[2]Lebedev Physics Institute RAS Moscow, Russia

ЗНЧ 2017 Снежинск

Outline

1. **Inertial electrostatic confinement fusion (IEC) scheme.**

   DD syntheses at small scale set –up.
2. **IEC scheme based on nanosecond vacuum discharge (NVD) with deuterated Pd anode. Experiments on DD fusion and PIC simulations.**
3. **PIC modeling of proton – boron nuclear burning in the potential well of virtual cathode at nanosecond vacuum discharge.**
4. **Concluding remarks**

Pioneers of IECF at 50-th of XX century - O.Lavrent’ev, F.Farnsworth, R.Hirsch, W.Elmore et al

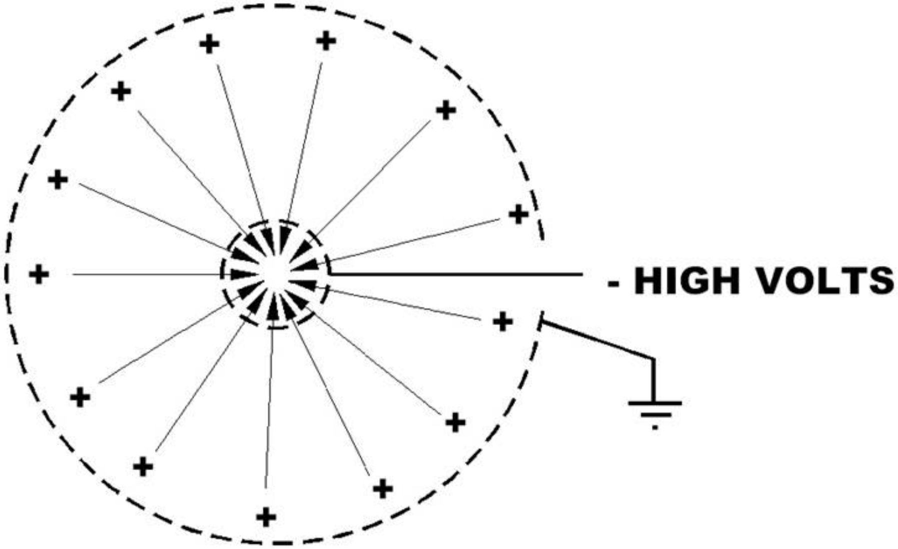

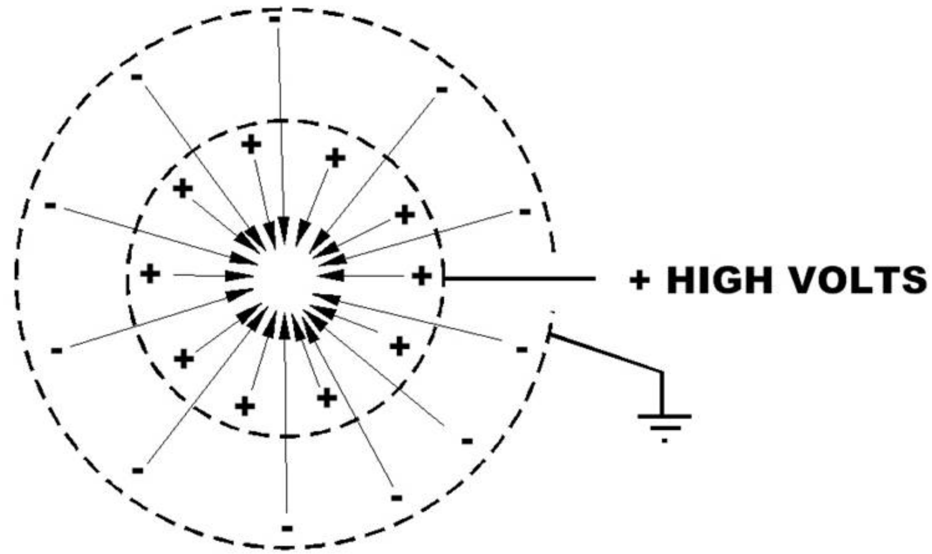

"On the Inertial-Electrostatic Confinement of a Plasma", William C. Elmore, James L. Tuck, Kenneth M. Watson, *The Physics of Fluids*, v. 2, no. 3, May-June 1959.

"Inertial-Electrostatic Confinement of Ionized Fusion Gases", Robert L. Hirsch, *Journal of Applied Physics*, v. 38, no. 11, October 1967.

Magnetic Electrostatic Plasma Confinement. T.Dolan. Plasma Phys. Control Fusion.36 (1994) 1539 (see references therein)

Inertial electrostatic confinement fusion (IECF)

general scheme,
example of single potential well

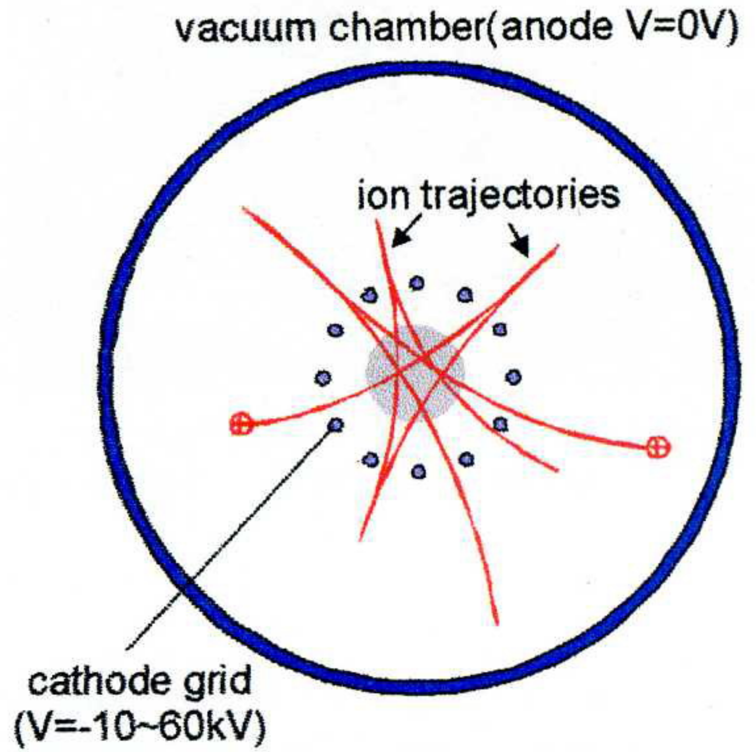

1. An IEC configuration with a gridded cathode.

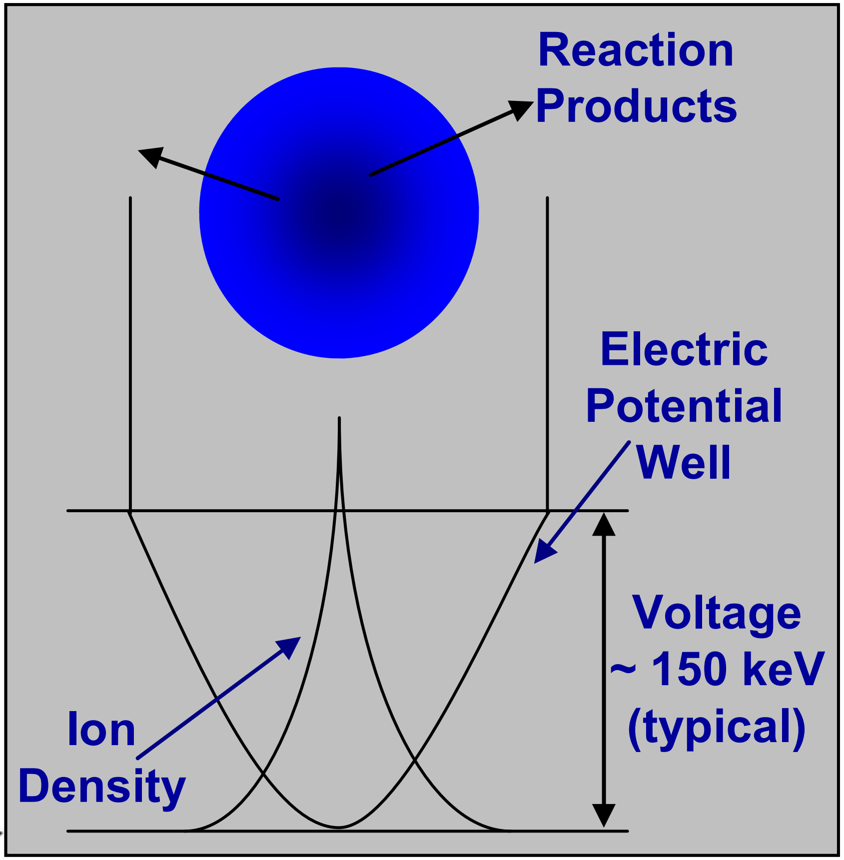

Младший сержант срочной службы (радиотелеграфист) Олег Александрович Лаврентьев. Остров Сахалин, 1950 г.

Inertial Electrostatic Confinement (IEC) at LANL and Tokio

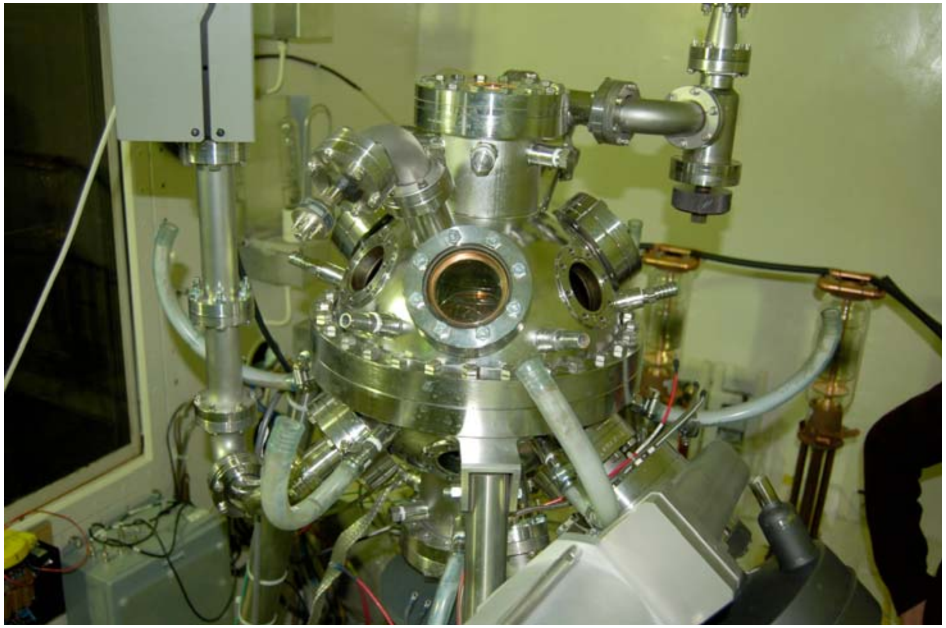

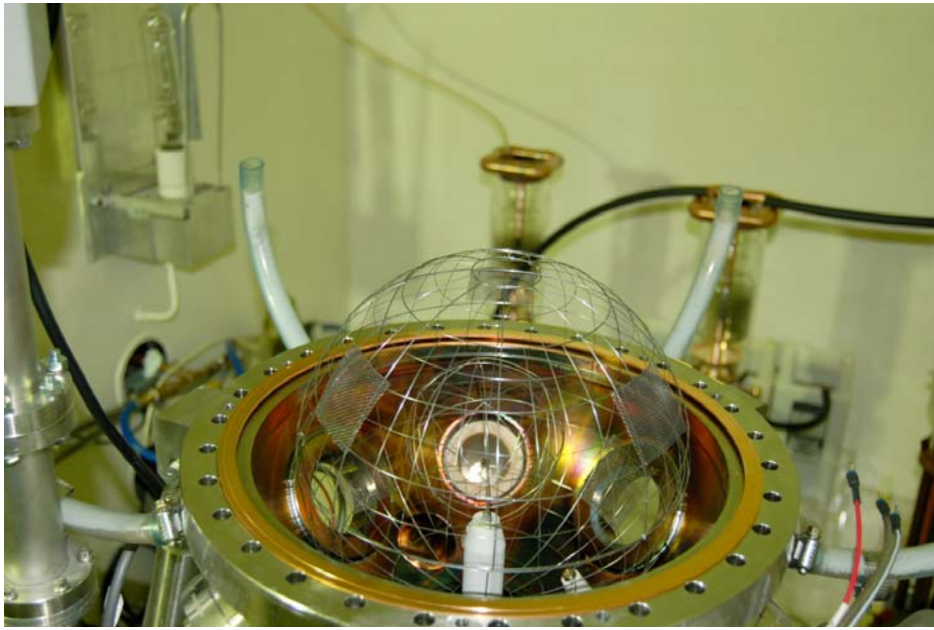

- • Electrostatic fields by grids: confine and accelerates ions to the center - easy to accelerate ions to fusion energy (50 - 150 kV) e cell)
- • Converging ion beams produce fusion reactions in the center
- • Proven neutron source:

  - $2x10^{10}$ n/s with D-T by Hirsch (1968)

  - $1.5x10^{8}$ n/s with D-D by U. Wisconsin (2002)

  - $6.8x10^{9}$ n/s (pulsed) with D-D by Tokyo Inst. Tech. (2005)
- Low efficiency device - fast ion loss via collisions and the grid loss

High current pulsed operation Tokyo Institute of Technology

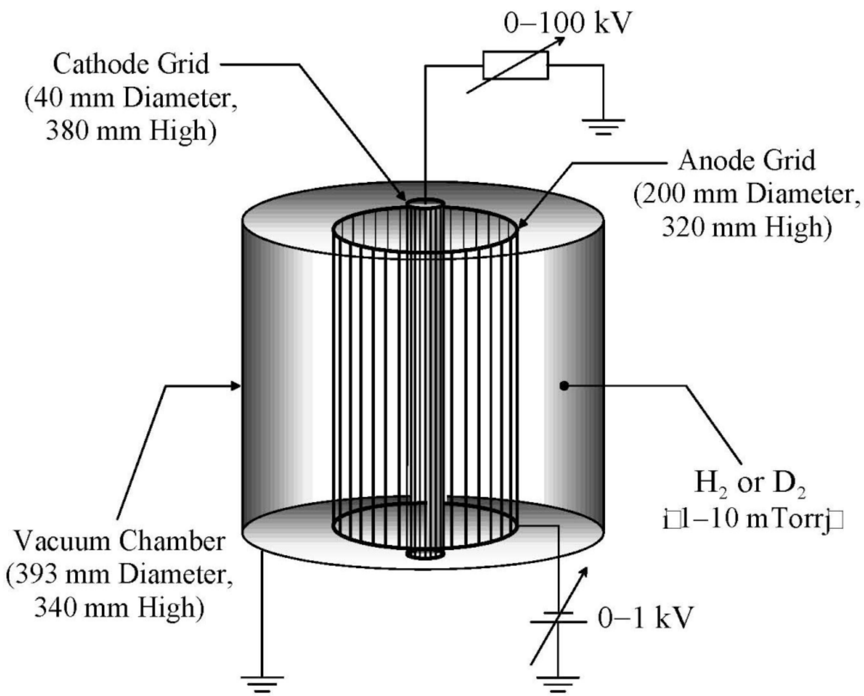

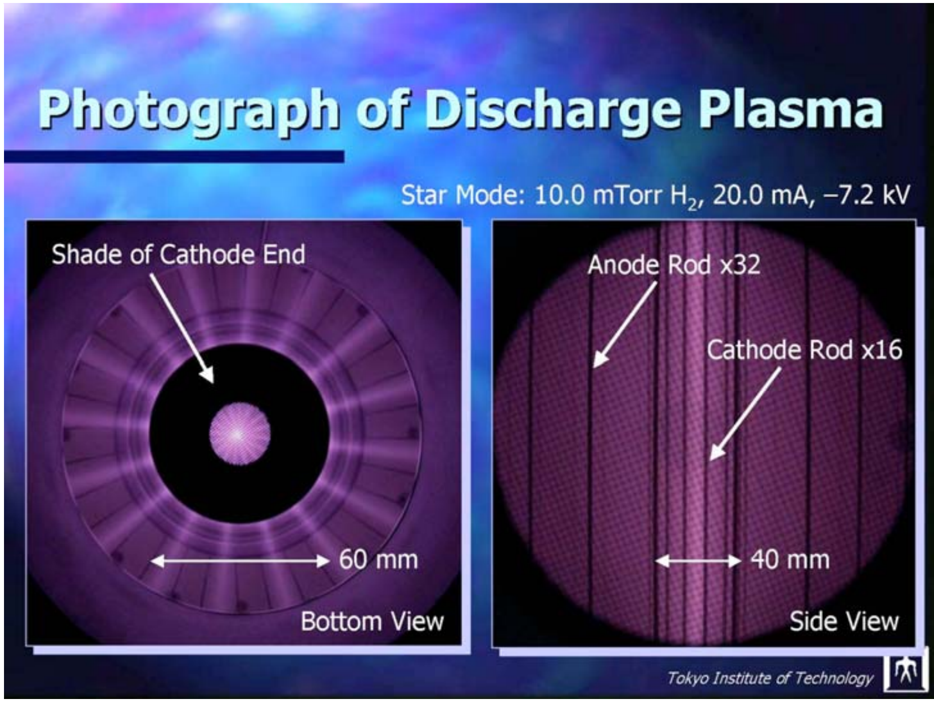

- High current pulsed operation --> high neutron yield
- - D-D neutron yield of 6.8x10 9 n/s - 10A@70 kV using cylindrical IEC
- Very low efficiency - low ionization fraction and large CX loss
- Cylindrical Device: Better Symmetry than Spherical system in practice and easier diagnostic access

Ditmire et al *PRL* 84(2000)634

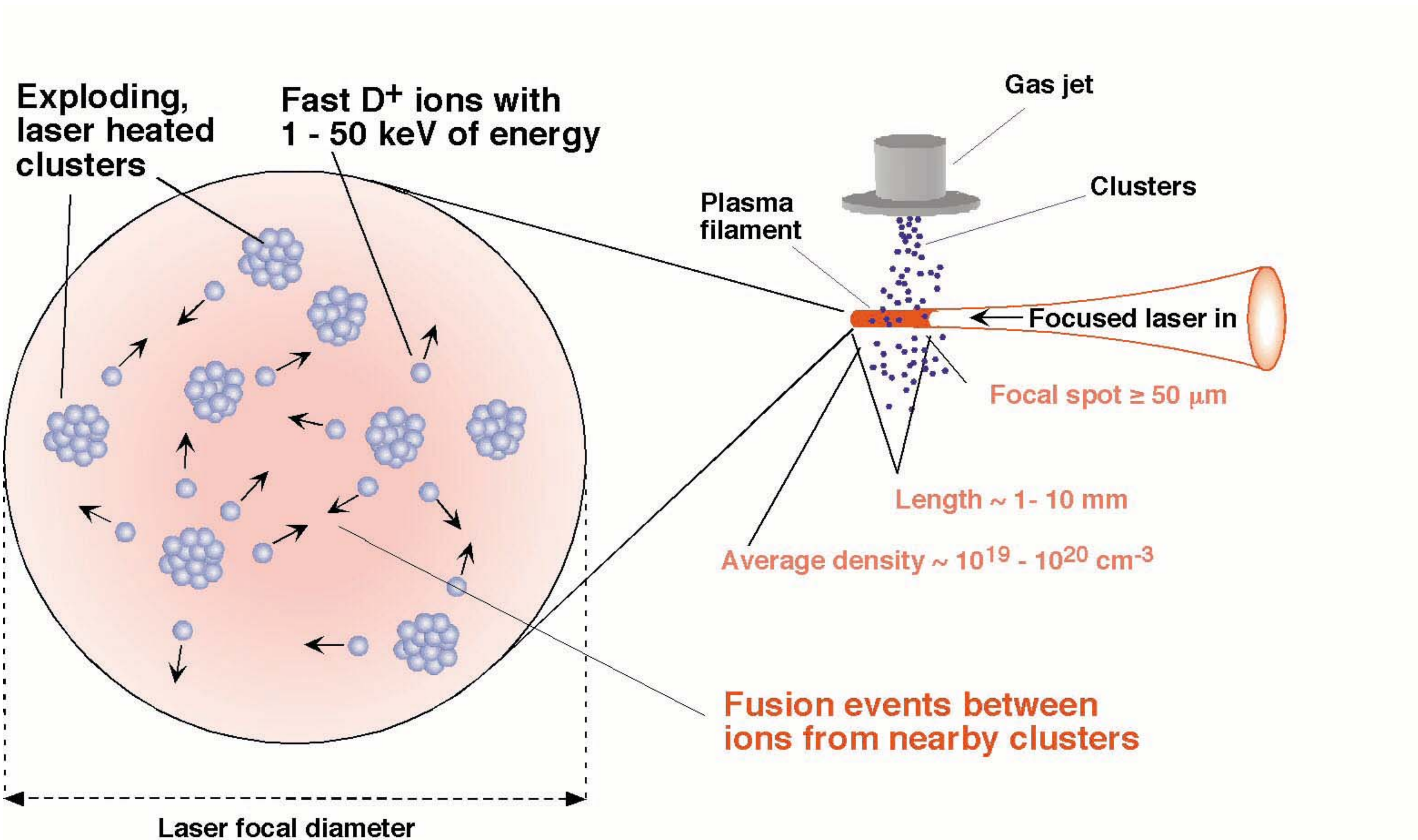

IECF scheme for DD nuclear synthesis based on vacuum discharge (M.Skowronek and Yu.K.Kurilenkov 2003, 2006 J.Phys A)

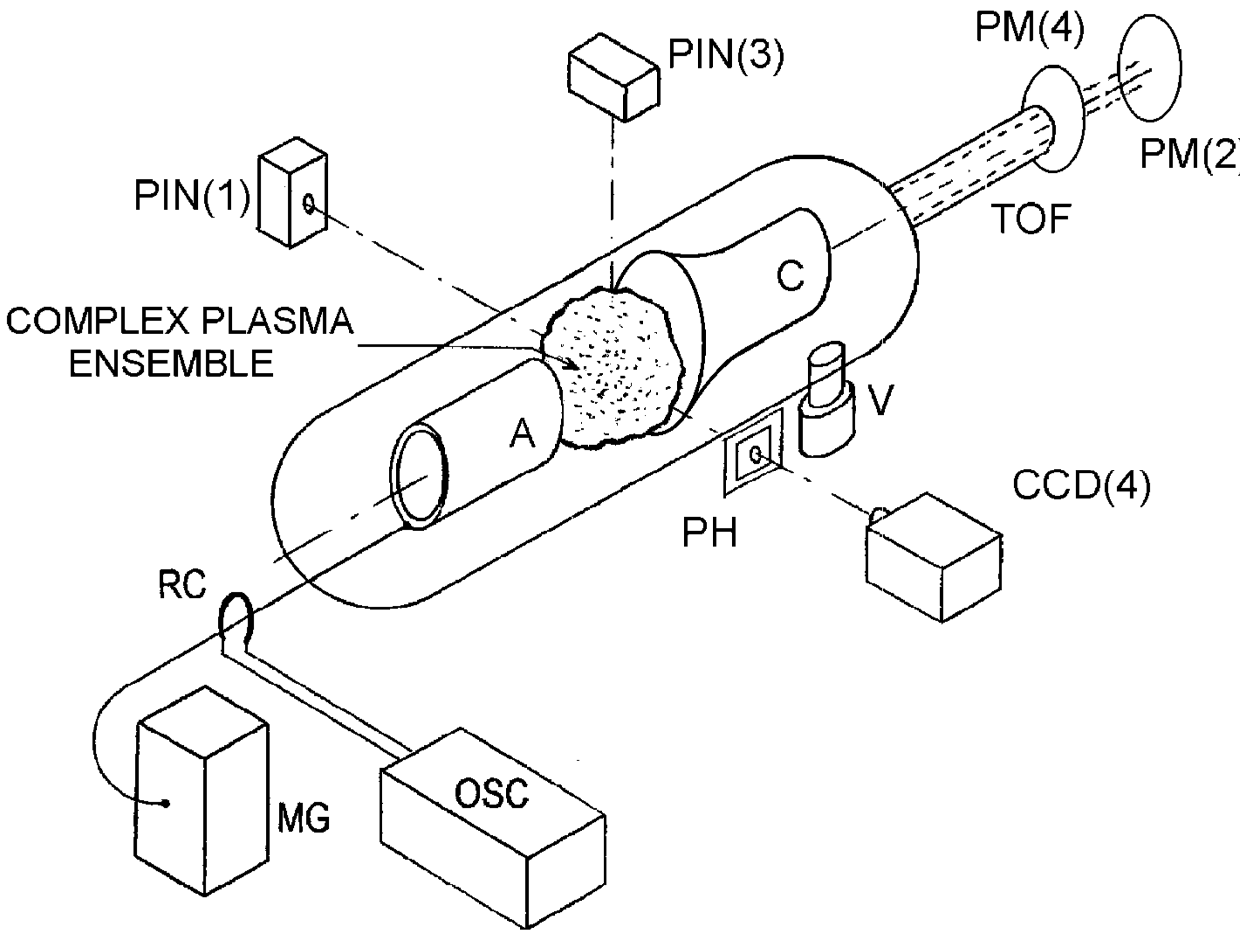

- Parameters of discharge: ≈ 1 J of total energy, U=70kV, t=50 nsec I_{max} =1kA, TOF = 30-90 cm P_{min} ≈ 10^{-7} mbar.

view for experimental set up at university laboratory

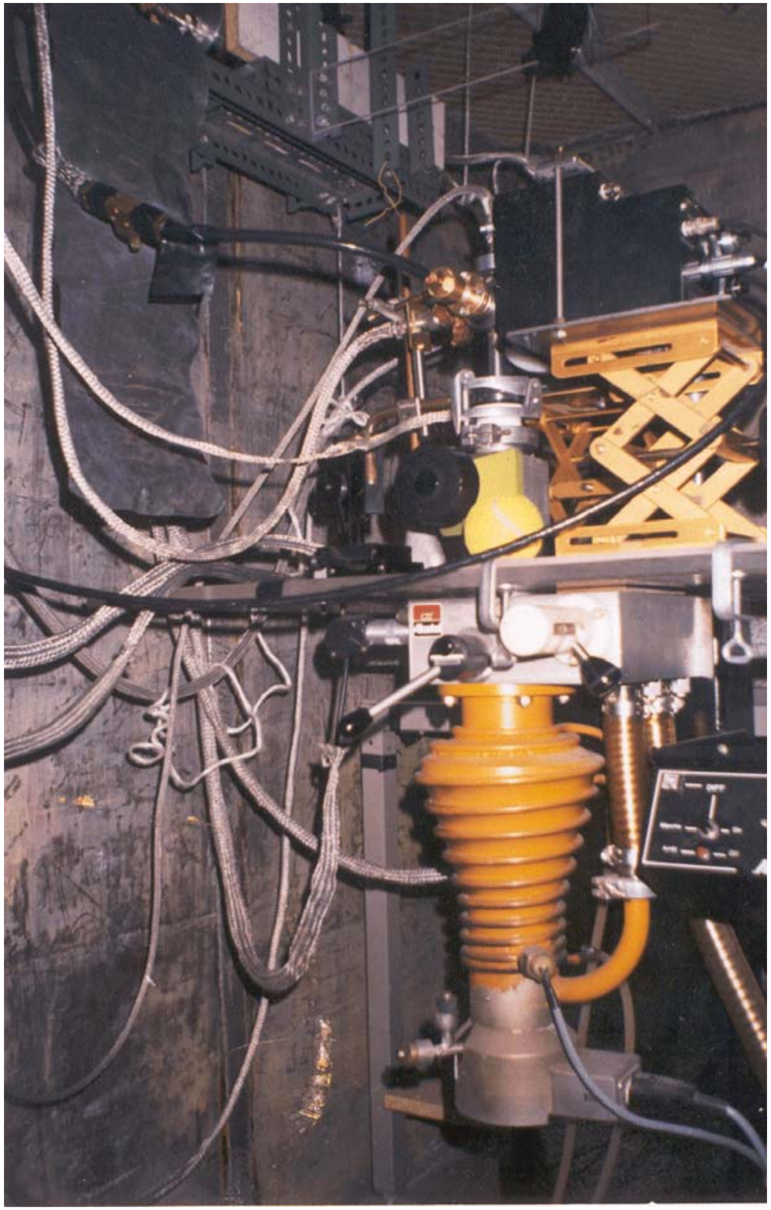

Electrodes

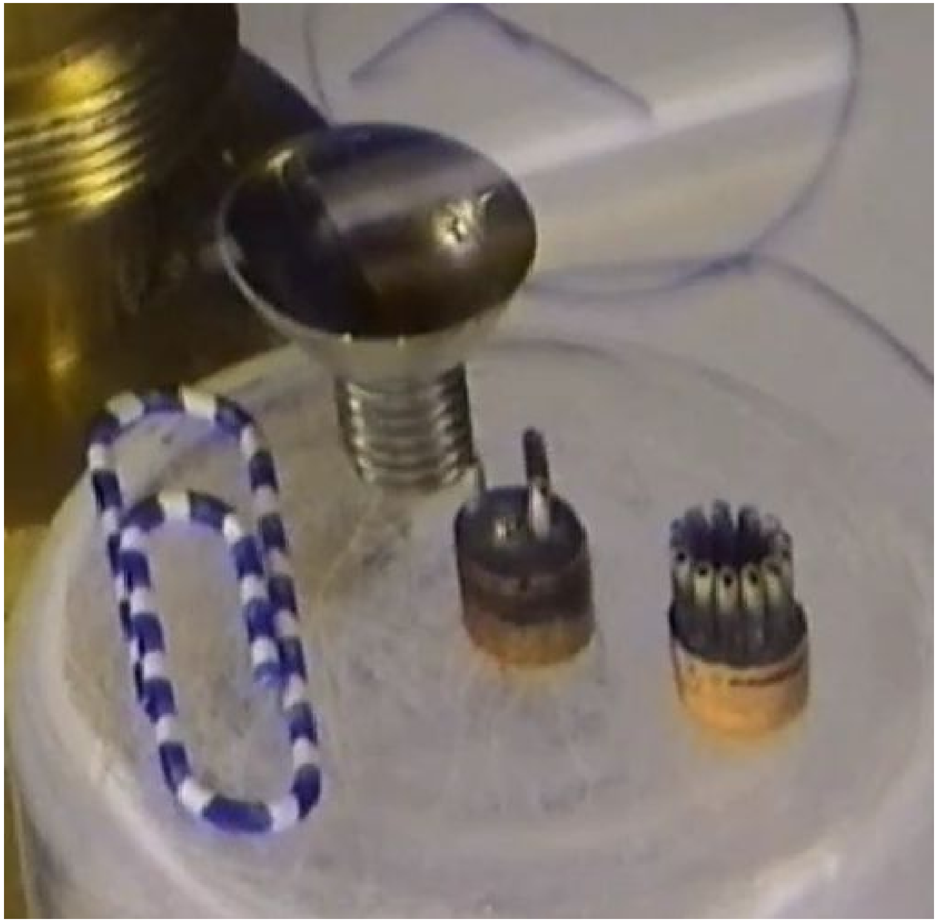

DD nuclear synthesis: particles dynamics by KARAT code.

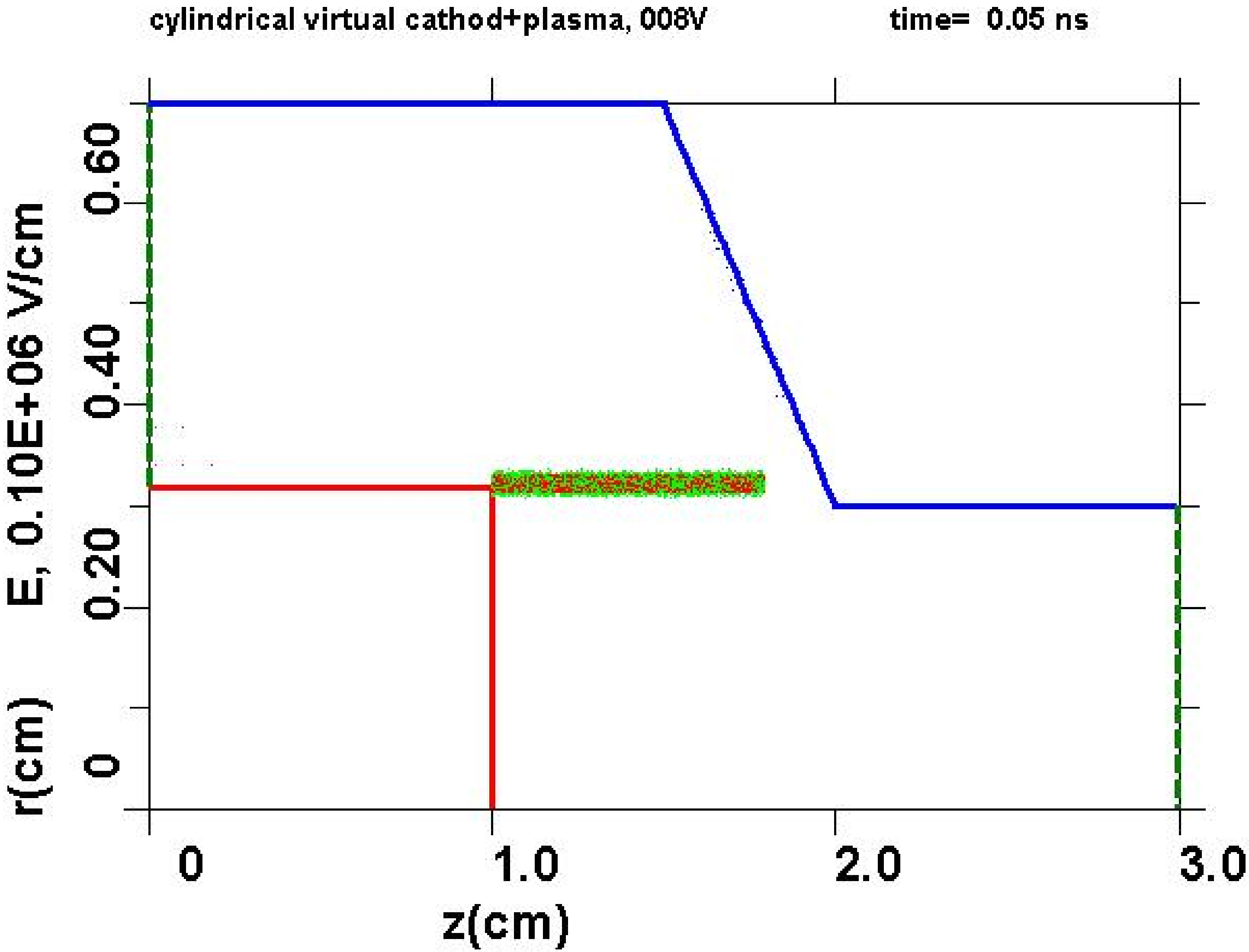

KARAT simulations

DD nuclear synthesis …..

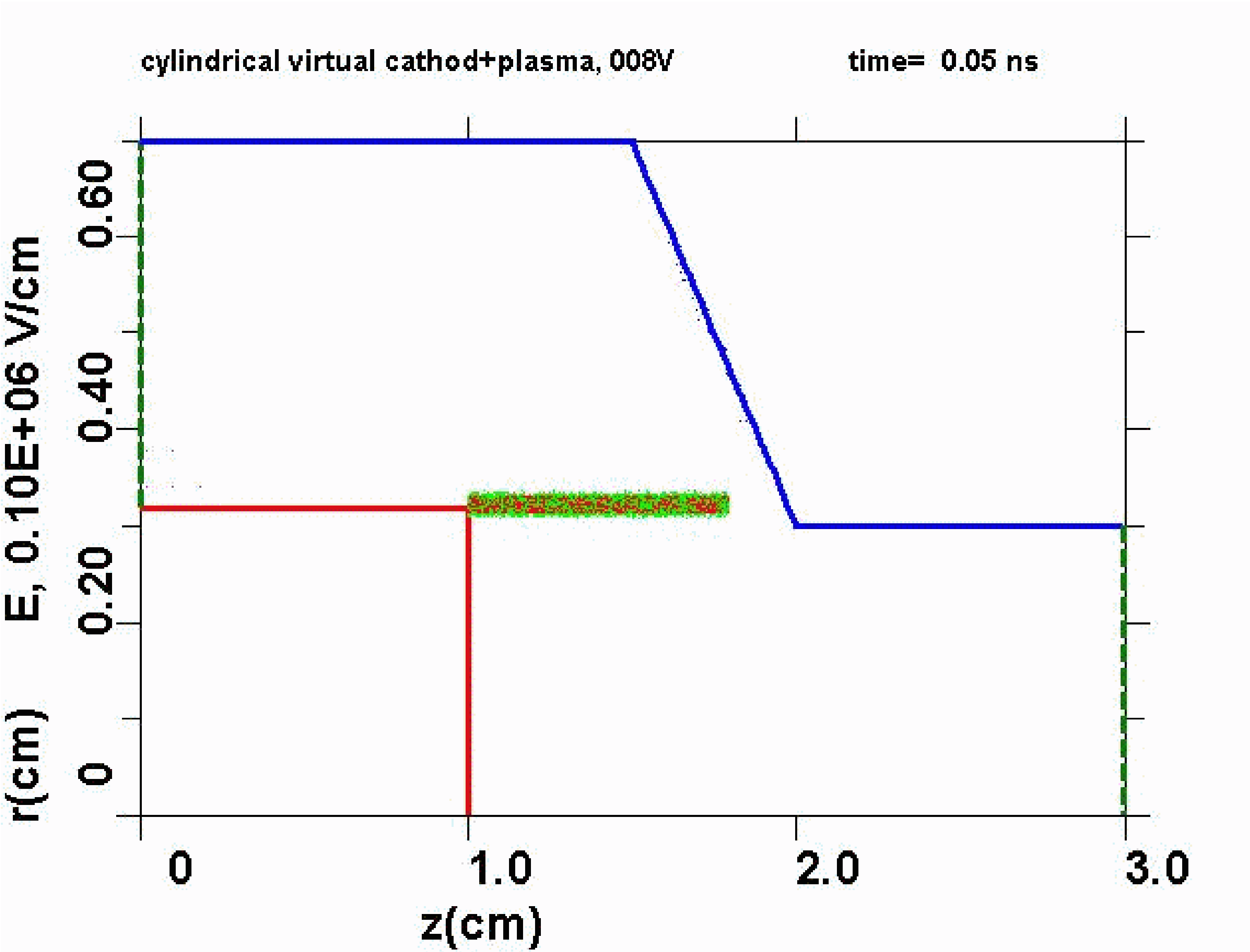

KARAT simulations

Example of particles dynamics by KARAT code (blue – beam electrons, red – ions accelerated by the field of VC, green- anode erosion plasma)

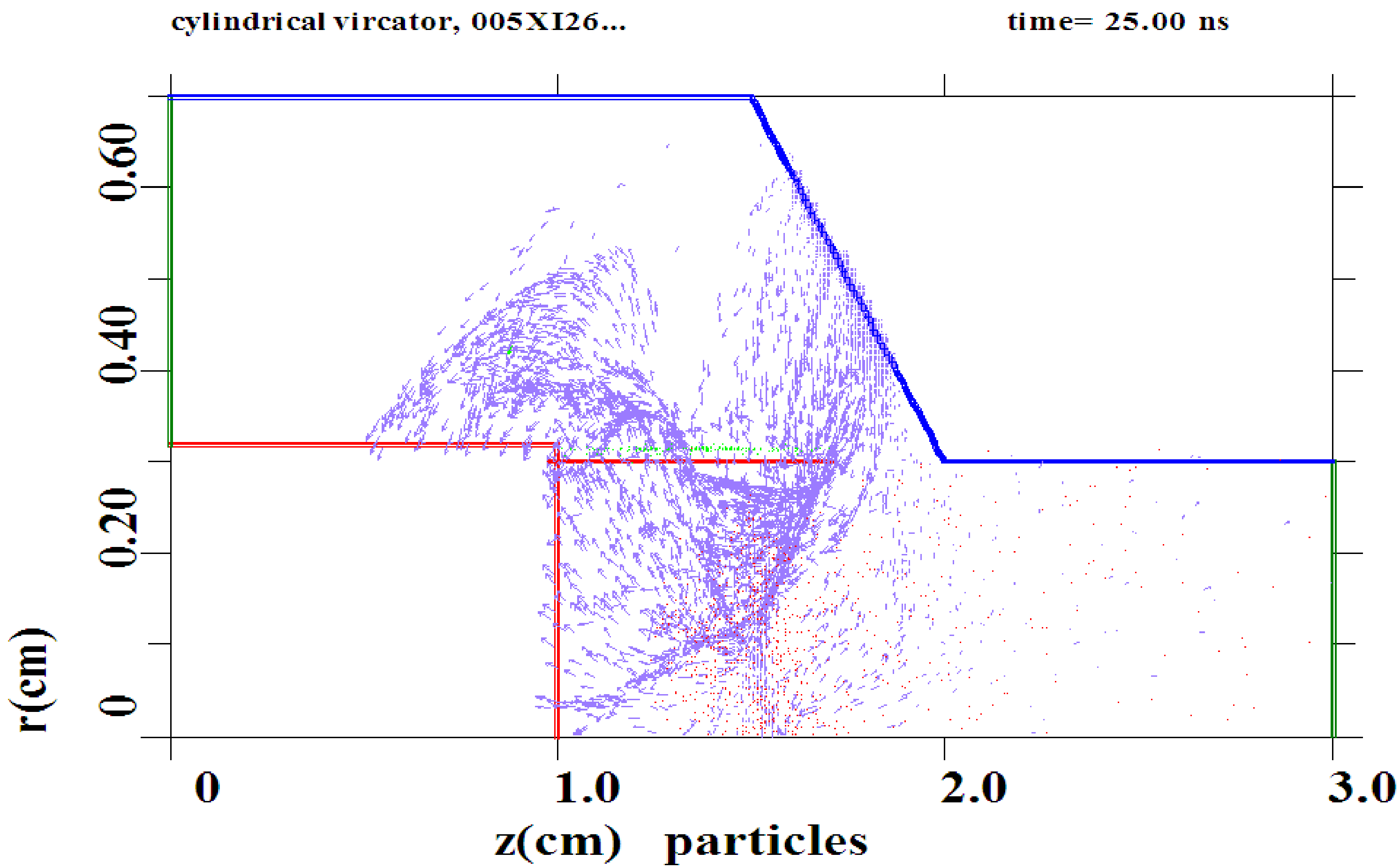

Typical single potential well (PW) at interelectrode space

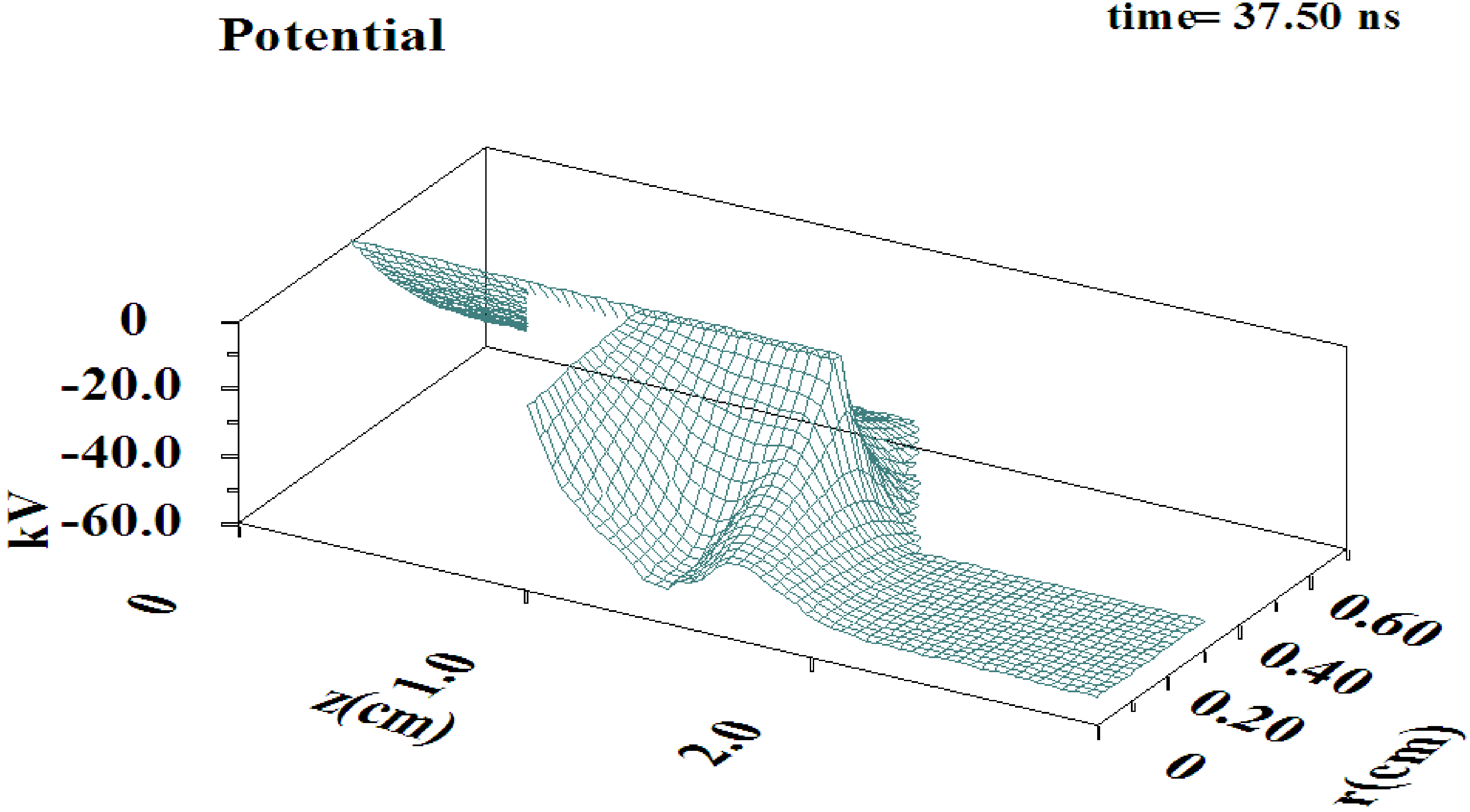

PIC modeling: electron (blue) and ions (red) dynamics at interelectrode space (under virtual cathode formation ; green- “erosion plasma” from loaded Pd tubes)

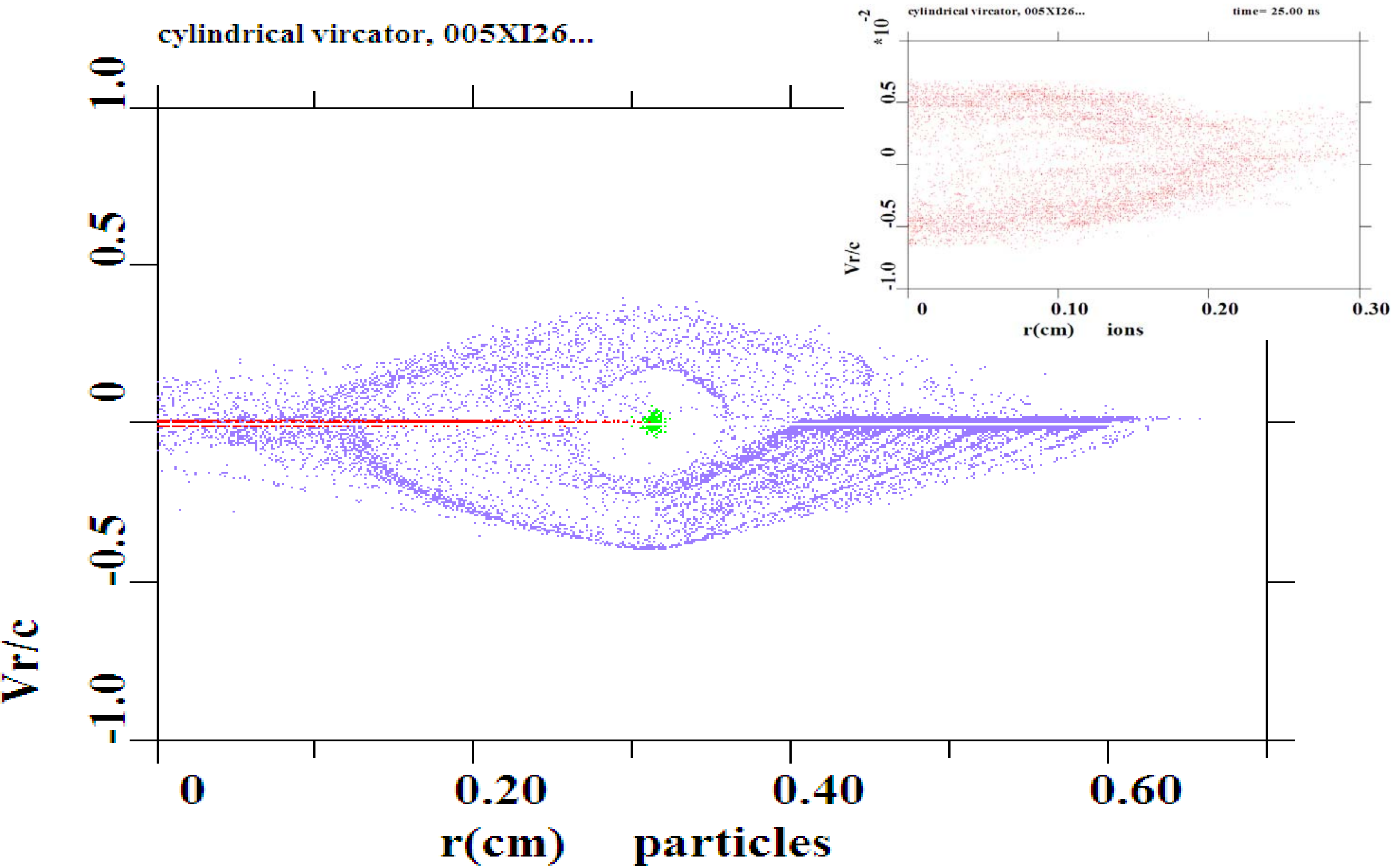

Energies of ions and beam electrons as function of their radial position

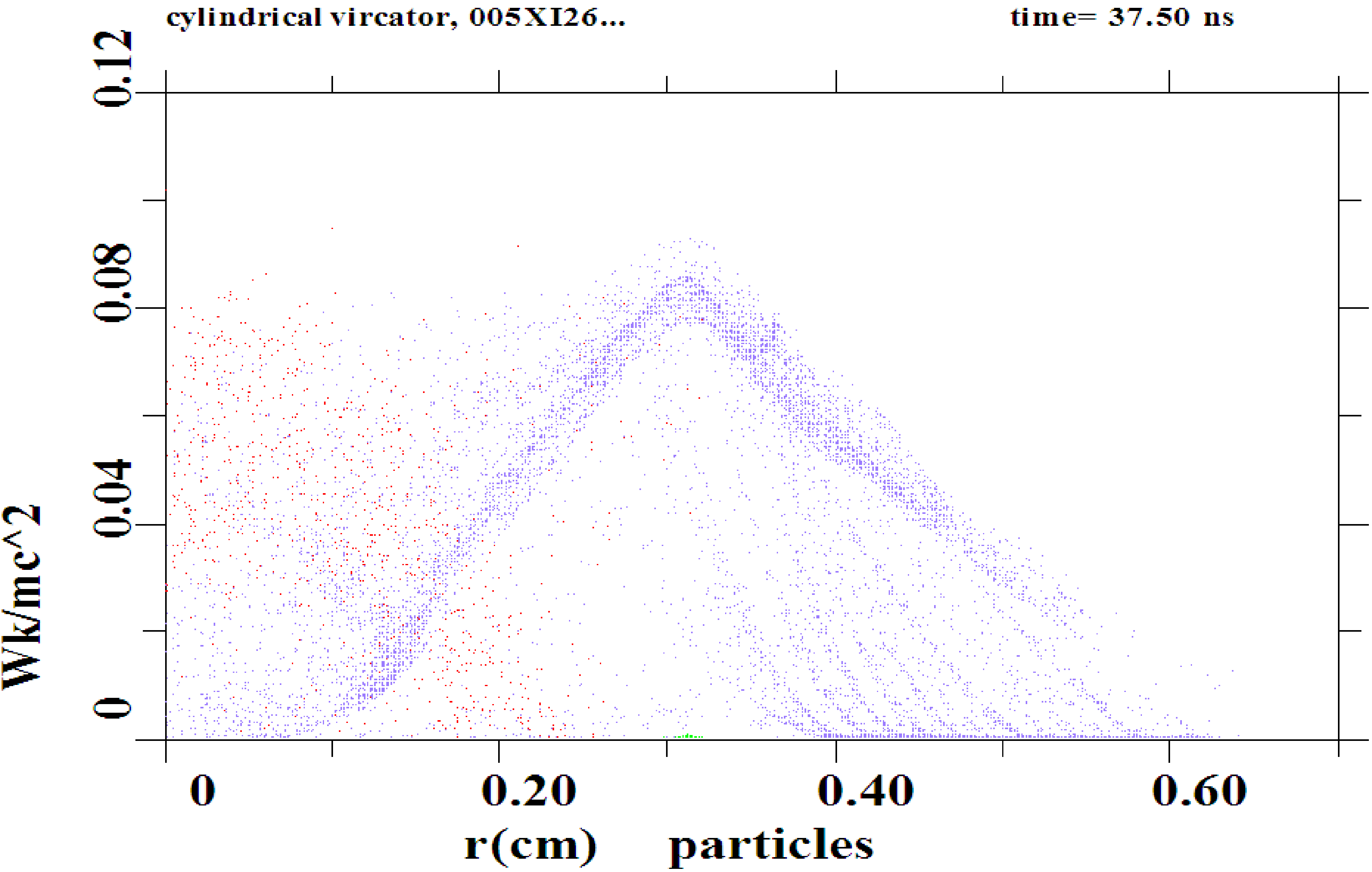

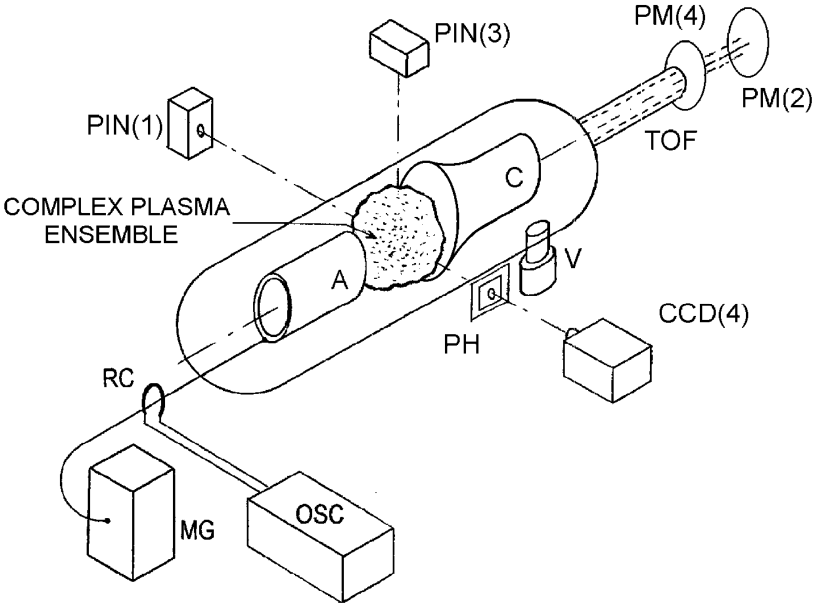

Observation of DD microfusion events accompanied by moderate neutron yield
(1005d2)

D(D,n)He^3 → ~ 2,45 MeV neutrons

46, 6 nsec/m TOF delayed signal

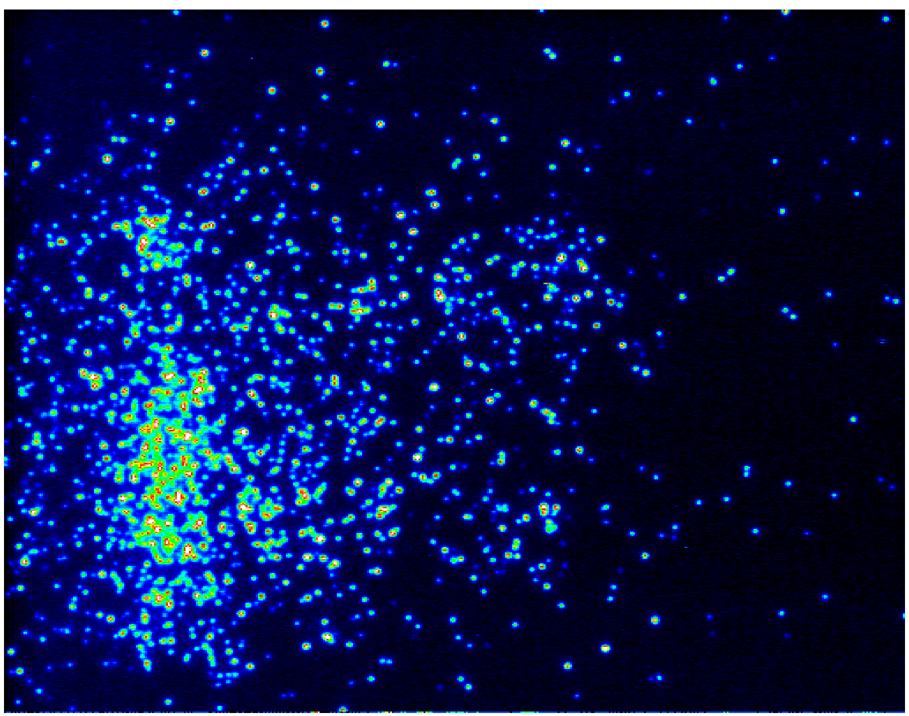

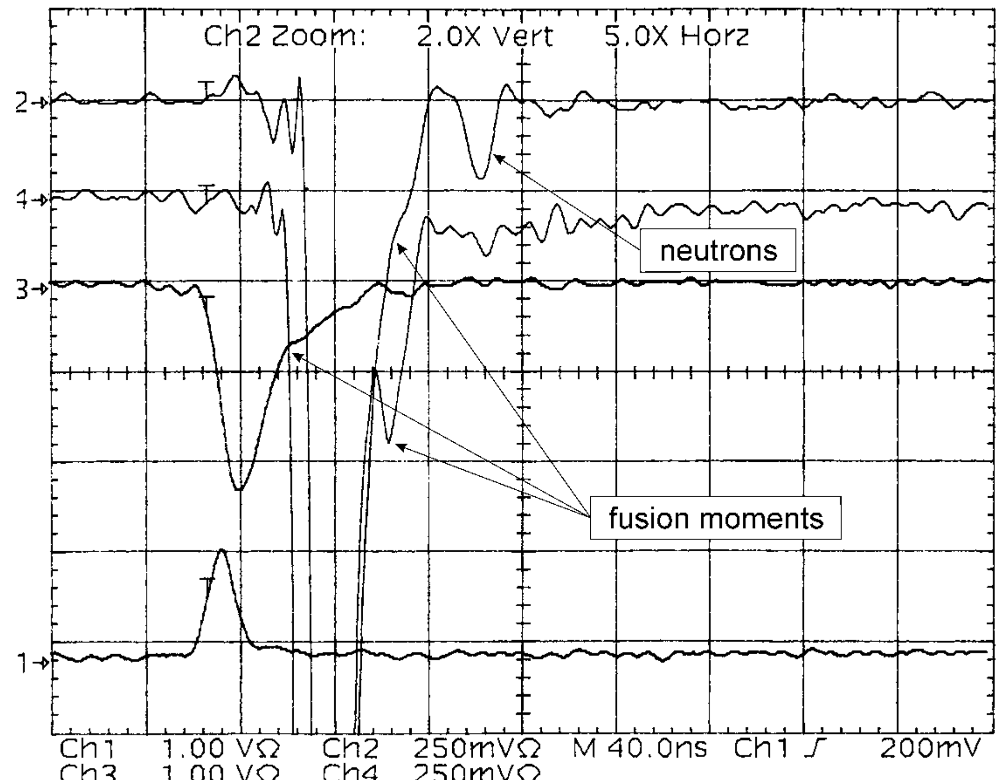

Neutron yield is observed when virtual cathode and potential well are forming along the pulse as well as at very initial stage of discharge also(1005d5)

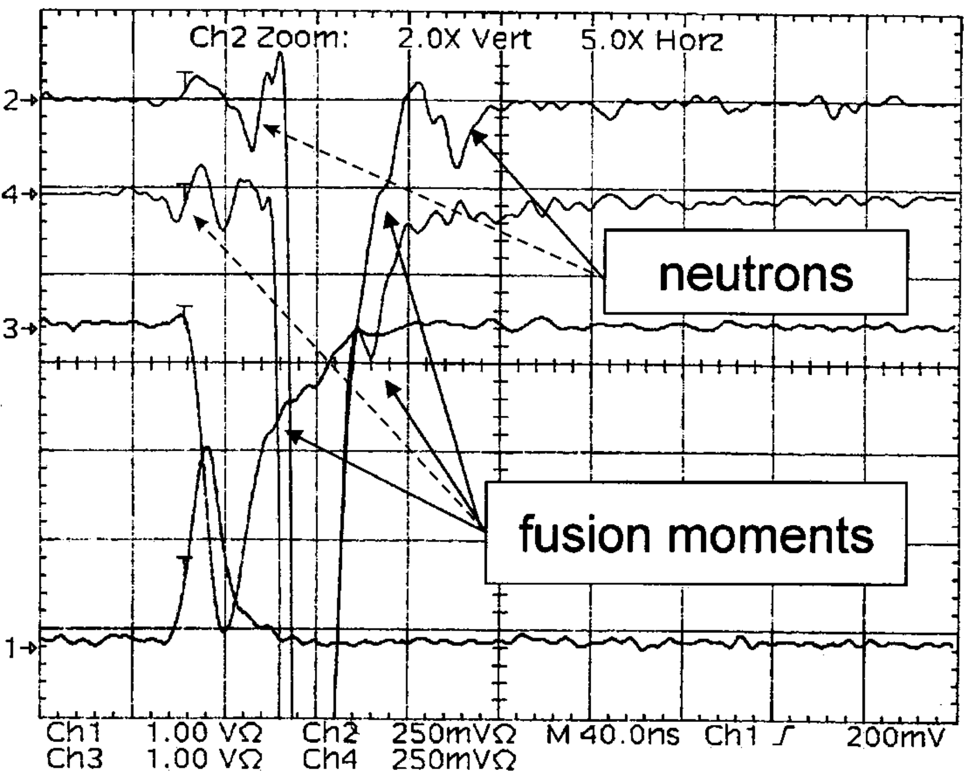

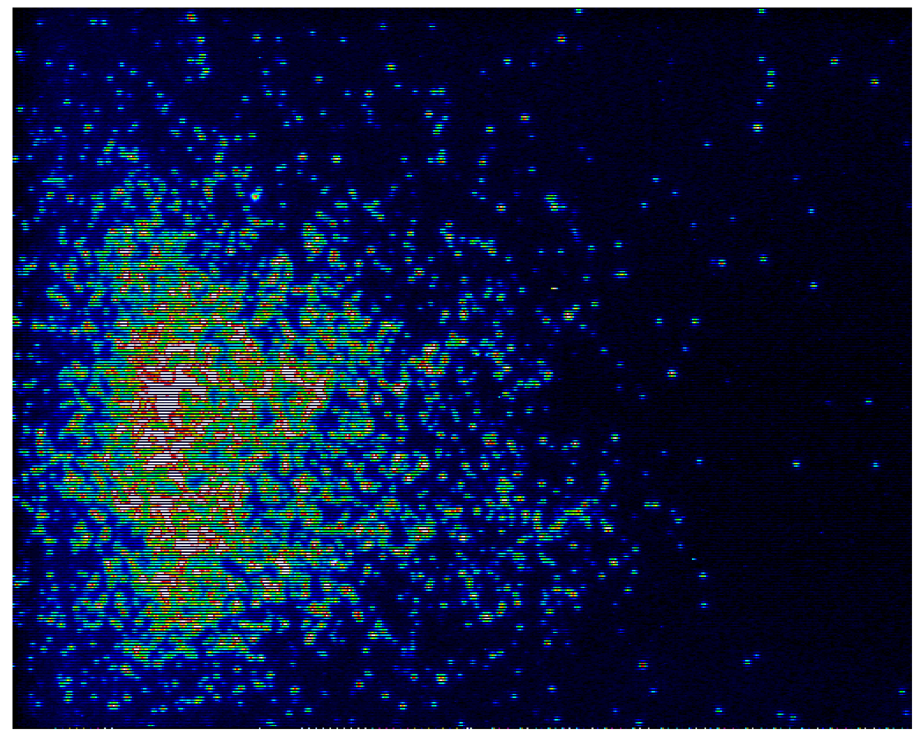

Periodically Oscillating Plasma Sphere (POPS)

- **Ion beam fusion concept: high power density and Q>1 are incompatible**
  - Beam distribution required for high fusion power density
  - Ion-Ion Coulomb collisions spreads beam distribution and beam focus
  - $\langle\sigma v\rangle_{i\text{-}i} \gg \langle\sigma v\rangle_{fusion}$: no net fusion power
- Barnes and Nebel (circa 1997): Constant density electron background in a sphere (by external electron injection) --> spherical harmonic potential well for ions
- Ions created by ionization and oscillate radially in the well
- POPS frequency for singly charged ions:

$$f_{POPS} = \frac{\sqrt{8V_{well}/M_{ion}}}{2\pi r_{VC}}$$

- Harmonic oscillator - same freq. regardless of amplitude --> simultaneously converge to the center with maximum kinetic energy

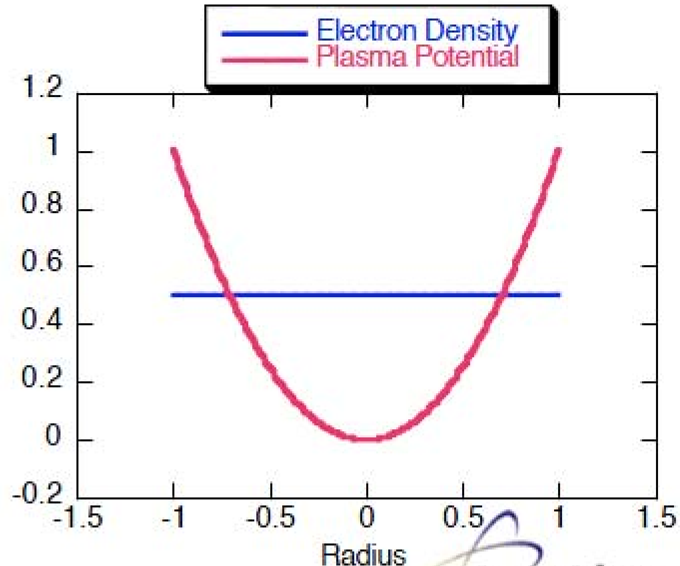

NNSA

Los Alamos
NATIONAL LABORATORY

Два предельных случая: превалирует максвелловское или пучковое распределение ионов по энергиям

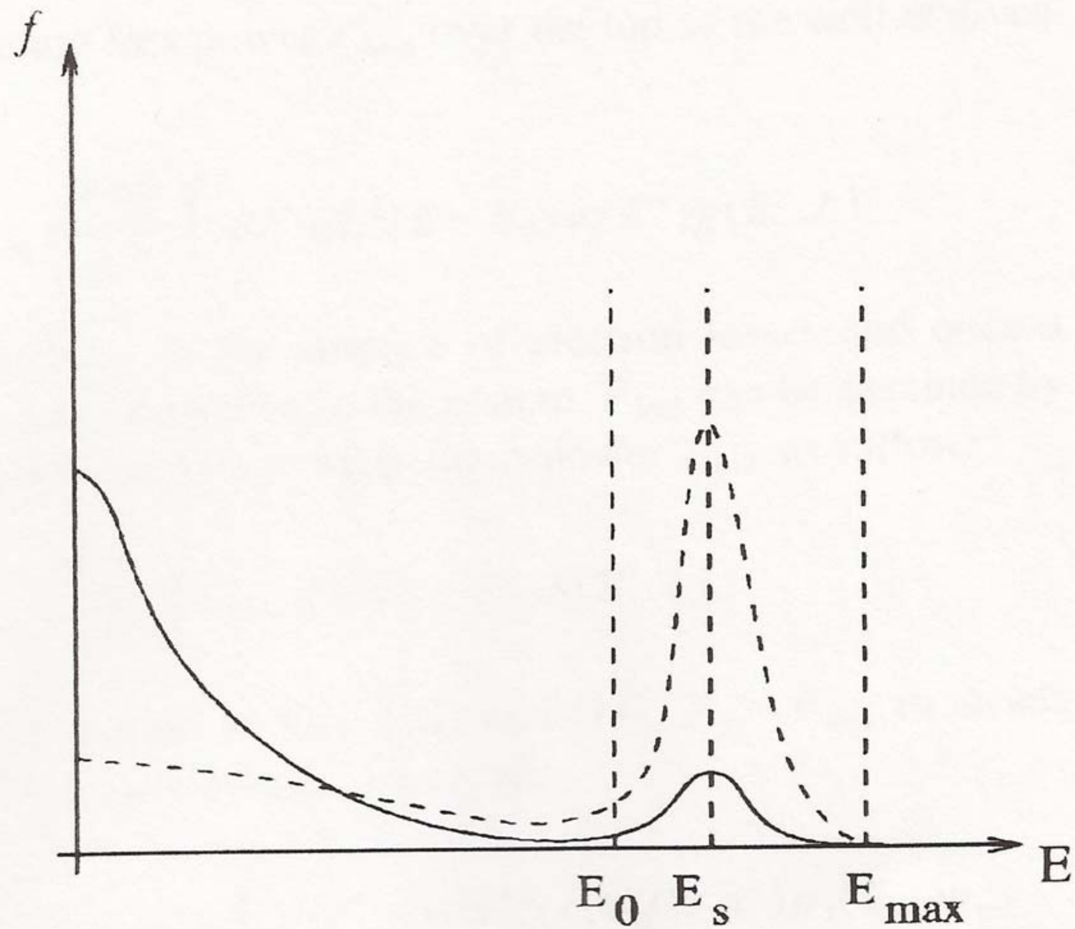

FIG. 4. Sketch of two opposite limits of the beam-Maxwellian equilibrium: the solid line corresponds to a case in which the Maxwellian population is dominant; the dashed line corresponds to a case in which the beam contribution is dominant.

Phase of POPS Oscillation

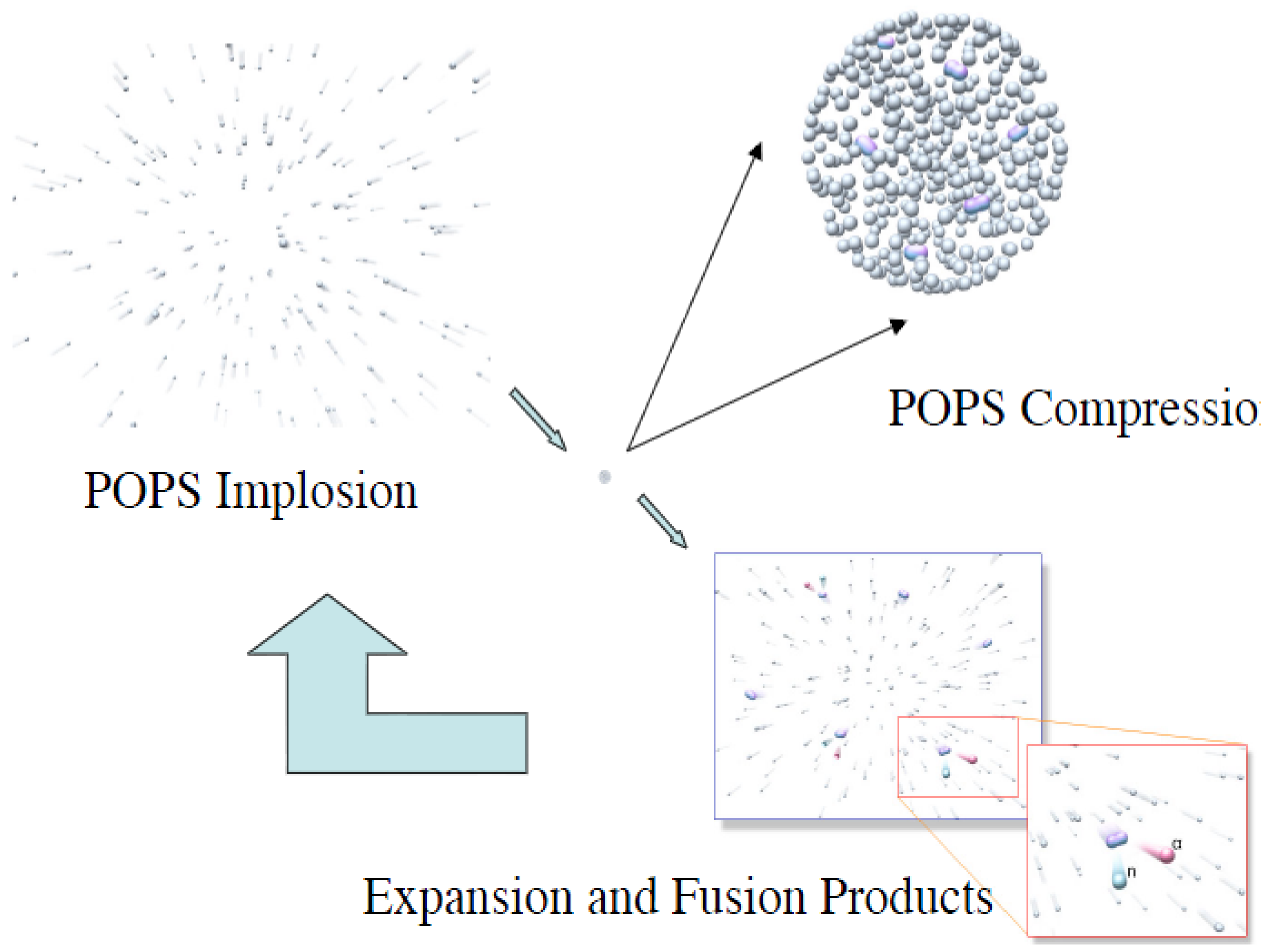

NNSA

Los Alamos
NATIONAL LABORATORY

Scaling of POPS frequency

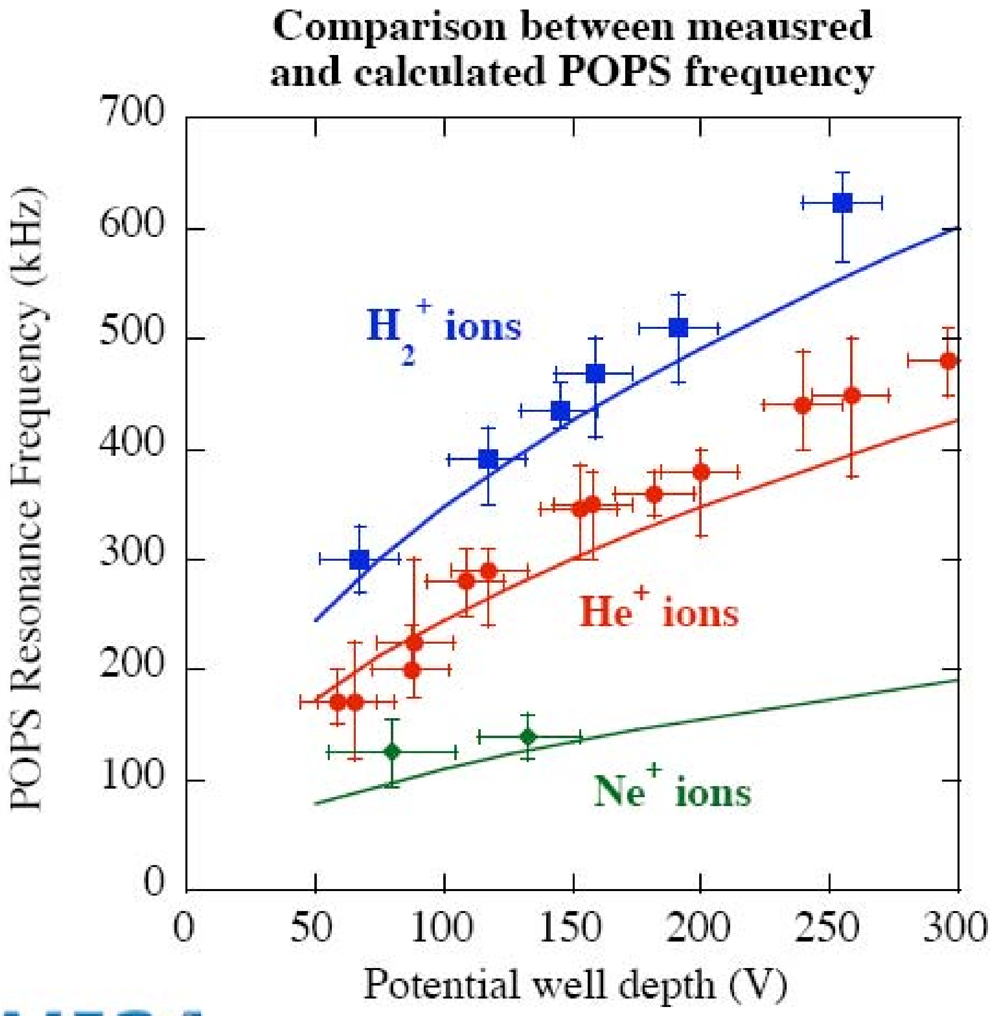

- 3 ion species (H_2^+, He^+ and Ne^+) have been used.
- Resonance frequency exhibit $V_{well}^{1/2}$ scaling
- Resonance frequency exhibit $1/(\text{ion mass})^{1/2}$ scaling

$$f_{POPS} = \frac{\sqrt{8V_{well} / M_{ion}}}{2\pi r_{VC}}$$

- POPS frequency calculation with $r_{VC} = r_{grid}$ (no free parameter)
- **Excellent agreement with theoretical calculations (in absolute values)**

POPS Compression and Potential Applications

- Two factors for practical fusion devices based on POPS
  - -Fusion efficiency ($Q = P_{fusion}/P_{input}$)
  - -Fusion power density ~ compression $(\theta)^2$

$$P_{fusion} \approx \frac{3 f^2 \varphi_0^2 \theta^2}{2\pi e^2 r_{grid}} < \sigma v >$$

- Higher compression --> higher fusion power density --> more practical
- Various potential applications based on achievable compression ratio
- D-T mixed fuel --> lower compression requirement

Fuel	Application	Compression ratio (r_{max}/r_{min})	Neutron rate	Number of Modules (r = 1 cm)
D-D	Nuclear Assay (HEU, HE, CW)	26	$\sim 1.0 \times 10^{11}$ n/s	1
D-D	Neutron Tomography	83	$\sim 1.0 \times 10^{12}$ n/s	1
D-D	PET Isotope Production	200	$\sim 1.0 \times 10^{15}$ n/s	172
D-D	Fusion (1GWth)	2000	$\sim 1.6 \times 10^{21}$ n/s	$\sim 2.8 \times 10^{7}$
D-T	Fusion (1GWth)	86	$\sim 1.6 \times 10^{21}$ n/s	$\sim 2.8 \times 10^{7}$

NNSA

Los Alamos NATIONAL LABORATORY

On the variation of the regimes of DD neutron yield in time

1) **Single** neutron peak

$T_{VC} \approx T_{pulse}$ = 50 nanoseconds

2) **Multiple** yield (two or more neutron peaks of different intensity)

3) **Pulsating** (oscillatory) neutron yield

$T_{VC} << T_{pulse}$ $T_{osc} \approx$ 12-13 ns

- the time of formation (reconstruction) of virtual cathode (**VC**) and potential well (**PW**) in vacuum discharge

$$T_{VC} \sim C\, U / I_L$$

(Barengolts and Mesyats JETPh 2000)

CL limiting current

$$I_L \sim U^{3/2} / d^2_{eff}$$

Variation of A-C distance d_{eff} in experiment allows to change I_L and relation T_{vc} / T_{pulse}, and , correspondingly, to change the regimes of neutron yields

DD fusion: TOF registration of DD neutrons

Example of increasing pulsating neutron yield

- 0525tri7

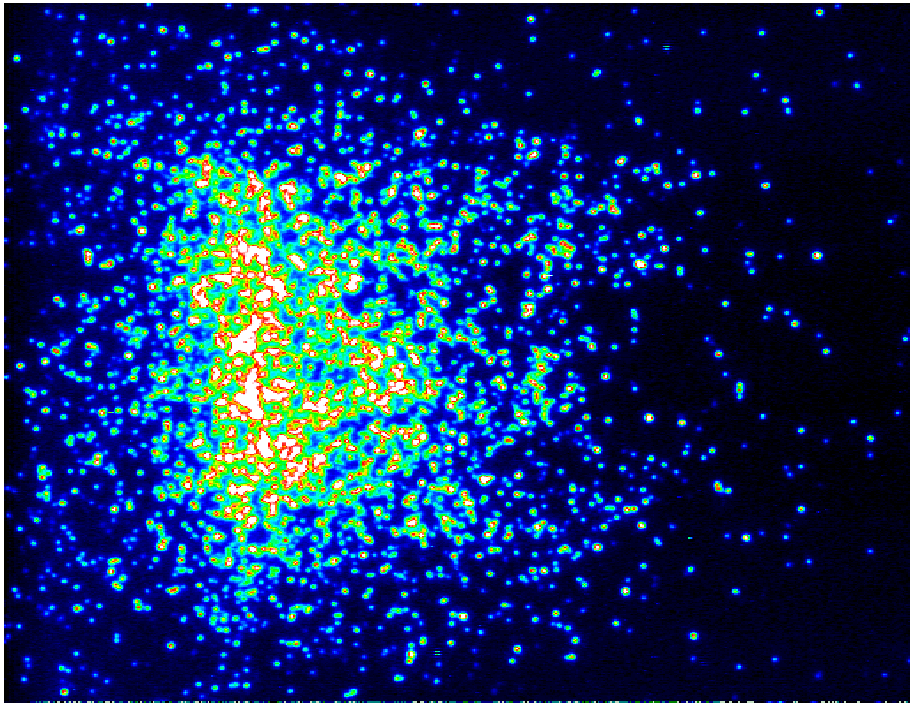

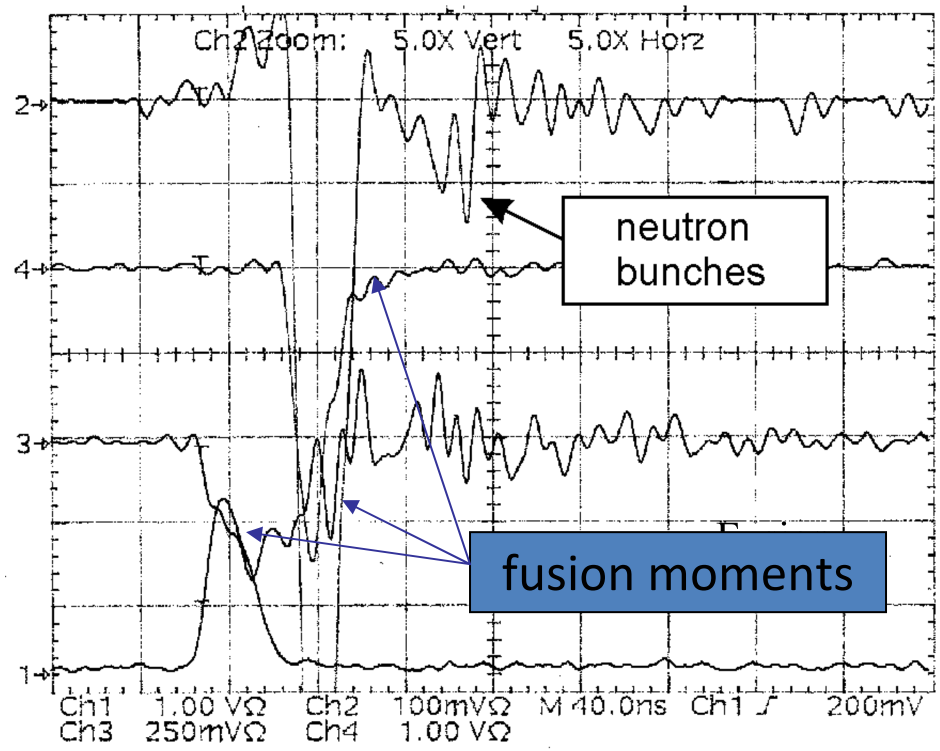

Well-defined multiple fusion events (MFE) and pulsating neutron yield (PM2+Pb , 0525tri9)

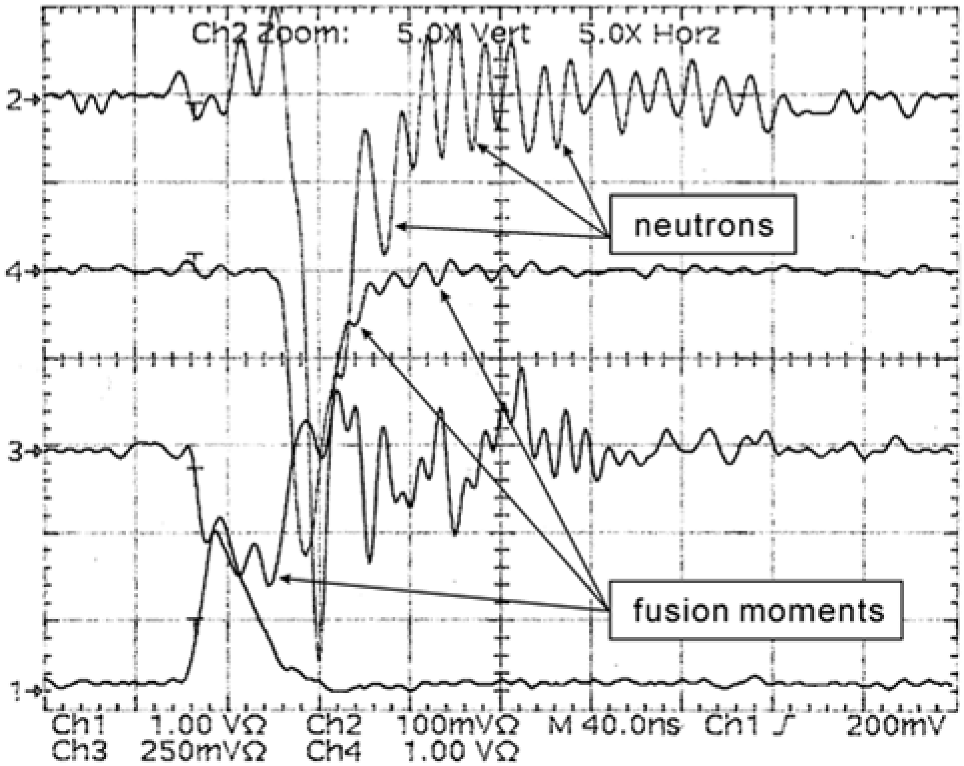

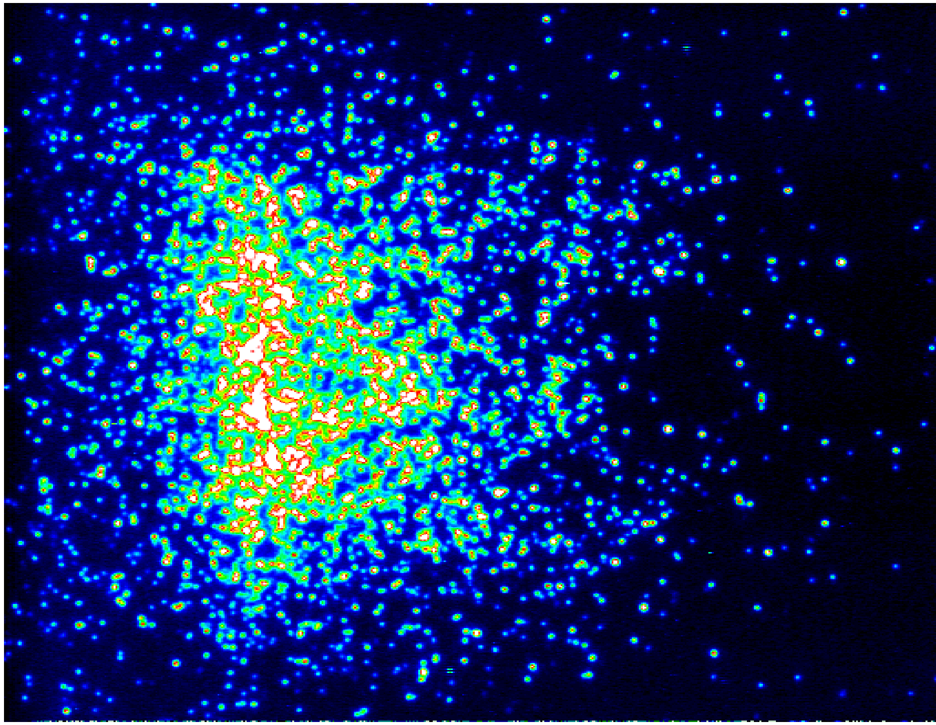

particular example of dilute x-rays dust

(two double neutron peaks, and damped oscillations, ch.2, 0518D10)

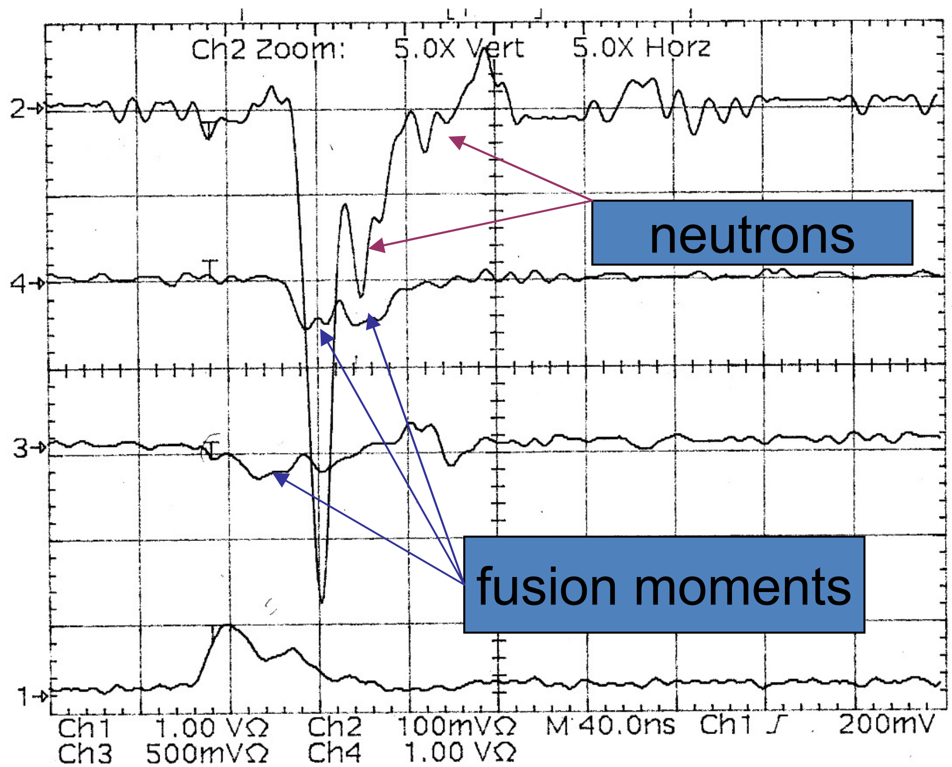

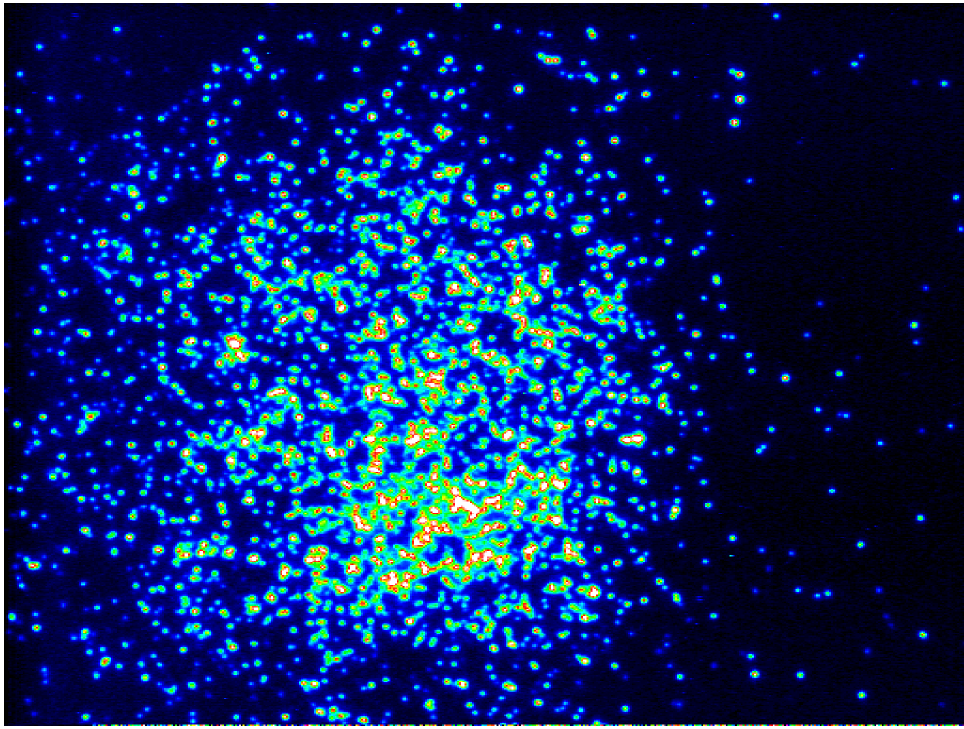

Example of double *stationary* potential well at interelectrode space

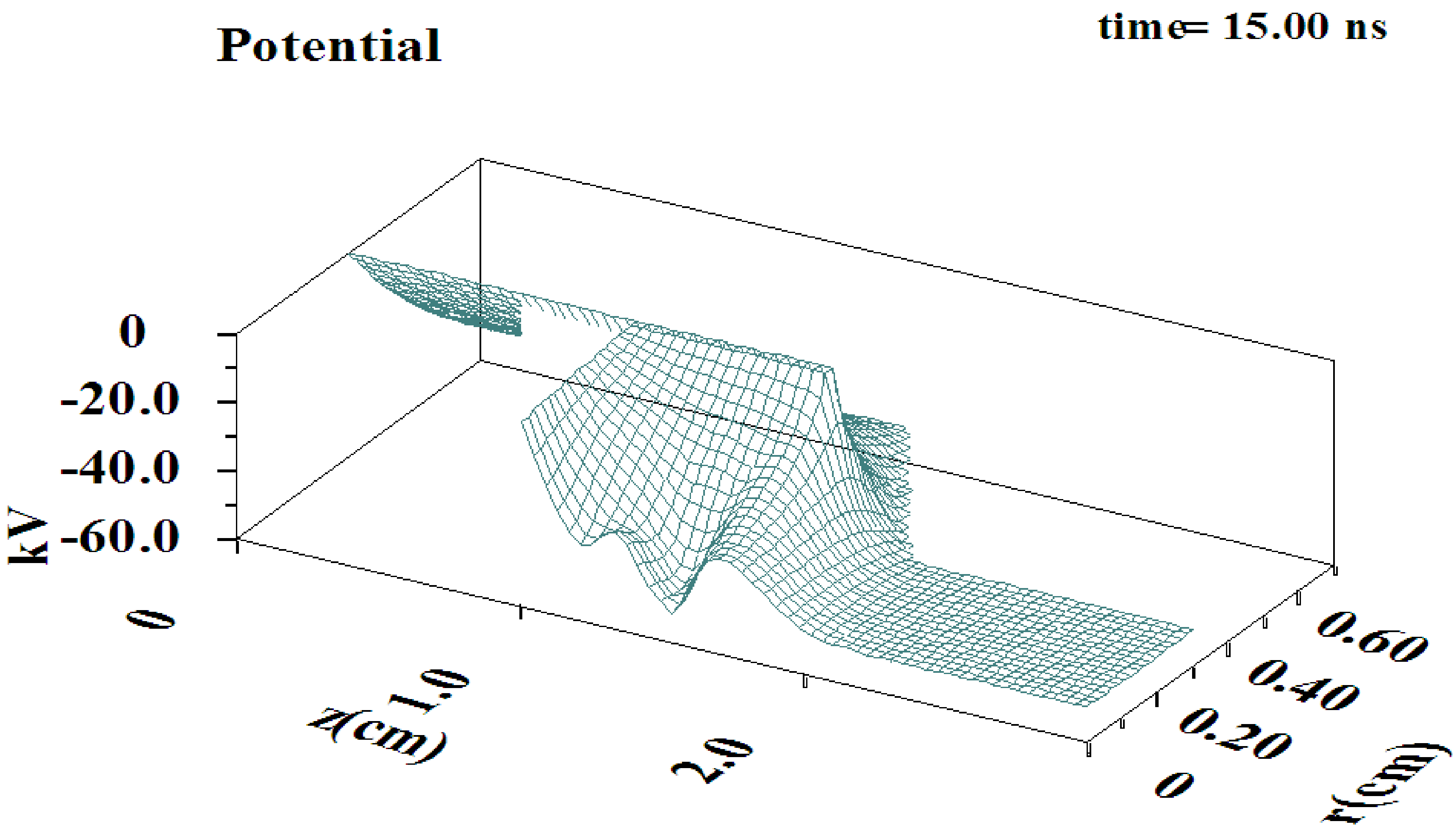

Experimental set-up for IECF study with Periodically Oscillating Plasma Spheres (POPS)

(Los Alamos 2005-2010, $f_{POPS} < 1MHz$, $\phi_{PW} < 1$ keV)

6 Electron emitters

- Управляющий катод
- Импульсы напряжения ~ 10 мкс

Spherical greeds

Nanosecond vacuum discharge (NVD)

J.Phys.A **39**(2006)43 Yu.K Kurilenkov et al

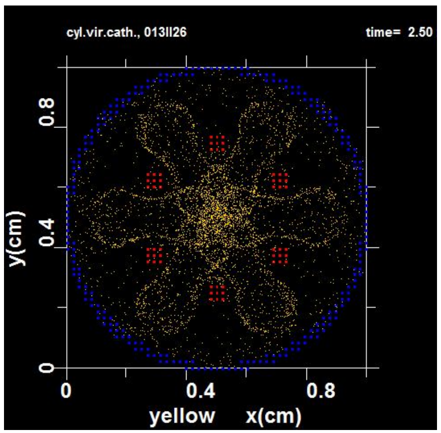

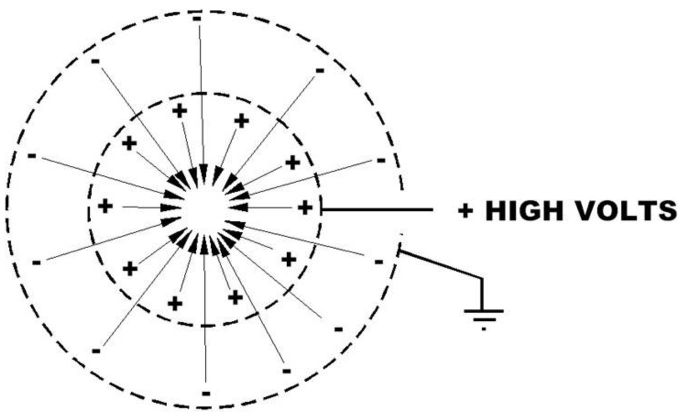

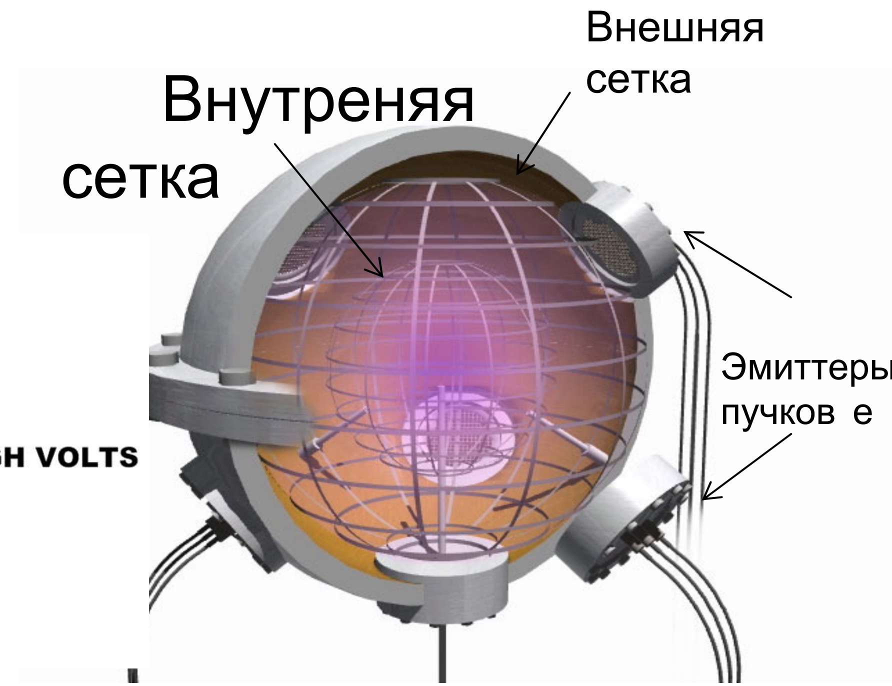

Autoelectron beams from cathode do appear automatically when voltage applied at NVD. Thus, POPS-like scheme is simplified essentially and becomes more efficient due to favorable scaling of fusion power density, $\mathbf{P \sim \theta^2 \phi^2 / r^4_{VC}}$ which increases with the inverse of virtual cathode (VC) radius $\mathbf{r_{VC}}$ and increasing of potential well (PW) depth ϕ_{PW} (f≈ *80 MHz, PW depth* φ_{PW} *~ 55 кeV)*

*Схема установки для синтеза с инерционным электростатическим удержанием (IECF) в Лос-Аламосе, LANL*J.Park, R.Nebel *et al* Phys.Plasmas **12**, 056315 (2005)

Distribution functions for deuterons at different distances from Z (r = 0.0, 0.1, 0.2)

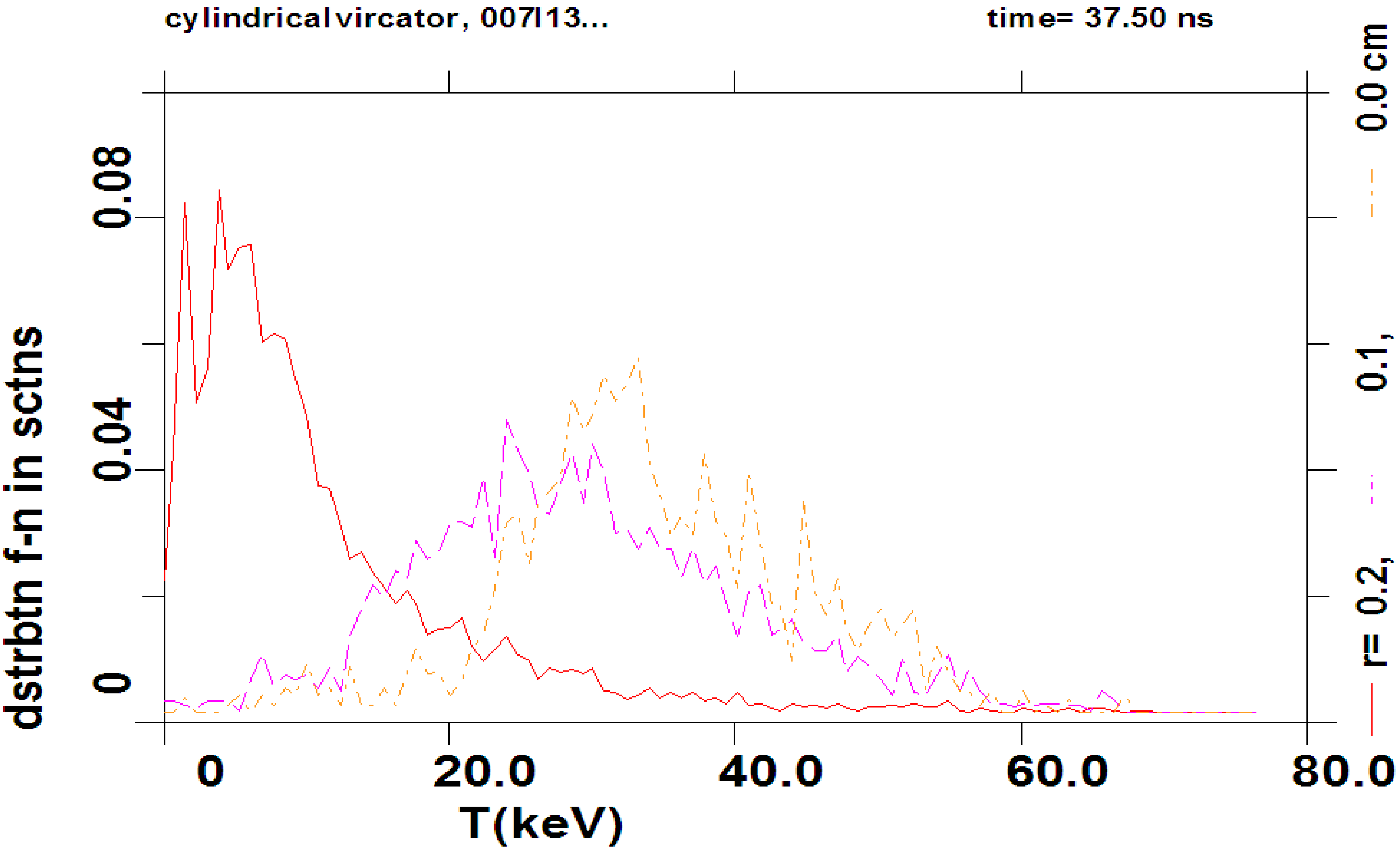

dense ensembles with total *trapping of fast ions and partially “diffused“ hard x-rays*
(inside of cluster ensemble)

Diffusion (delay) of lower energy hard x- rays (ch.1,3). Release of harder x-ray. Enhanced neutron yield from the « ball »

(sensitivity of ch.2 is 500 mV, 0426D1)

Neutrons leave the « ball » earlier than diffused lower energy x-rays

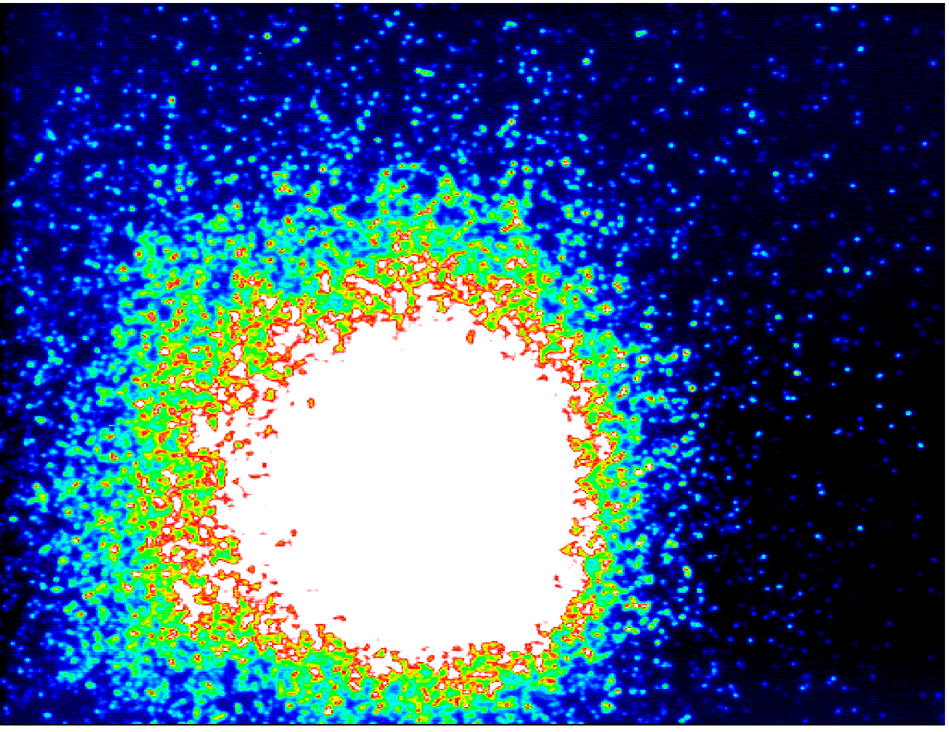

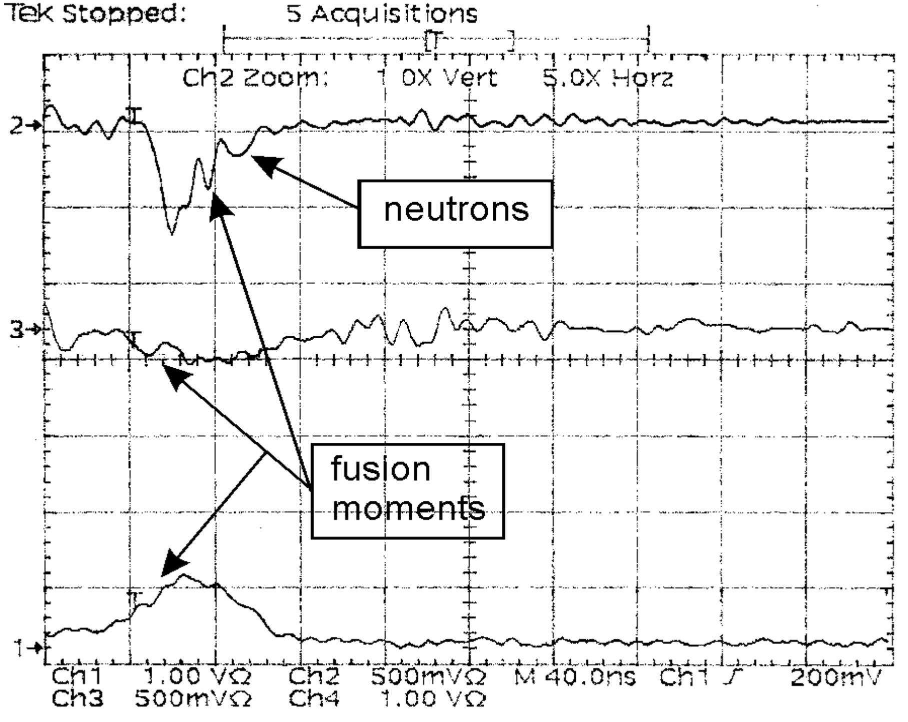

essential x-rays diffusion and manifestation of higher pulsating neutron yield (due to *multiple fusion events)*

(example of « microreactor »-like regime)

- 1018D3, ch.2 -1 V, ch.4- 500 mV

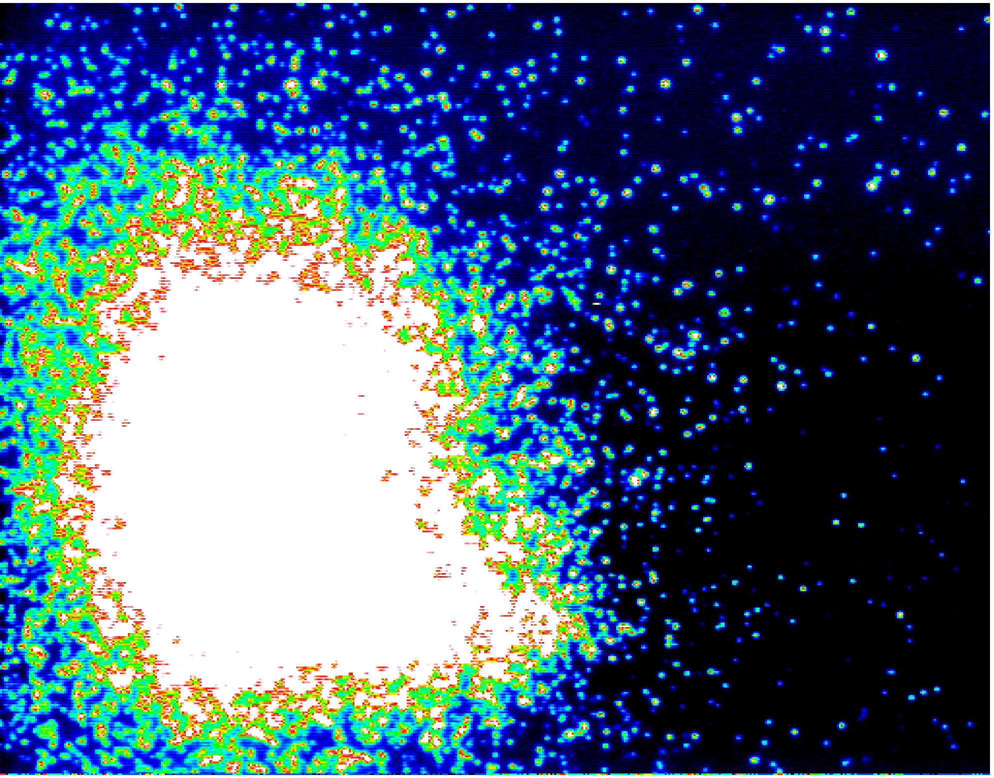

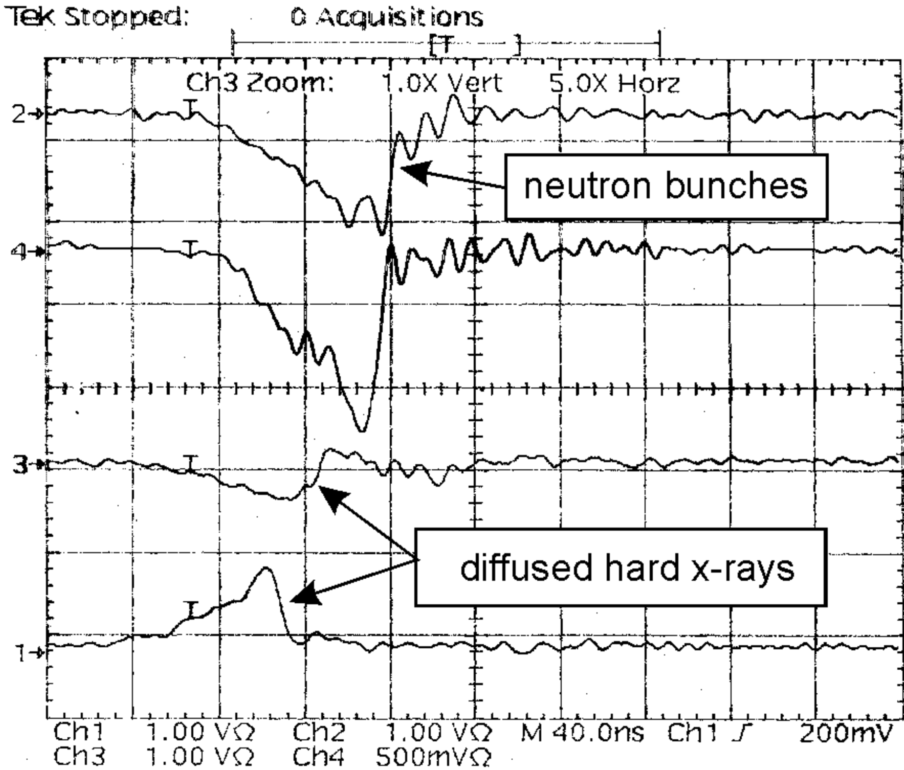

Another shape of dense ensemble with multiple fusion (« microreactor ») and essential x-rays trappingю **High pulsating neutron yield and *very low level of x-rays yield (chs 1,3)*(it provides the registering of just neutrons mainly at PM4 also)**

- 1018D5, ch.2 -1 V, ch.4- 500 mV

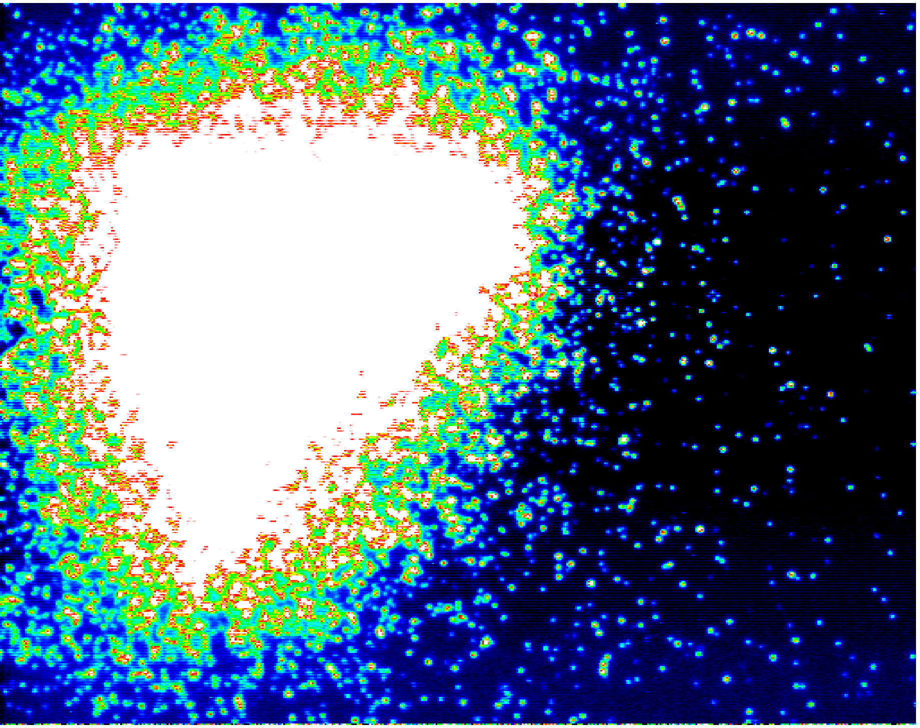

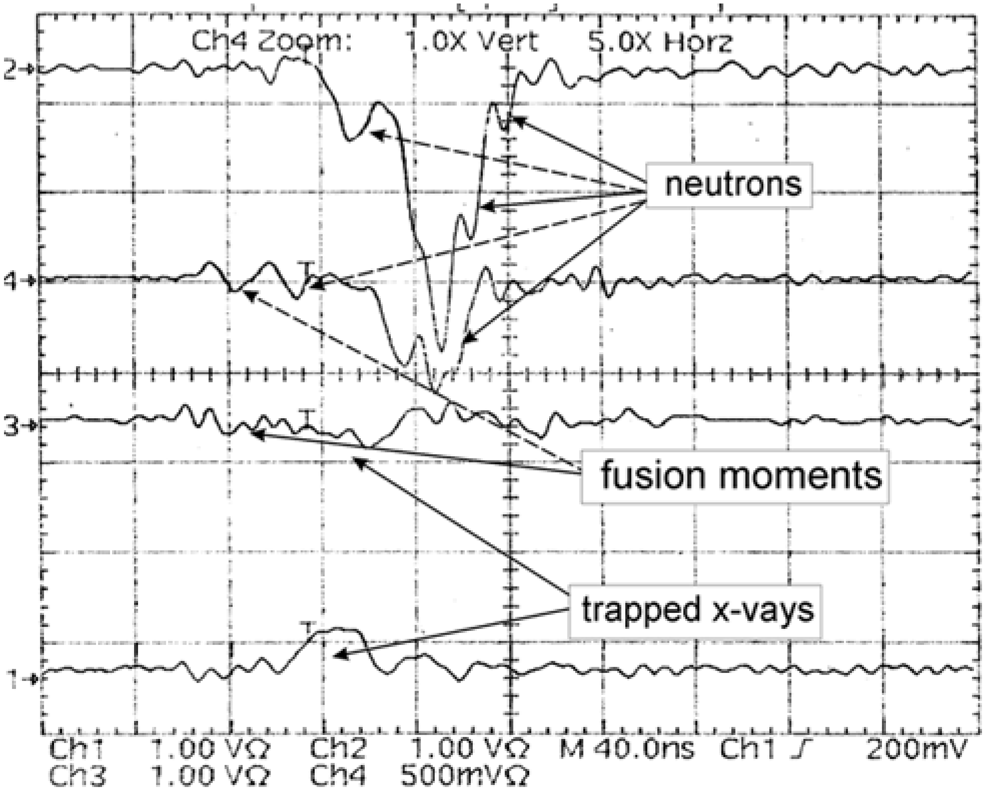

Key Fusion Fuels

D + T → n (14.07 MeV) + ^{4}He (3.52 MeV)

D + D → n (2.45 MeV) + ^{3}He (0.82 MeV)

→ p (3.02 MeV) + T (1.01 MeV)

{50% each channel}

D + ^{3}He → p (14.68 MeV) + ^{4}He (3.67 MeV)

p + ^{11}B → 3 ^{4}He (8.68 MeV)

^{3}He + ^{3}He → 2 p + ^{4}He (12.86 MeV)

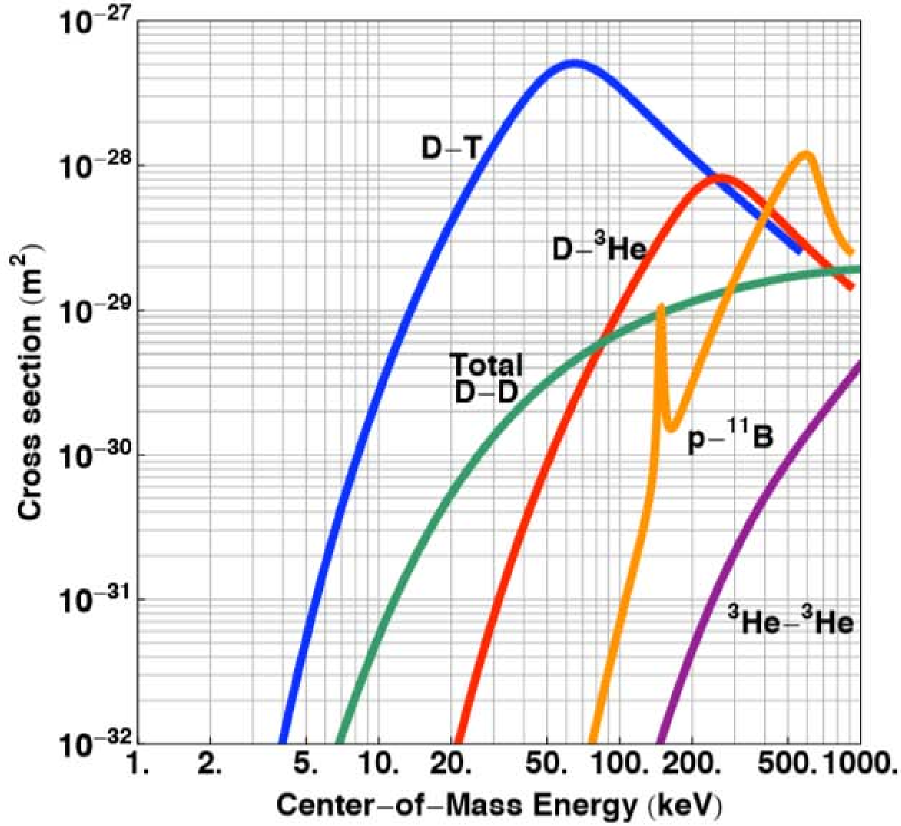

reaction p+ $^{11}B \rightarrow \alpha + {^8Be^*} \rightarrow 3\alpha$

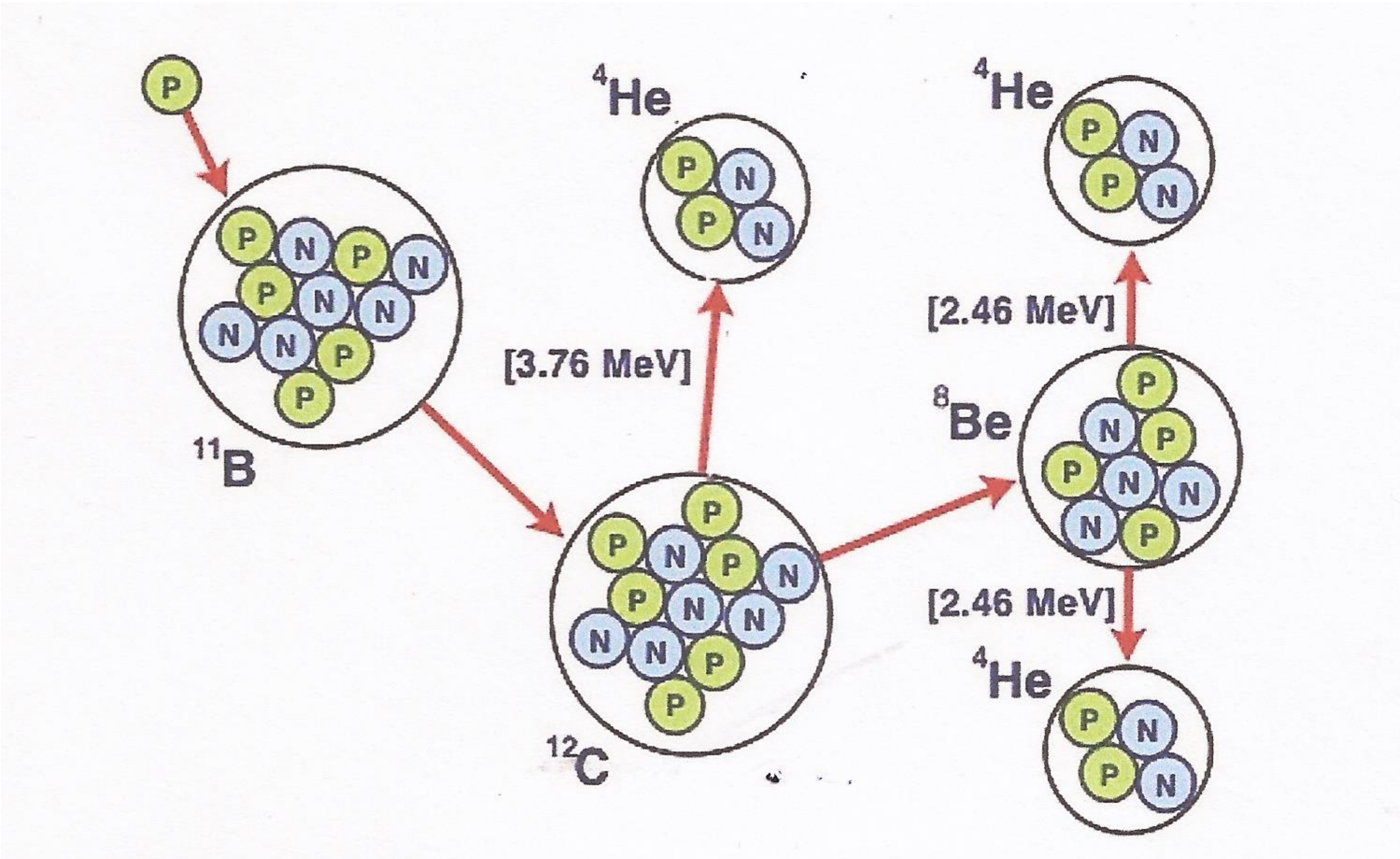

Nature Communications 4:2506 doi:10.1038/ncomms3506 (2013)

Fusion reactions initiated by laser-accelerated particle beams in a laser-produced plasma

C. Labaune[1], C. Baccou[1], S. Depierreux[2], C. Goyon[2], G. Loisel[1], V. Yahia[1], and J. Rafelski[3]

[1]*LULI, Ecole Polytechnique, CNRS, CEA, UPMC, F-91128 Palaiseau, France*
[2]*CEA, DAM, DIF, F-91297 Arpajon, France* and
[3]*Department of Physics, The University of Arizona, Tucson, Arizona 85721, USA*

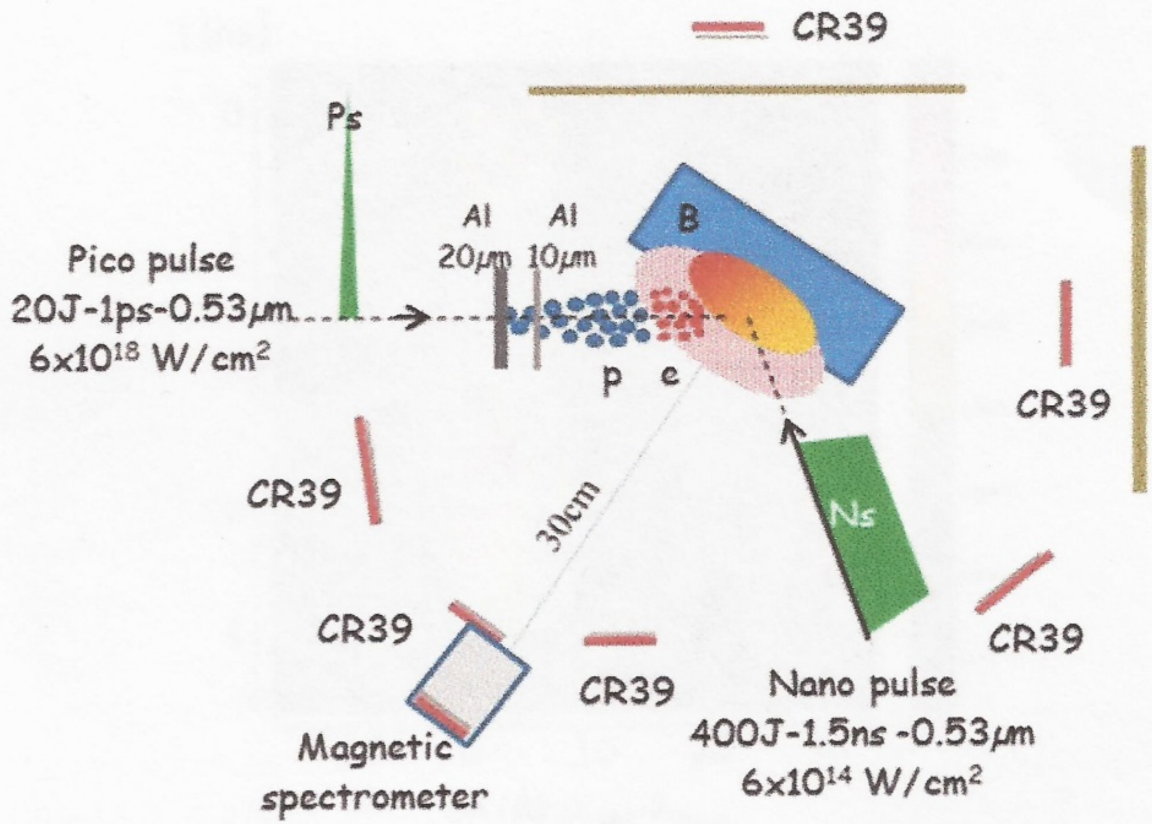

Proton –boron burning at NVD

2D PIC simulation: (a) anode (red) – cathode (blue) geometry in discharge gap of NVD where the virtual cathode is formed; green area- simulated "erosion plasma" consisting of protons and boron ions **(b)** the start of moving of protons (red ones) and boron ions (yellow) at potential well of virtual cathode to axis Z where p+ ^{11}B reaction will take place (U = 150 kV).

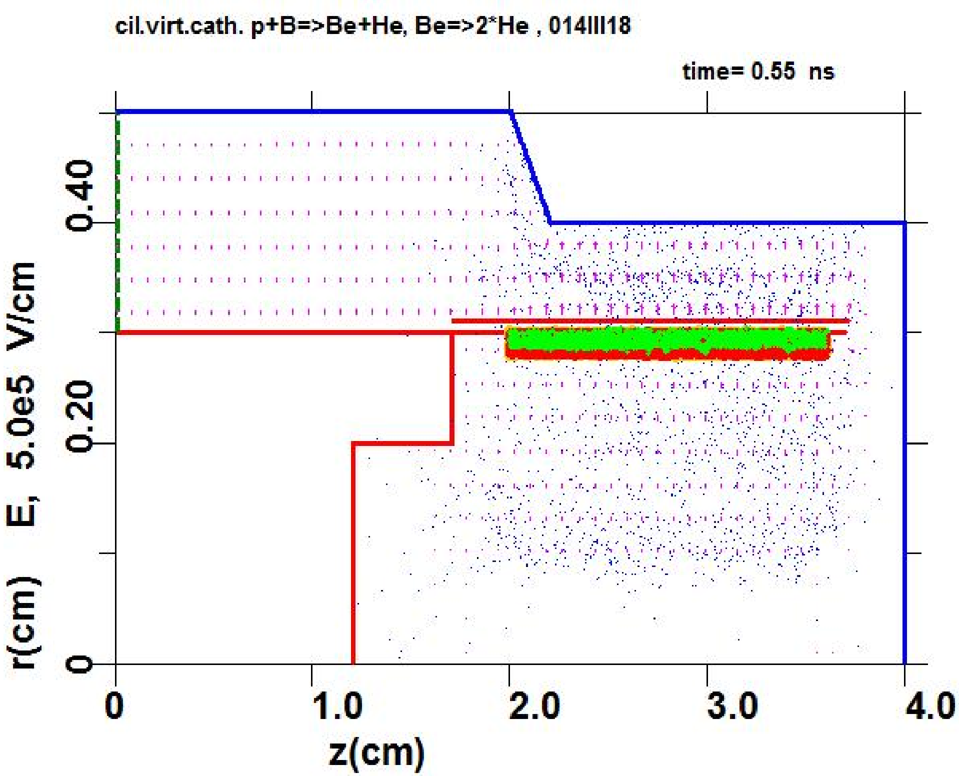

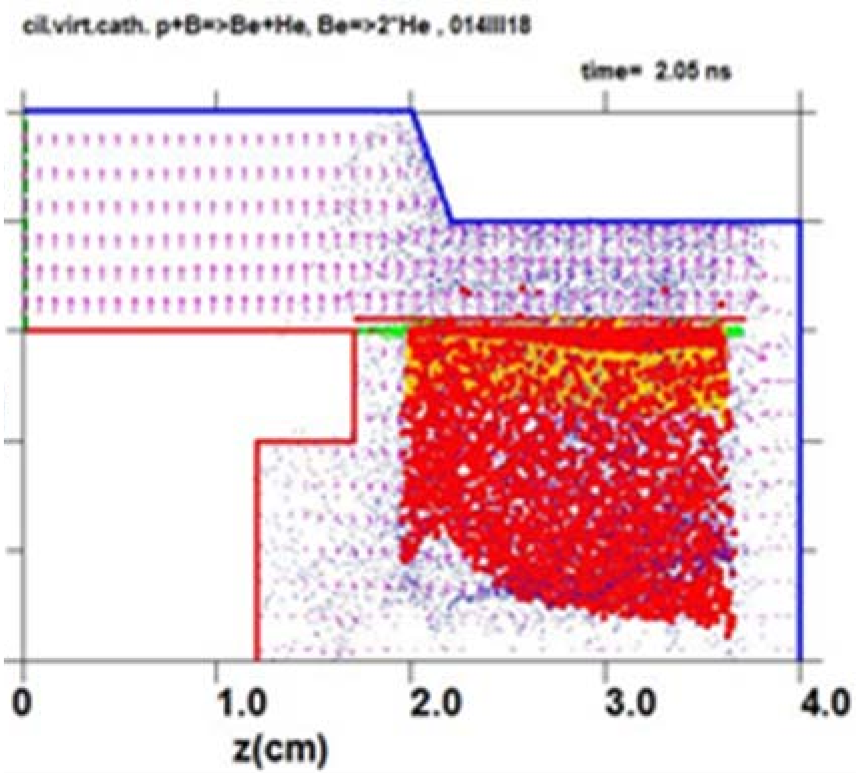

Further view of total particles ensemble at interelectrode space at 15-th and 20-th ns (including all products of p+B11 reaction listed further)

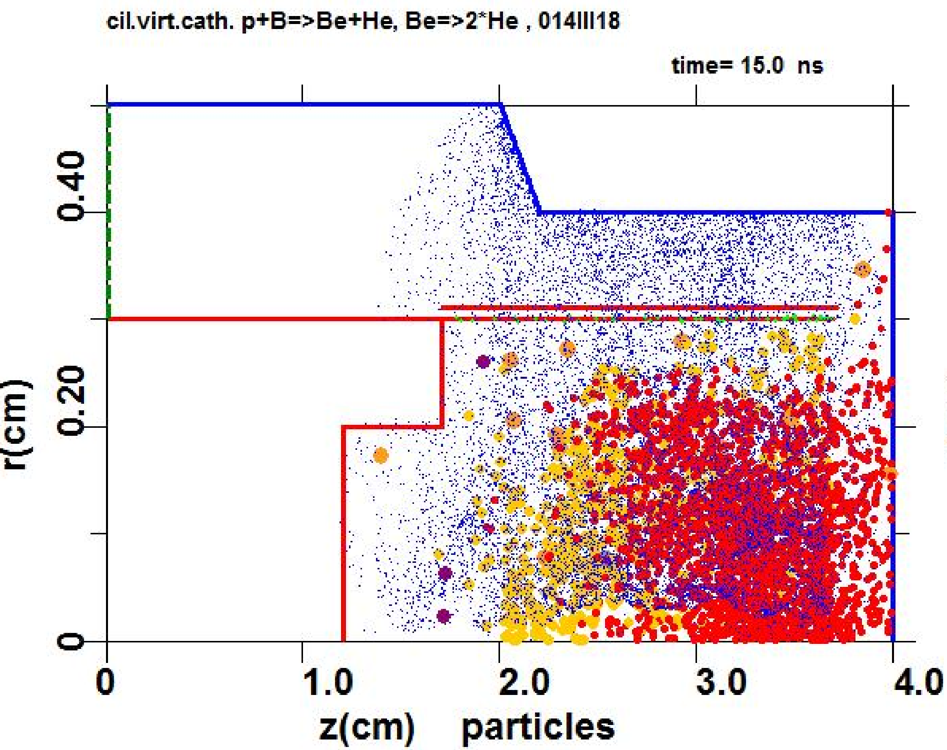

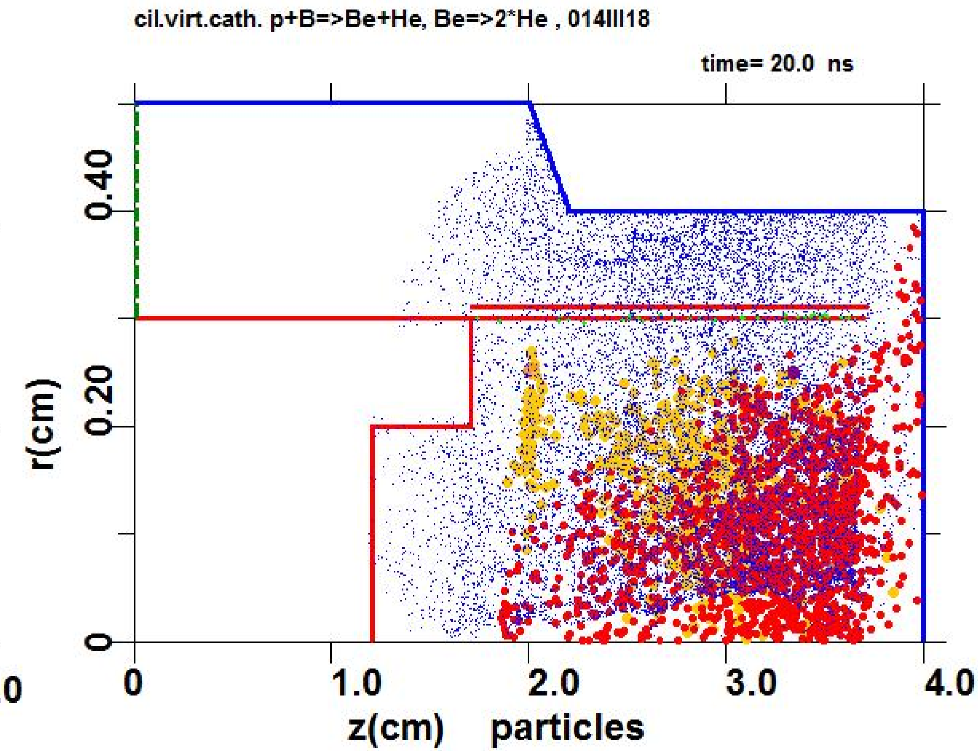

Potential well of the virtual cathode as possible micro-"reactor" for p + ^{11}B nuclear burning at nanosecond vacuum discharge (NVD).

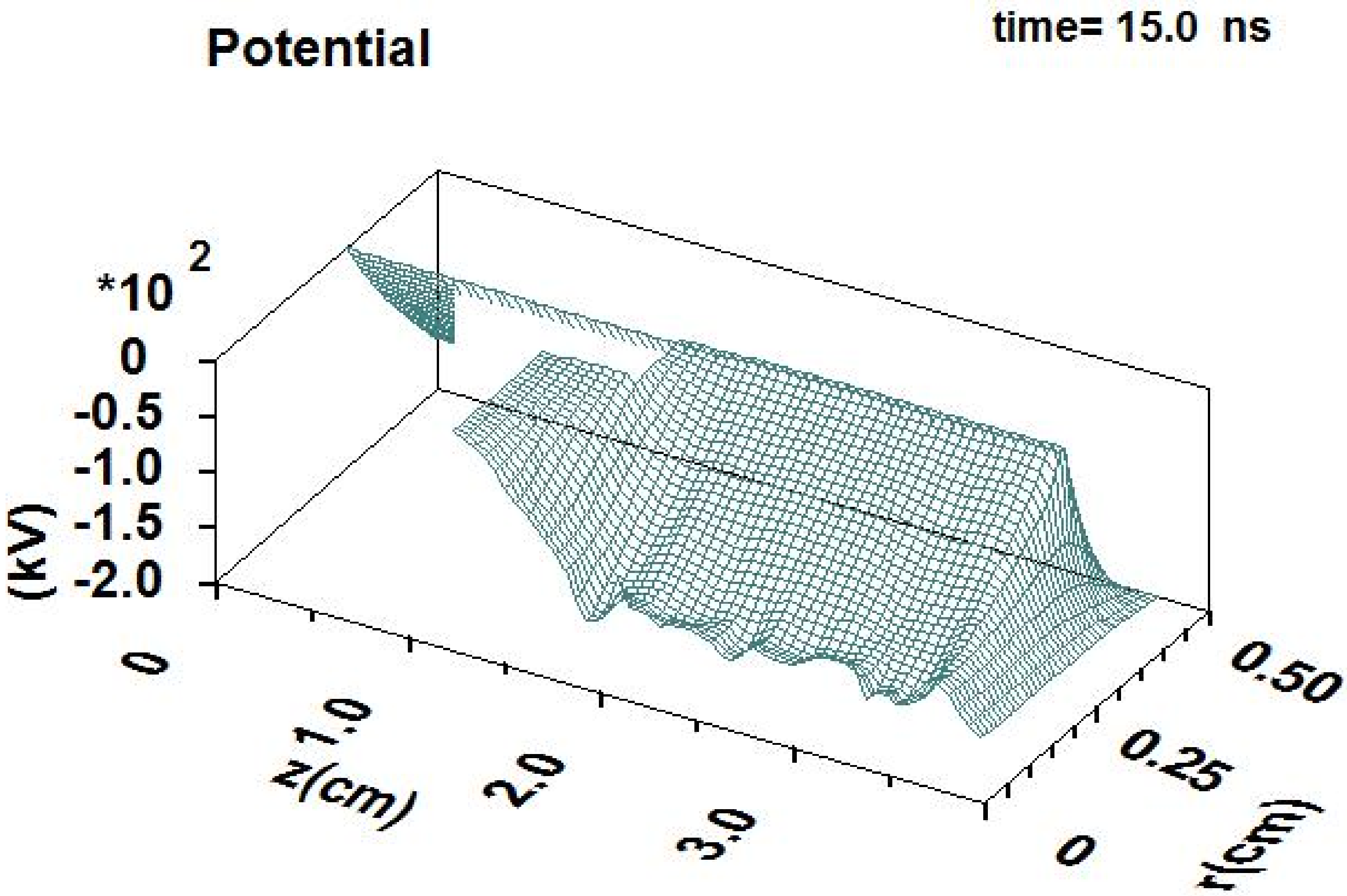

(a) Trajectories of particular groups of boron ions and protons during their oscillating around the axis Z at anode space (r- protons, y- boron ions)**(b)** Energy of chosen groups of protons and boron ions as a function of time in the process of oscillations in potential well (within the interval 0–20 ns)

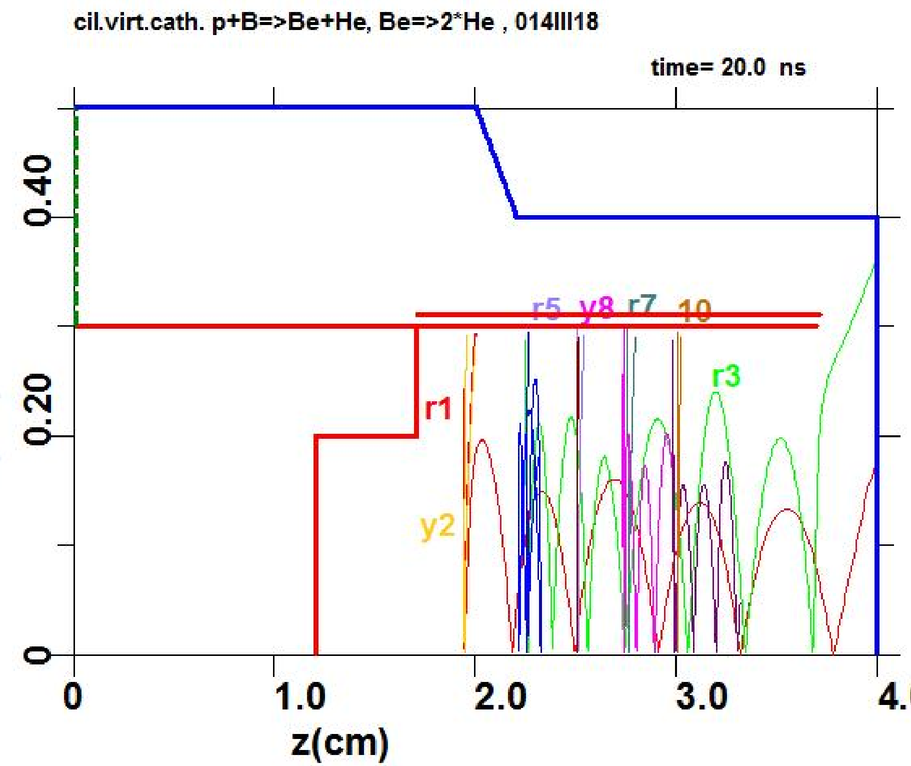

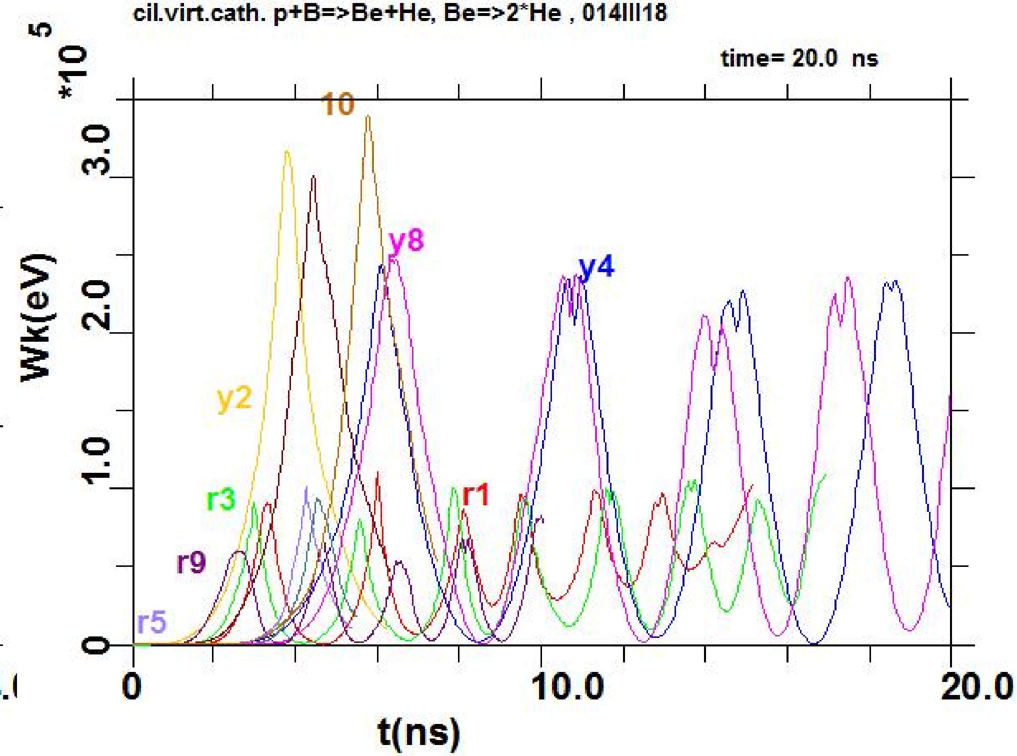

Velocities of all particles as a function of their position ***along the radius*** (phase portrait) of the anode–cathode geometry being studied (formation of virtual cathode in the area of r ≤ 0.1 cm at slow-downing of the electrons is presented, while protons and boron ions are accelerating in the potential well to the axis Z)

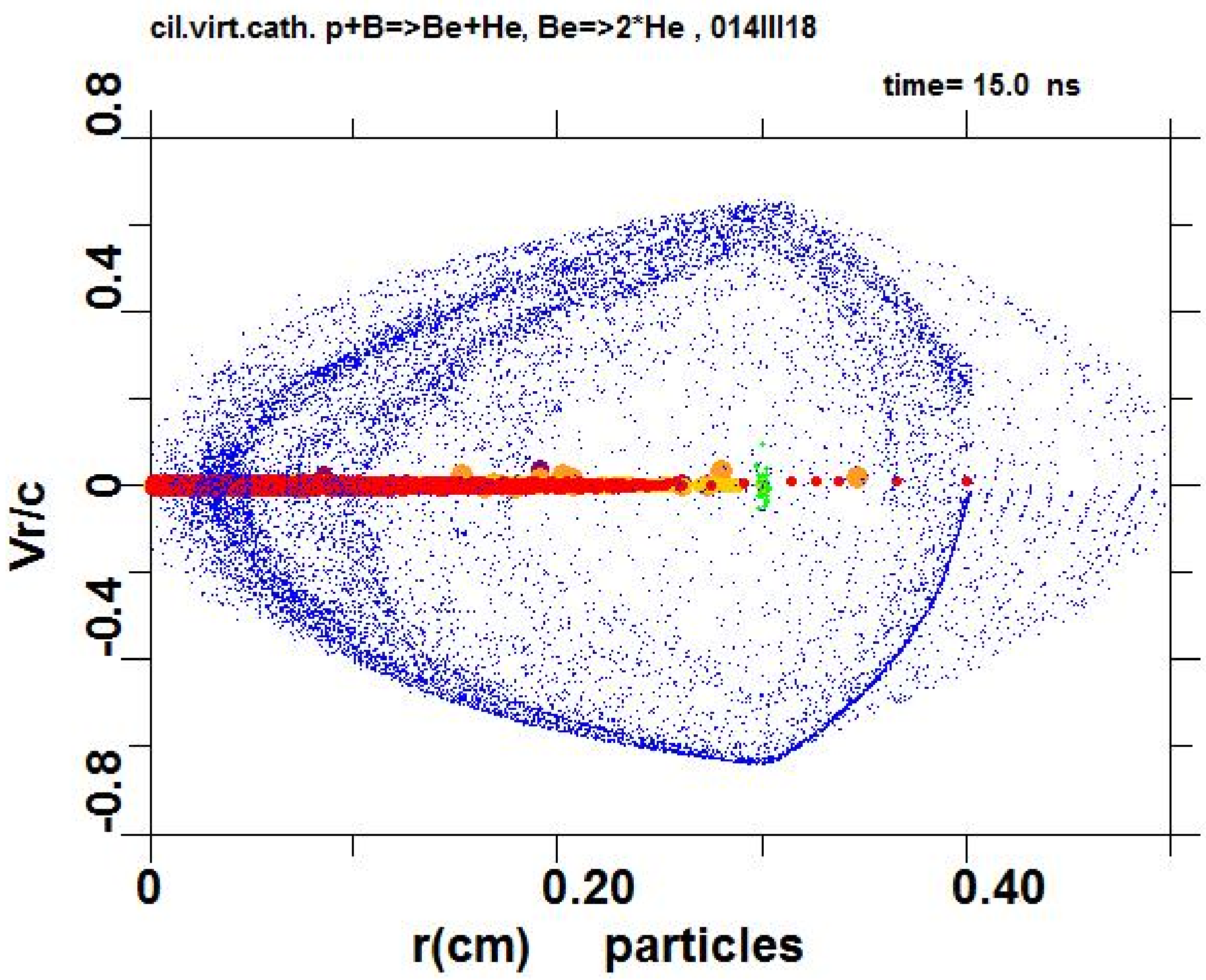

Energy of all particles in a nuclear reaction $p + {}^{11}B \rightarrow \alpha + {}^{8}Be^{*} \rightarrow 3\alpha$ as a function of their position ***along the radius*** (blue—electrons, yellow —boron ions, red — protons, violet – He^4, Z=+2 primary α - particles; gray - ${}^{8}Be^{*}$, Z=+2; dark orange – He^4 , secondary α – particles due to disintegration of ${}^{8}Be^{*}$)

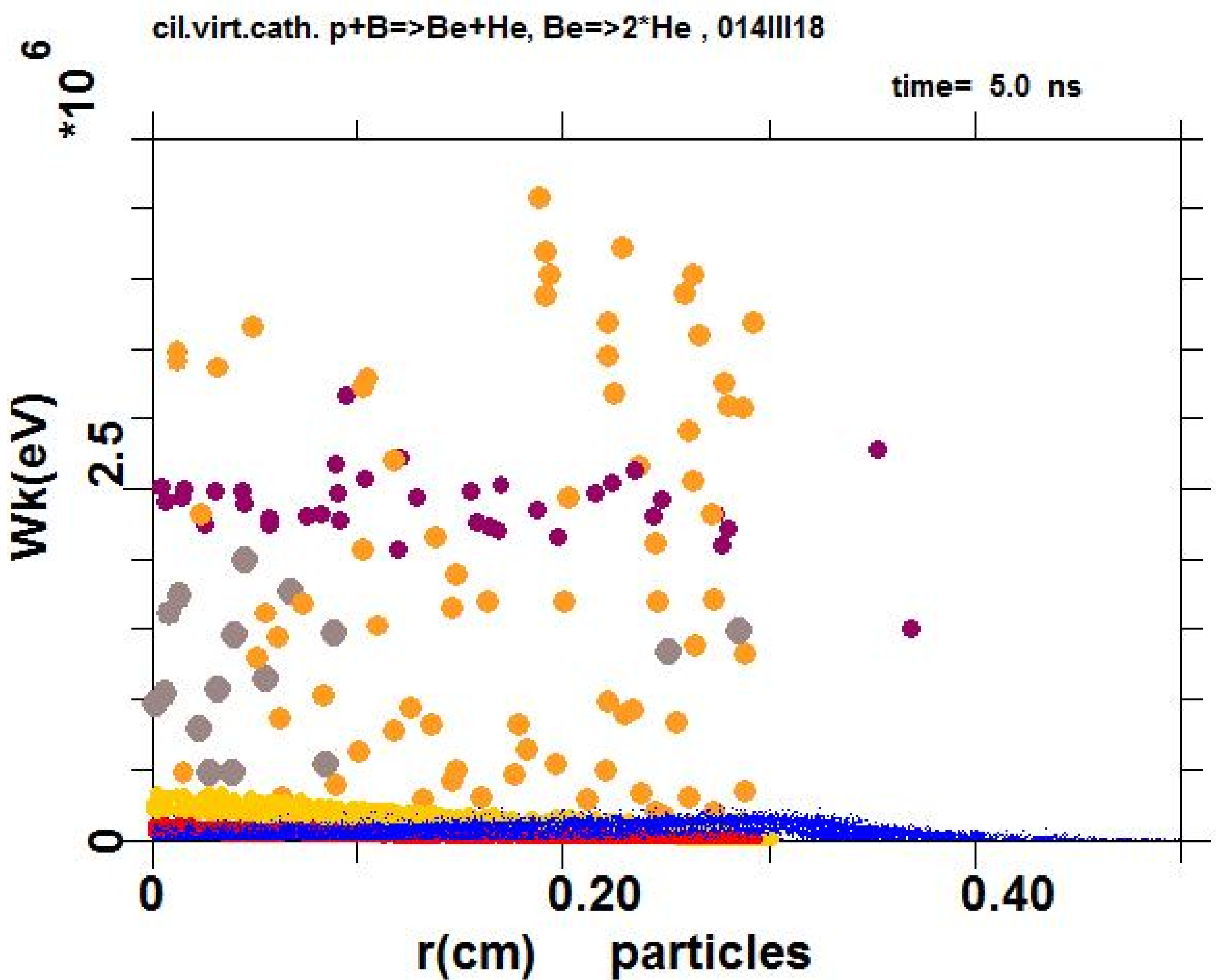

Energy of all particles in a nuclear reaction p+ $^{11}B \rightarrow \alpha + ^{8}Be^{*} \rightarrow 3\alpha$ as a function of their position ***along the axis Z*** (blue—electrons, yellow —boron ions, red — protons, violet – He^4, Z=+2 primary α - particles; gray - $^{8}Be^{*}$, Z=+2; dark orange –secondary α - particles)

5 ns

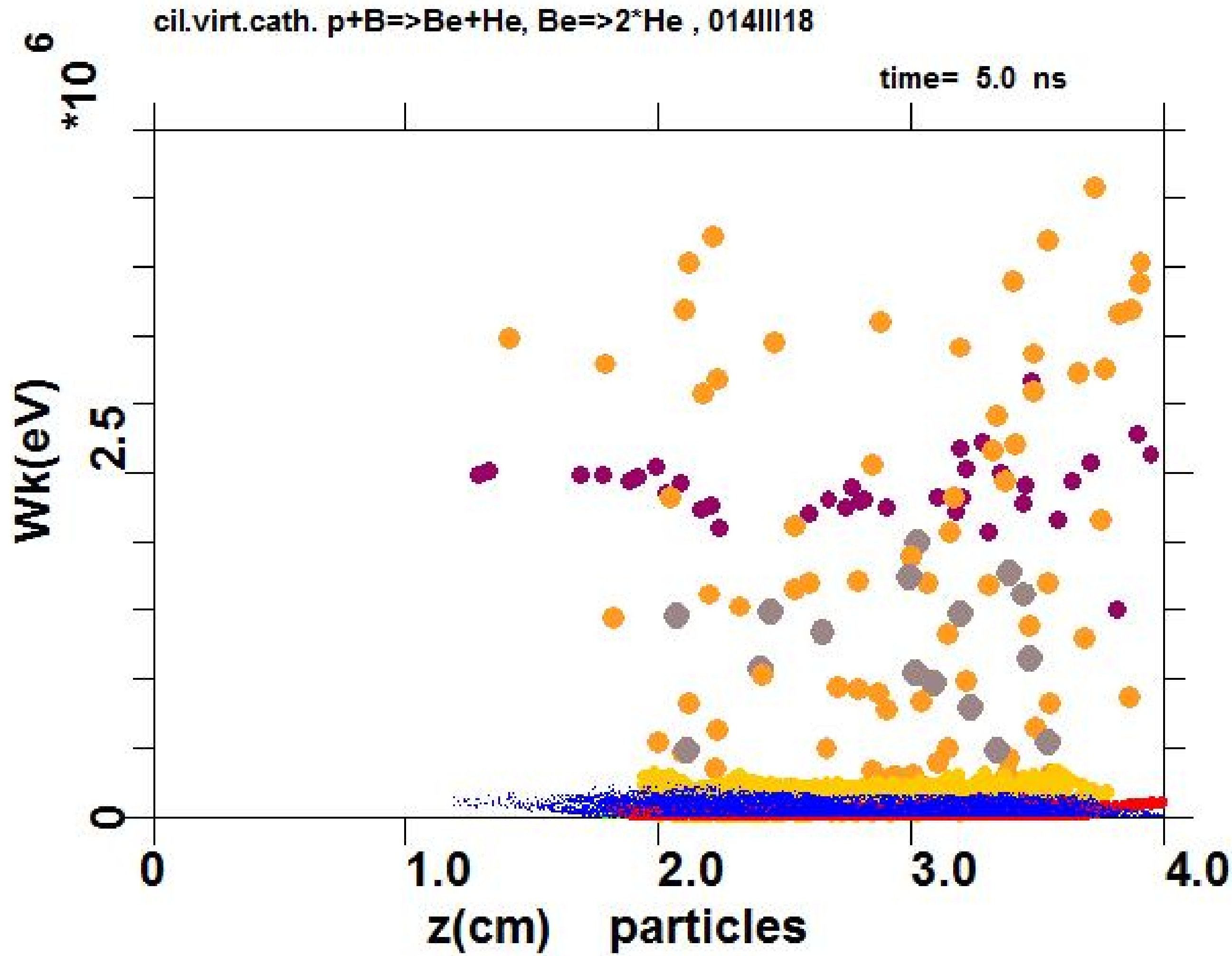

Same ones as on previous slides, but for t =15 ns

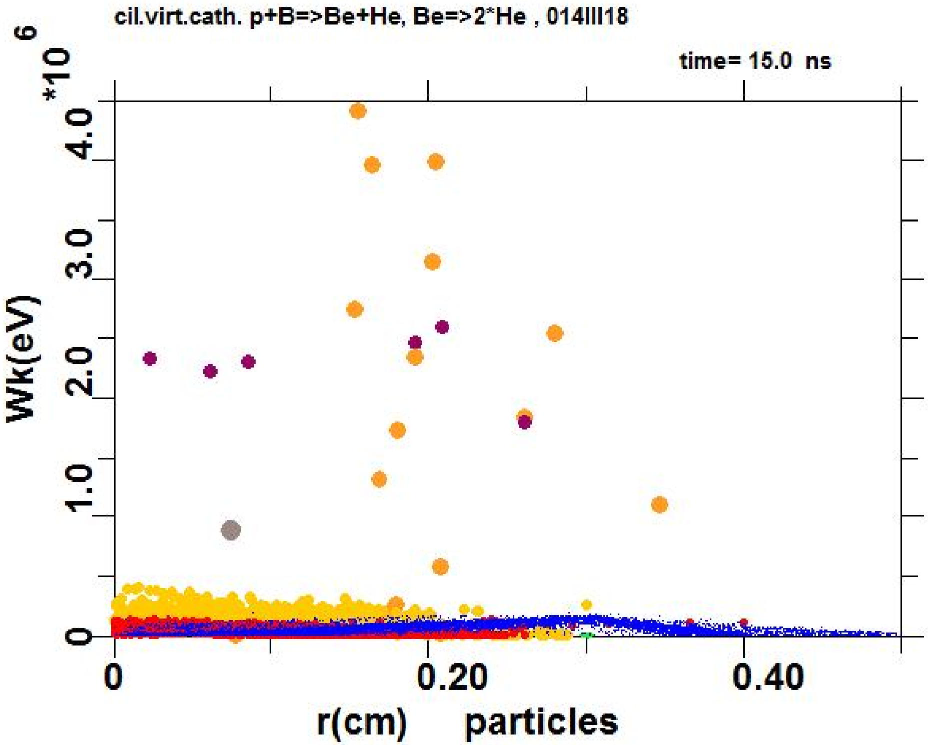

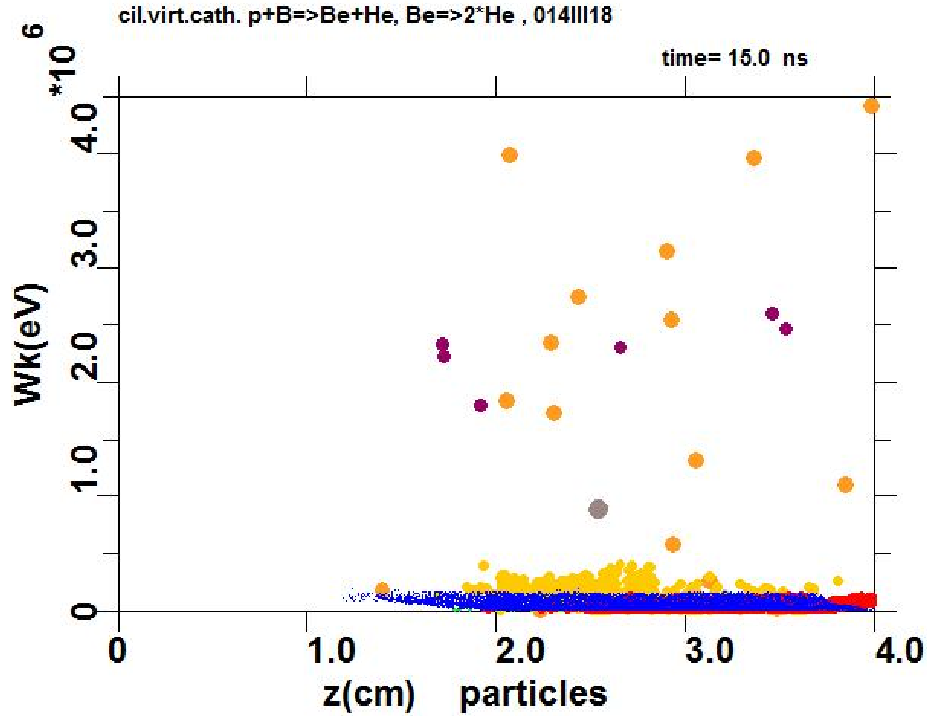

(a) The time histories of total number of particles throughout the first 20 ns (b - electrons of beam, g- anode plasma density, r- protons, y- boron ions) **(b**) the energy of electrons of beam along the radius: increasing energy before anode "grid", the decreasing of e-beam energy until virtual cathode formation at r < 0.1 cm

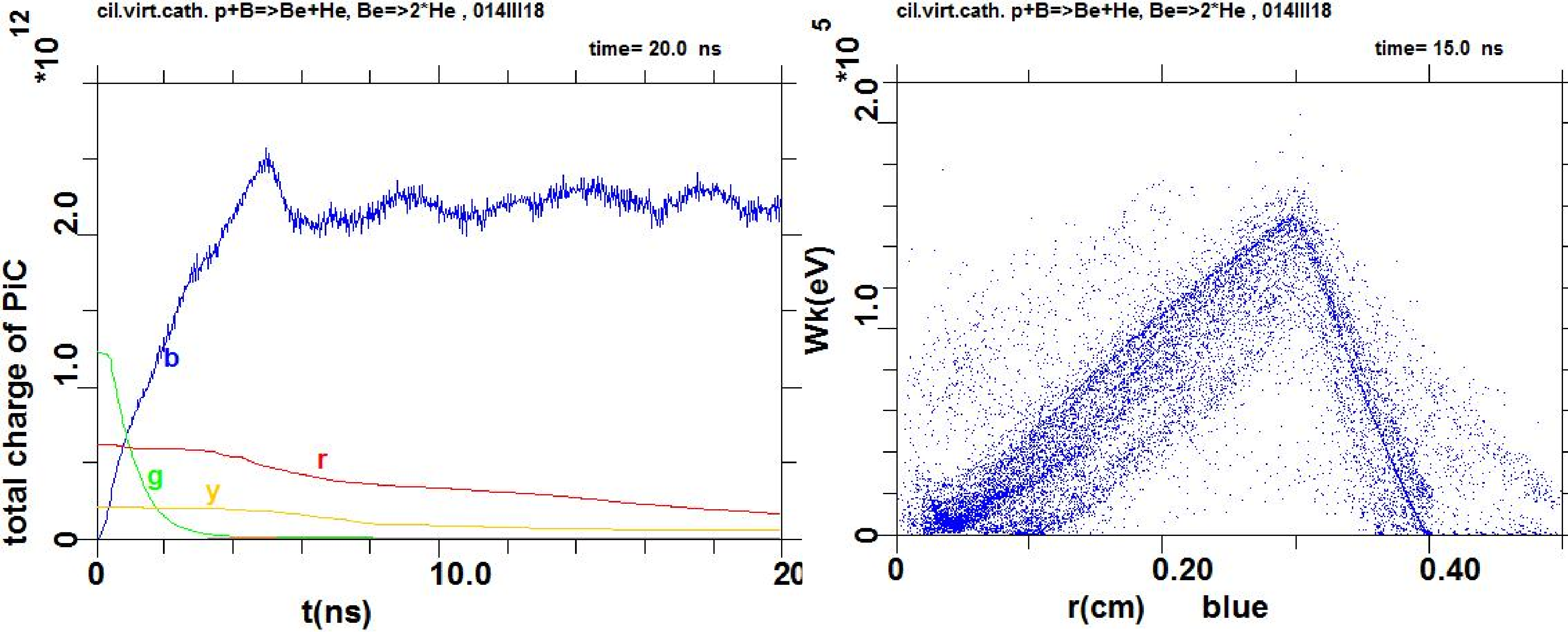

(a) an example of primary alpha-particle yield from unstable Carbon and **(a)** secondary alpha-particles yield from disintegration of $^{8}Be^{*}$.

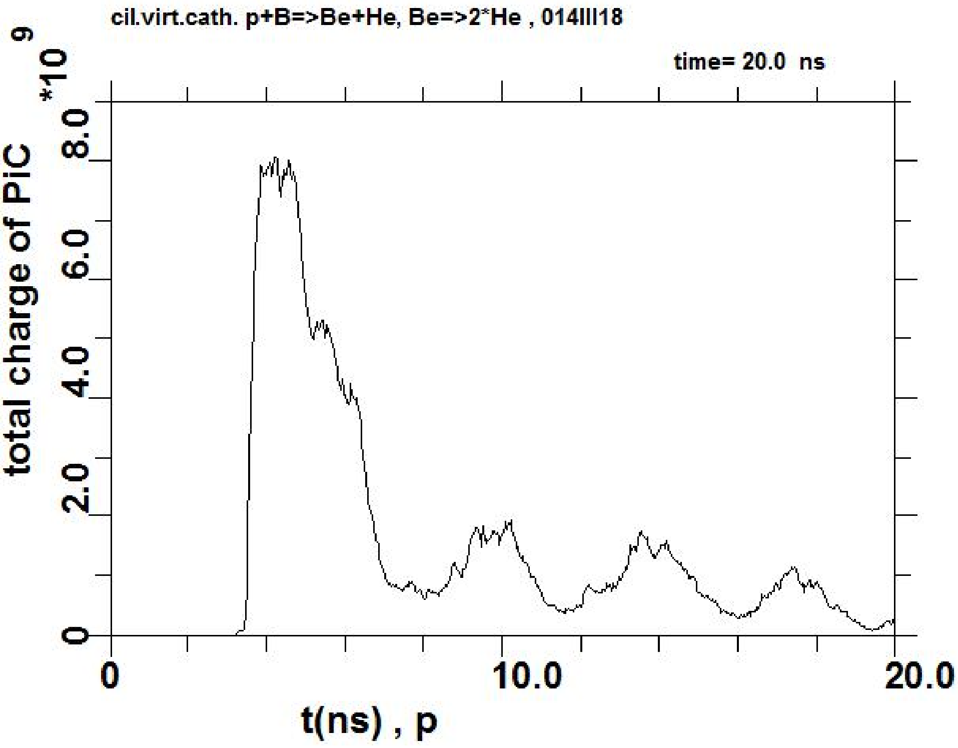

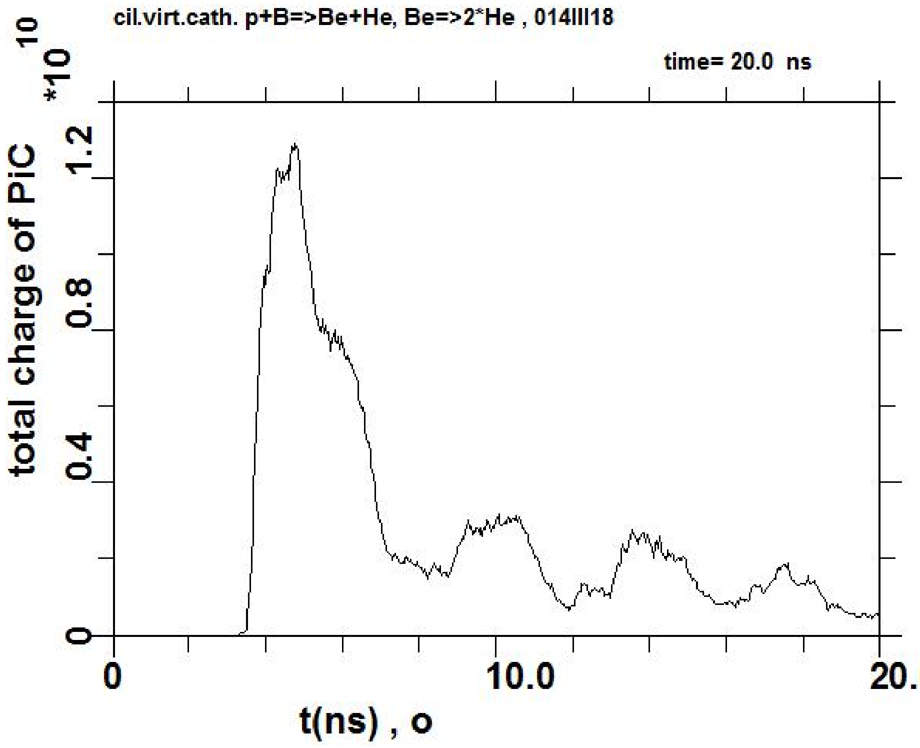

Мечта: Прямое преобразование энергии быстрых альфа-частиц в электричество (минуя тепловой цикл, трансформаторы и т.п.)
($p + {}^{11}B = 3\ He4 + 8{,}68$ МэВ) (from the book W Flint 2008)

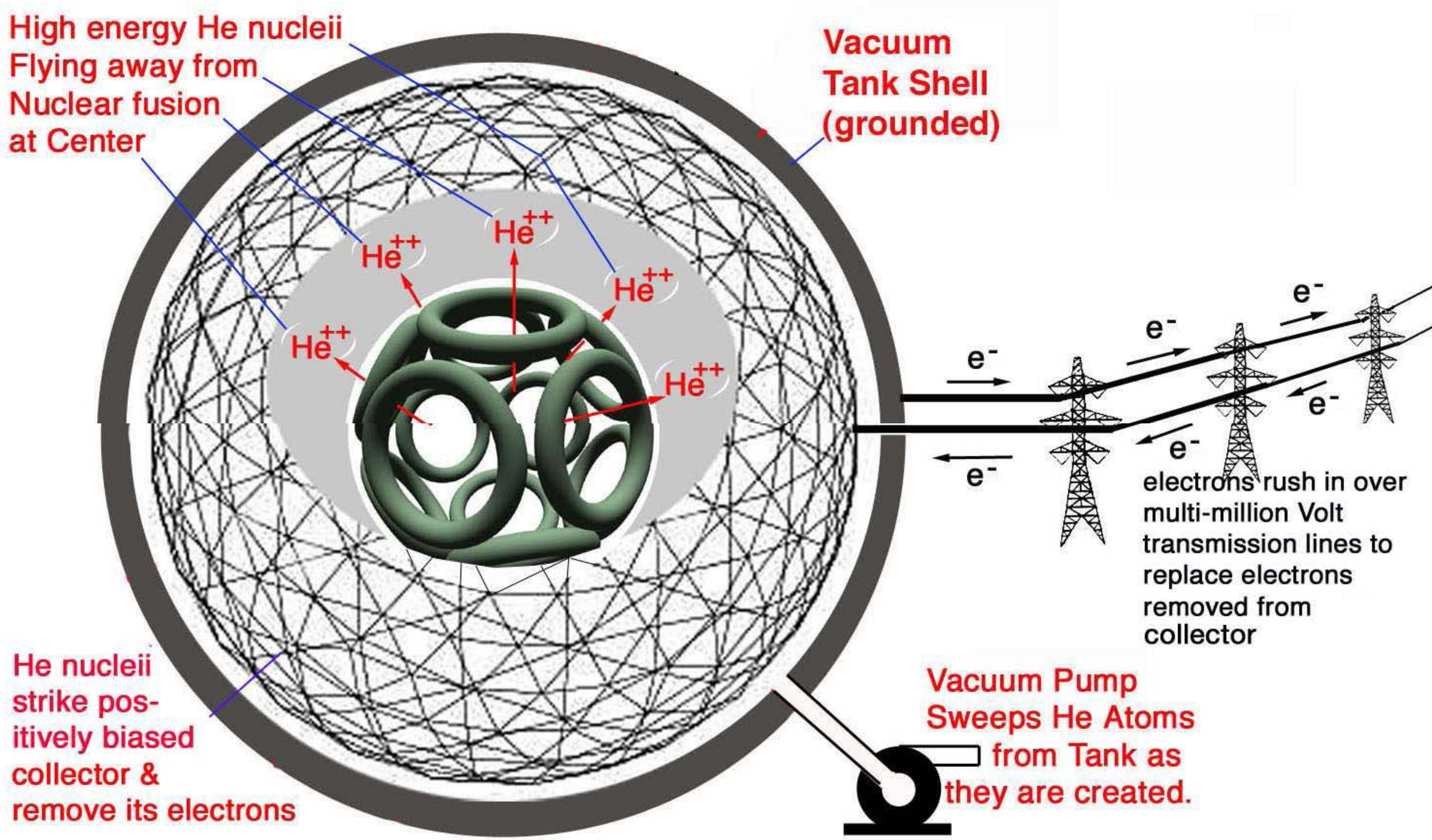

Concluding remarks

- Earlier, the estimated value of the neutron yield from DD microfusion demonstrated at interelectrode space is variable and amounts to ~ 10^5- $10^7/4\pi$ per shot under ≈ 1 J of total energy stored to create all processes.

- Simulations have clarified the physics of DD fusion at NVD: collective ions acceleration at the deep quasistationary potential well of virtual cathode followed by head-on collisional syntheses. The work extends available activity on IEC, especially, well-defined ions oscillations (like POPS, LANL)) and demonstrates the high values of fusion power density ($\sim \varphi^2 \boldsymbol{\theta}^2 / r^4_{ВК}$) at miniature-size discharge.

- Current PIC simulation illustrates the possibility of the using KARAT code to describe and optimize the p+ B^{11} synthesis conditions in the potential well of VC in the future experiments. The results presented allow us to be oriented in the processes of possible burning proton- boron in NVD, but they are still rather far from the optimum.

Kurilenkov Yu. K, Tarakahov and Gus'kov S.Yu. JPCS v 774 2016

Remark plus

1) Lowson criteria (1957 Proc. Phys. Soc. B70)

$n_i\,\tau \geq 10^{14} cm^{-3} c$ T ~ 10 keV

plasma in equilibrium

Q ≥ 2 → plasma ignition

2) IECF → non-equilibrium, not-ignited plasma

“wet wood burning” (J.Lowson view)

analogue of Lawson’s criterion for IEC with oscillations

$\tau\nu^2 > 3\times10^{13}\ s^{-1}$ 100MHz → $\tau \geq 1$ ms

(Guskov, Kurilenkov JPCS v 774, 2016)

Спасибо за внимание !

Polywell Fusion

<u>Combines two good ideas in fusion research</u>: Bussard (1985)

a) **Electrostatic fusion**: High energy electron beams form a potential well, which accelerates and confines ions

b) **High β magnetic cusp**: High energy electron confinement in high β cusp: Bussard termed this as "wiffle-ball" (WB).

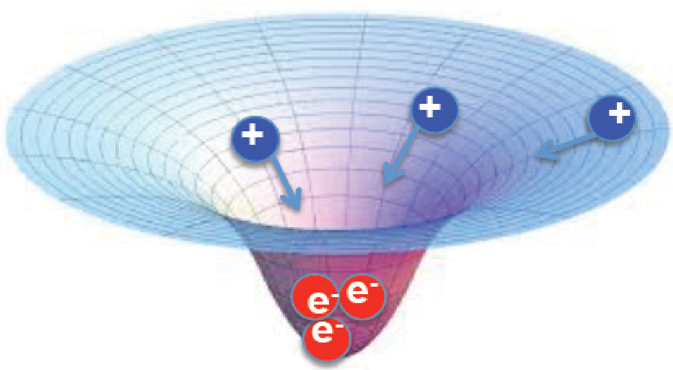

Potential Well: ion heating &confinement

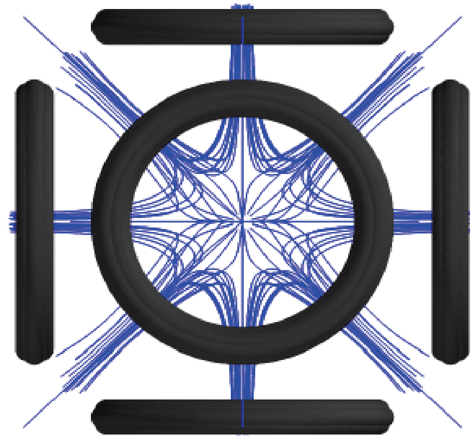

Polyhedral coil cusp: electron confinement

Plasma pressure/B-field pressure (β) ~ 1

Polywell realisations

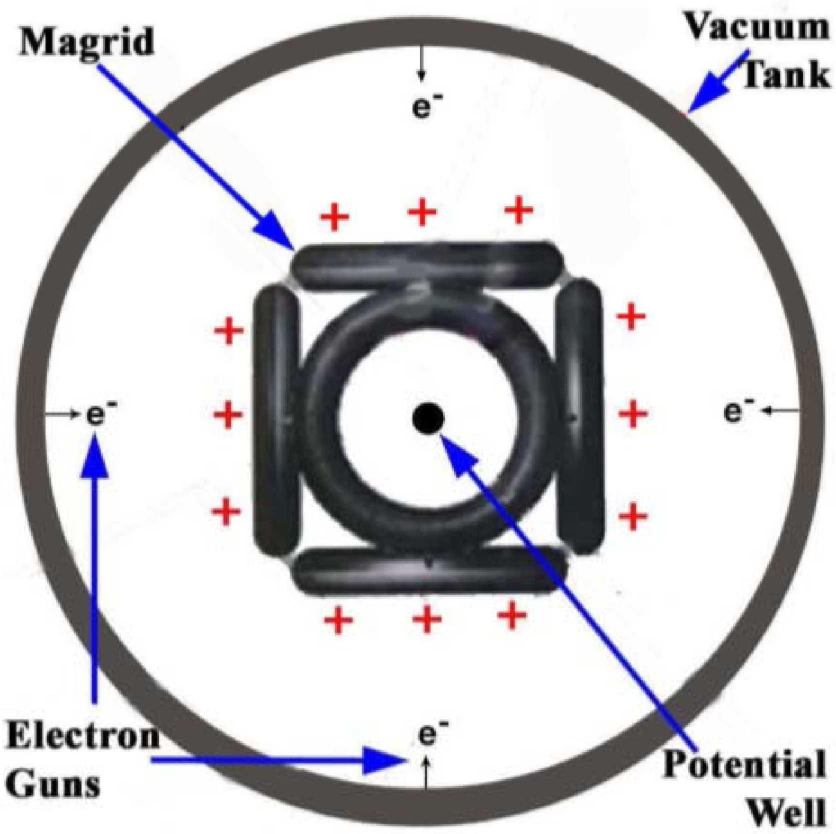

DD neutron yield estimations

- Our experiment: total yield $N_{neutrons} \sim 10^5 - 10^7 / 4\pi$

  (under assumption that yield is isotropic one !)

channels for fusion: beam-beam, beam –neutrals, beam- clusters, beam- anode

- Through POPS physics: $N_{neutrons} = ½ \, n_i^{\,2} <\sigma v> V\, t$

Poisson's Equation $n_e \sim \nabla^2 \phi \sim \phi/a^2$

Fusion power density : $p = 1/2\, \varphi^2\, \theta^2\, f^2 <\sigma v> /a^4 \sim \theta^2 \varphi^2 / r^4_{BK}$ (per one period of oscillation) , $\theta = r_{max} / r_{min}$ $f = n_i / n_e$

Total power p V : $P_{fusion} = 3\, \theta^2 f^2 \varphi^2 < \sigma \upsilon > /2\pi\, r_{VC}$

for cylindrical geometry $P_{fusion} \sim \pi a^2 L\, p \sim 1/a^2 \sim \theta^2 \varphi^2 / r^2_{BK}$

Fusion power at our discharge with IECF: POPS

$P_{fusion} \sim \theta^{\,2} f^2 \varphi^2 < \sigma v > L / 2\pi\, r^2_{VC}$, $N_{neutrons} \sim 10^5$ per collapse

Multi-Oscillation Burning (Guskov, Kurilenkov JPCS v 774, 2016)

Thermonuclear gain: $G \propto n_i \langle \sigma u_i \rangle \frac{\varepsilon_r}{\varepsilon} N_{ocs} t_{burn} = n_i \langle \sigma u_i \rangle \frac{\varepsilon_r}{\varepsilon} \tau \frac{t_{burn}}{t_{osc}} = n_i \langle \sigma u_i \rangle \frac{\varepsilon_r}{\varepsilon} \frac{\tau}{\theta}$

Oscillation period

$$t_{osc} = \frac{2 r_{grid}}{u_i} \approx 1.25 \cdot 10^{-7} \frac{r_{grid}(cm)}{\Phi_{kV}^{1/2}}$$

Burn duratuin in a single oscillation

$$t_{burn} = \frac{t_{osc}}{\theta} = \frac{1}{\nu \theta}, \qquad \theta = \frac{r_{grip}}{r_{burn}}$$

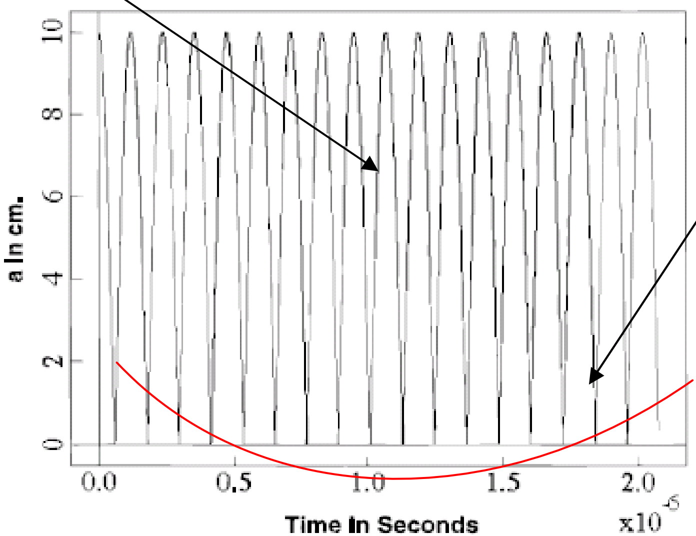

Fig. 4. Plasma radius versus time.

Lawson criterion - G>2 (Φ=100 kV)

$$\tau \nu^2 > 10^{13}$$

100 MHz (r_{grid} = 0.8 cm) $\Rightarrow$ $\tau > 1$ ms

Total burn time: $t = N_{osc} t_{burn} \equiv \frac{\tau}{\theta}$

$\tau, \quad \theta$

TOF registration of DD neutrons with energy 2,45 MeV
(delayed as ~ 46,6 ns/ m) (PM1 - 70 см, PM2 - 120 см)
Dynamics of x-rays and neutrons yields in the **regime 3** (tri 004).

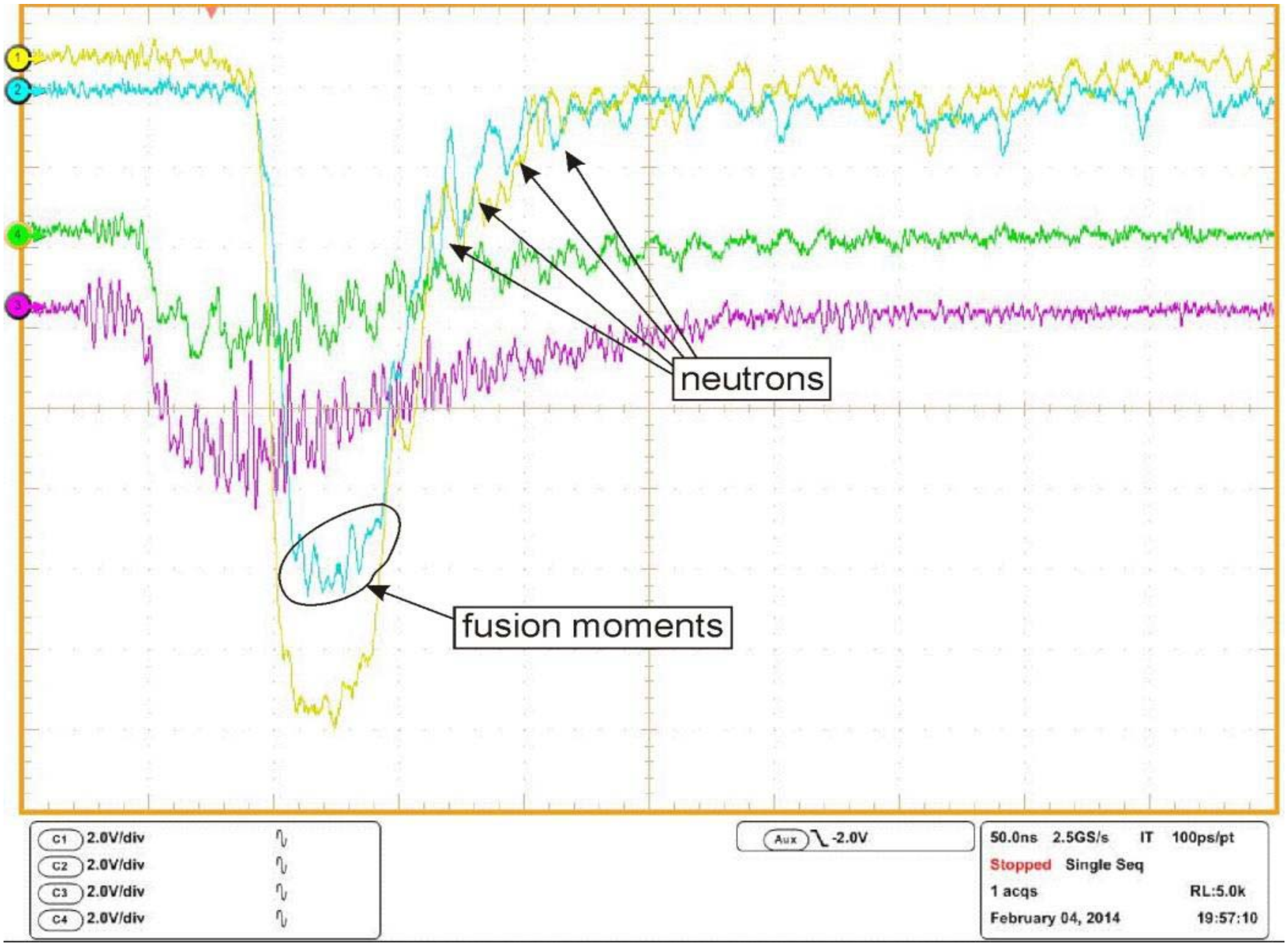

Next shot. Strong hard x-rays release (chs 1-4).

- 1018D7

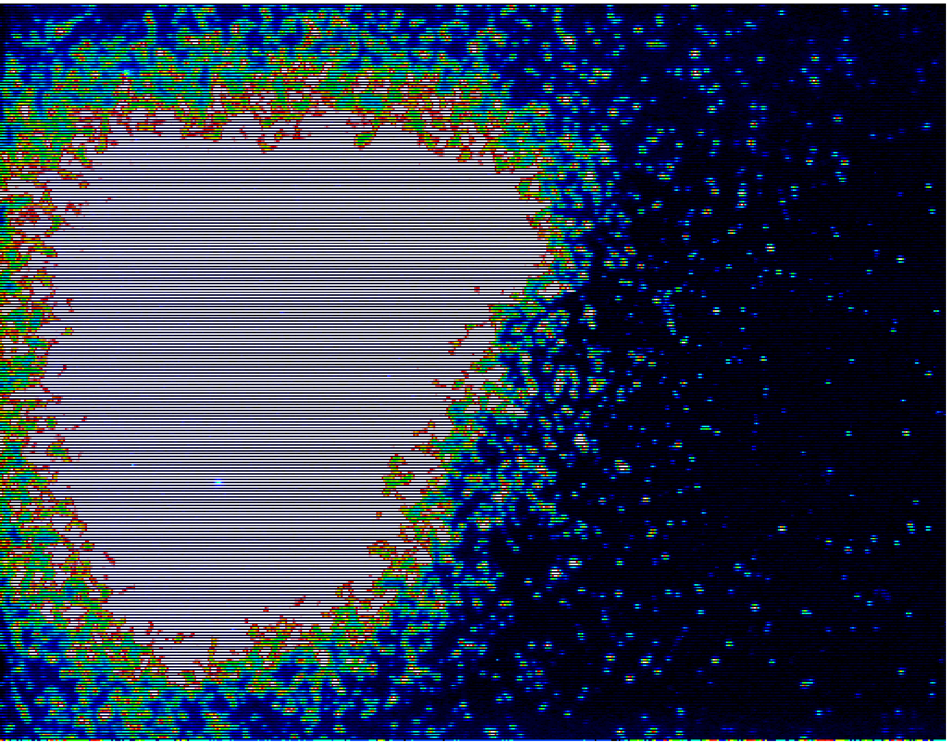

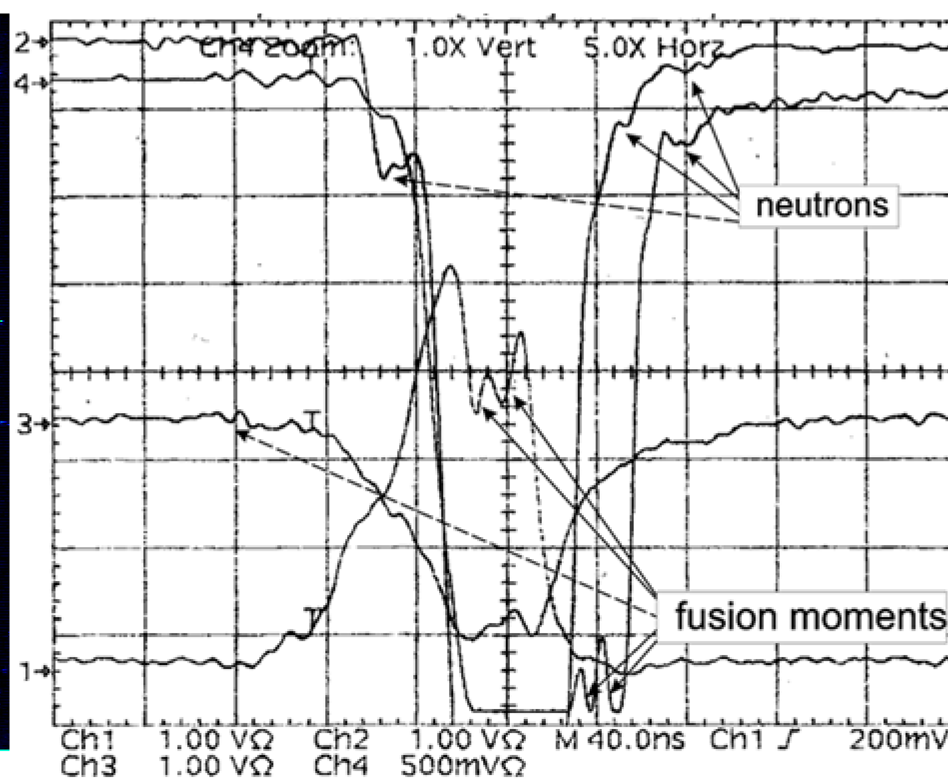

DD synthesis

D + D = T (tritium 1.01 MeV) + P (3.02MeV)

D + D = He3 (.82 MeV) + N (2.45 MeV)

neutrons signature - 46, 6 nsec/m time-of-flight (TOF) delayed signal

T – 13.8%
P - 41.4%
He3 – 11.2%
N – 33.6%

Установка ИЭУ со сферическим полым катодом и сферическим анодом (K.Yoshikawa et al. , 2003)

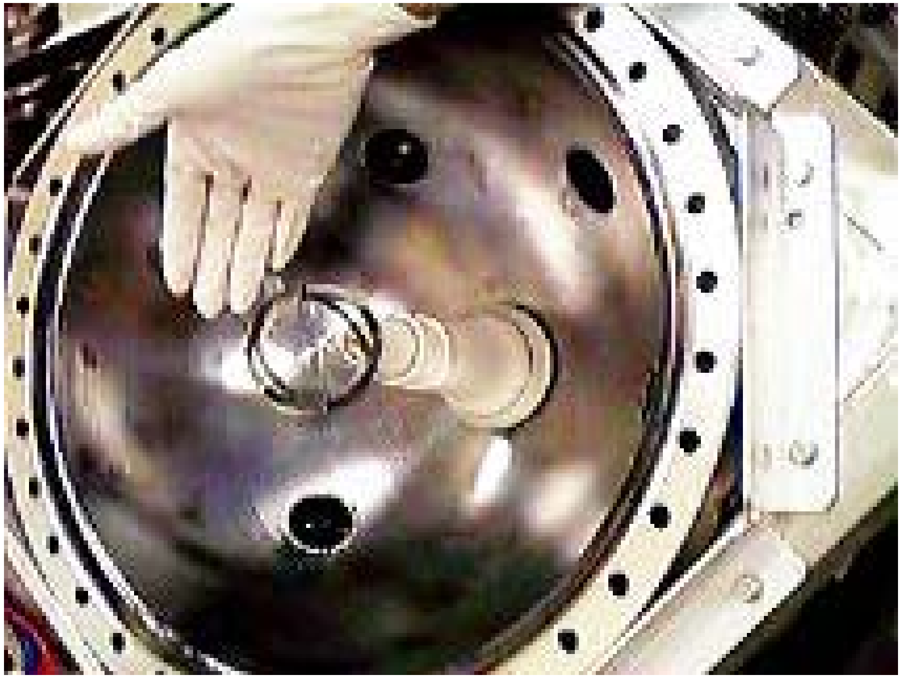

An IEC plasma within the hollow cathode K.Yoshikawa et al. (2006)

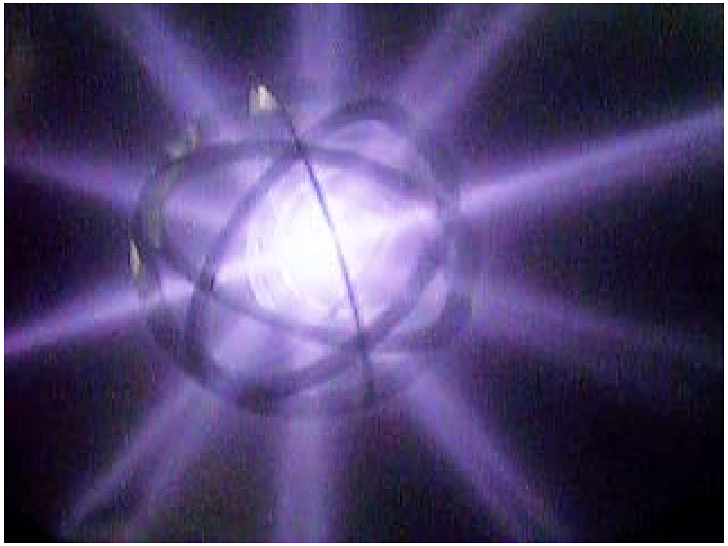

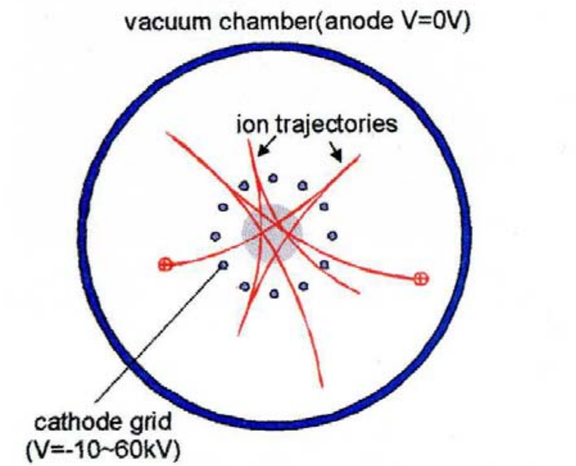

1. An IEC configuration with a gridded cathode.

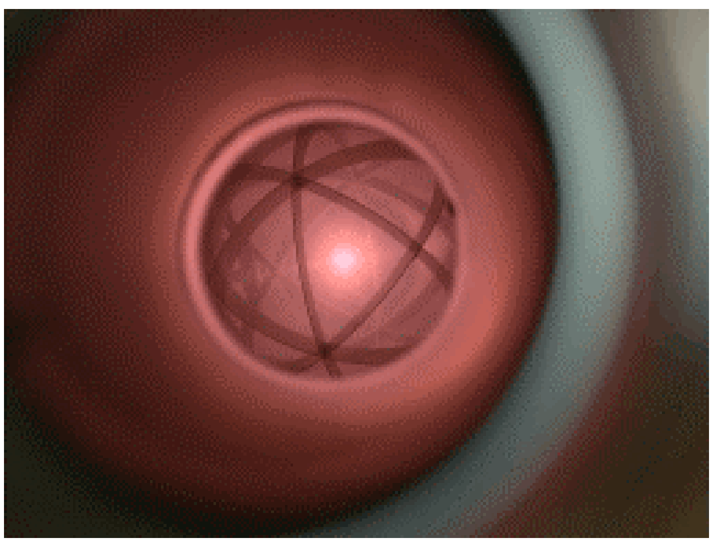

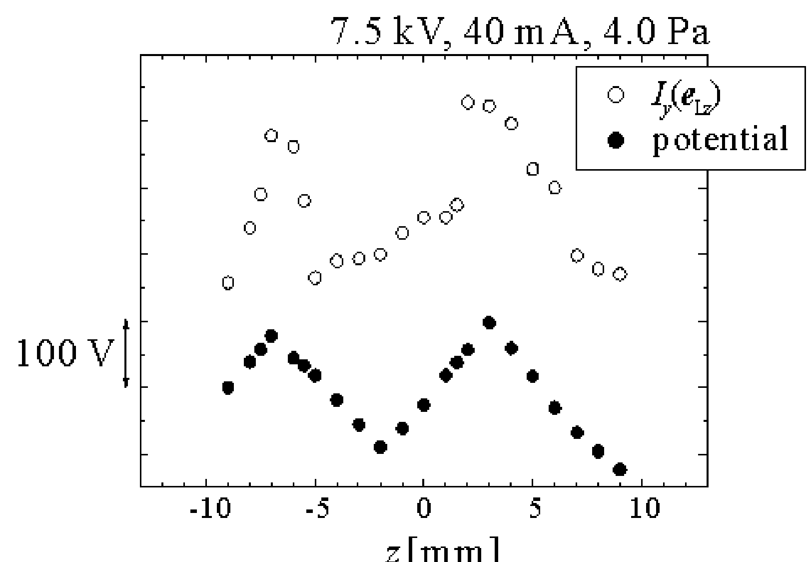

University of Wisconsin: Vacuum Chamber and Cathode Design Attempt to Minimize Field Perturbations

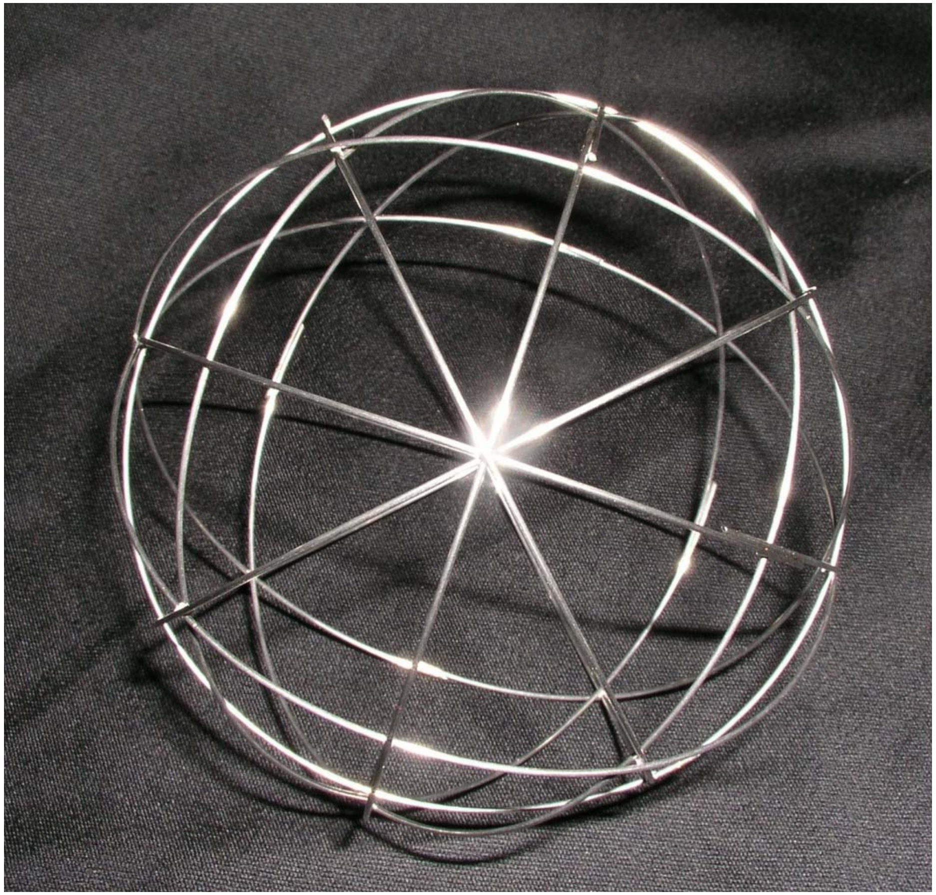

Оценка выхода DD нейтронов

Наш эксперимент: полный выход $\sim 10^5 - 10^7 / 4\pi$

(в приближении изотропного выхода)

Возможные каналы синтеза: ион-ион, ион –нейтрал, ион - кластер, ион- анод

POPS для канала ион-ион: $N_{neutrons} = \frac{1}{2}\, n_i^{\mathbf{2}} <\sigma v> V\, t$

Poisson's Equation $n_e \sim \nabla^2 \phi \sim \phi/a^2$

Плотность мощности синтеза:

$p = 1/2\, \boldsymbol{\varphi^2 \theta}^2\, f^2 <\sigma v>/a^4 \boldsymbol{\sim \theta}^2 \boldsymbol{\varphi^2 / r^4_{ВК}}$ (на один «коллапс» ионов)

$\boldsymbol{\theta = r_{max} / r_{min}}$ $f = n_i / n_e$

Полная мощность p V : $\mathbf{P}_{\mathbf{fusion}} = 3\, \theta^2 f^2 \boldsymbol{\varphi^2 < \sigma \upsilon > / 2\pi\, r_{VC}}$

Полная мощность (для цилиндричесой геометрии) :

$\mathbf{P}_{\mathbf{fusion}} \boldsymbol{\sim \theta}^2 f^2 \boldsymbol{\varphi^2 < \sigma V > L / 2\pi\, r^2_{ВК}}$, $N_{neutrons} \sim 10^5$

Scaling : high fusion power density (~ φ^2 / r^4_{VC}) at miniature cylindrical discharge (total power ~ φ^2 / r^2_{VC}). Is it possible to increase fusion efficiency at $r_{VC} \rightarrow 0$, and to get Q > 1 under decreasing of r_{VC} value up to micro- and nano sizes ?

Композитный материал: углеродные нанотрубки в Pd матрице (с электроосаждением тонких слоёв Pd)

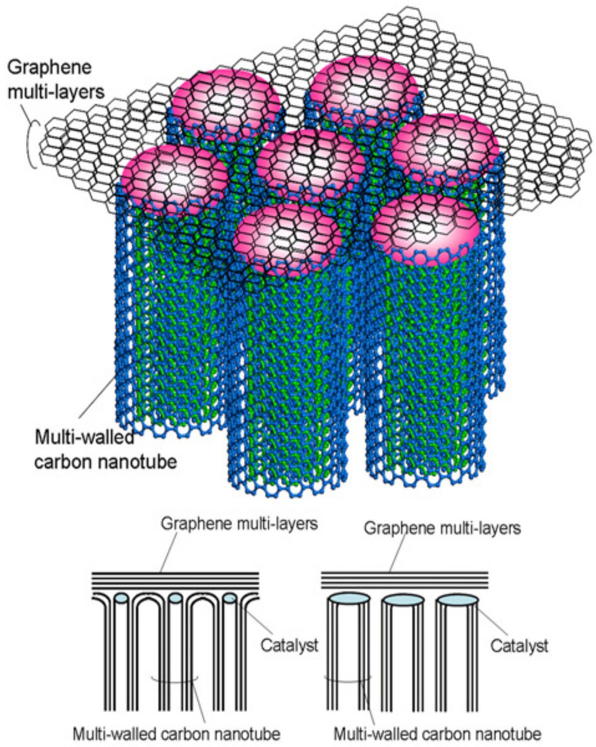

Поверхность отожжённой Pd фольги: наличие пор и каналов микронных размеров(~ 10^5 на см^2)

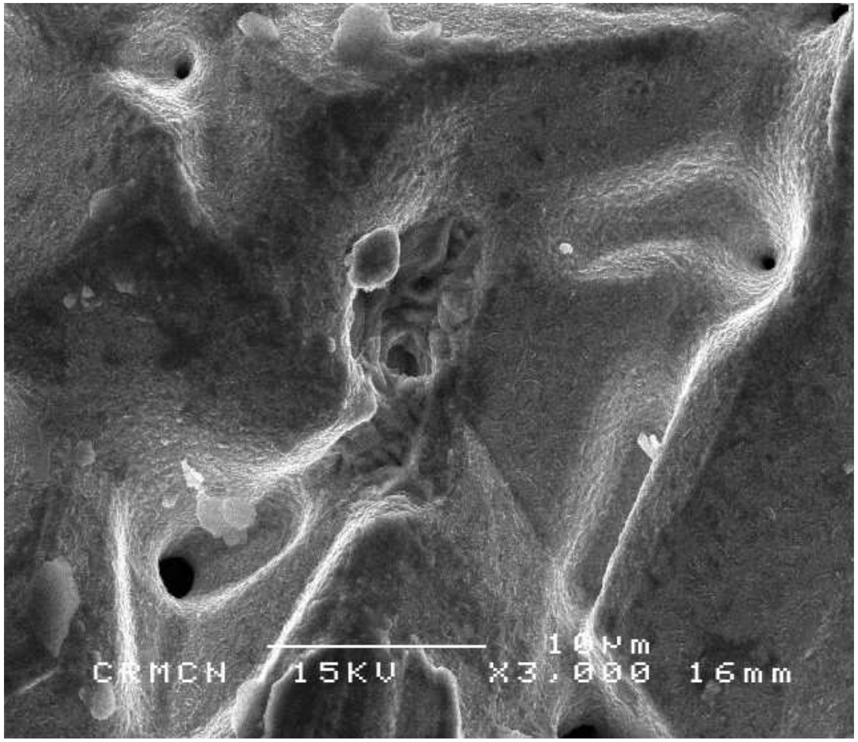

Neutron yield is observed when virtual cathode and potential well are forming along the pulse (solid arrow) as well as at very initial stage of discharge (dotted) –- double DD synthesis

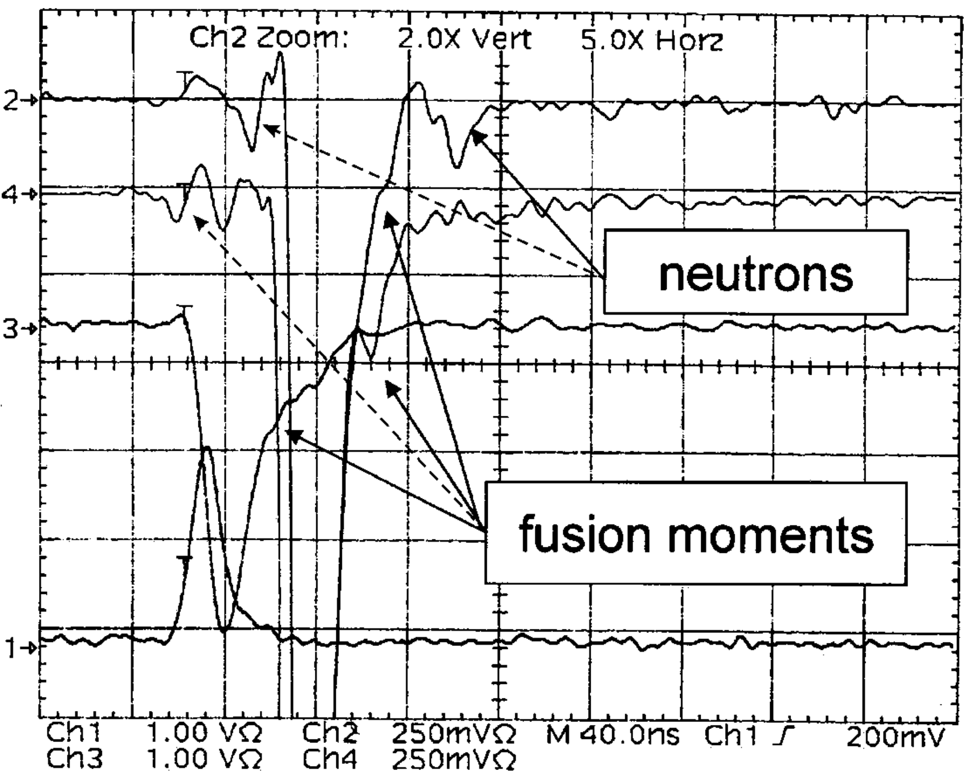

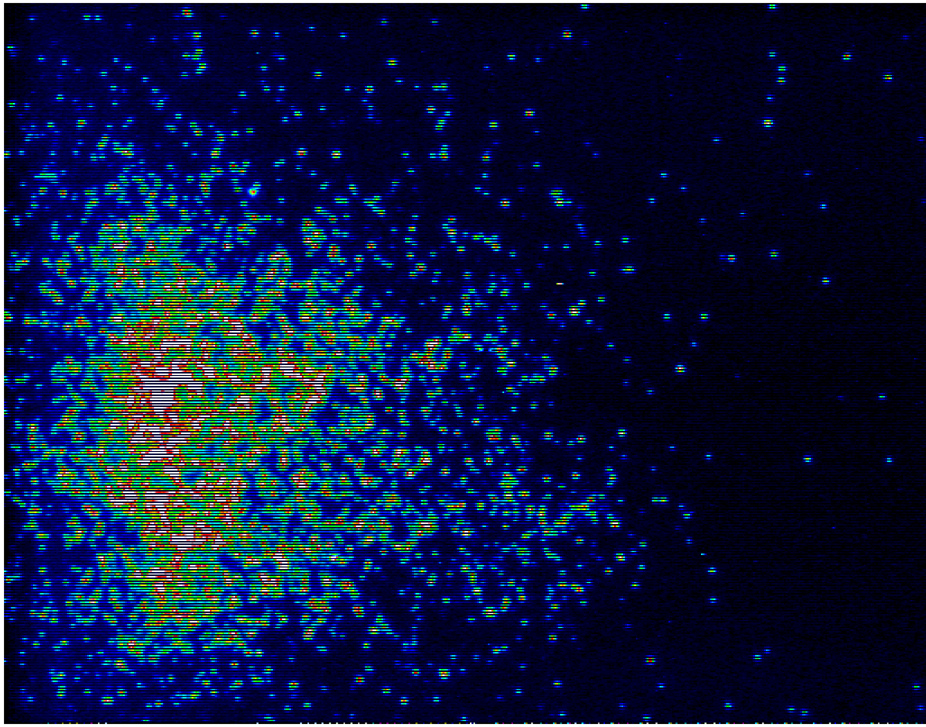

a) Regime 5 , where the piece of paraffin have been located between plasma source and photomultipliers PM4, PM2 (“triple “ anode)
b) Regime 6 for anode with 12 Pd tubes (“coronal’ anode). Neutron signal from initial stage of discharge do prevail.

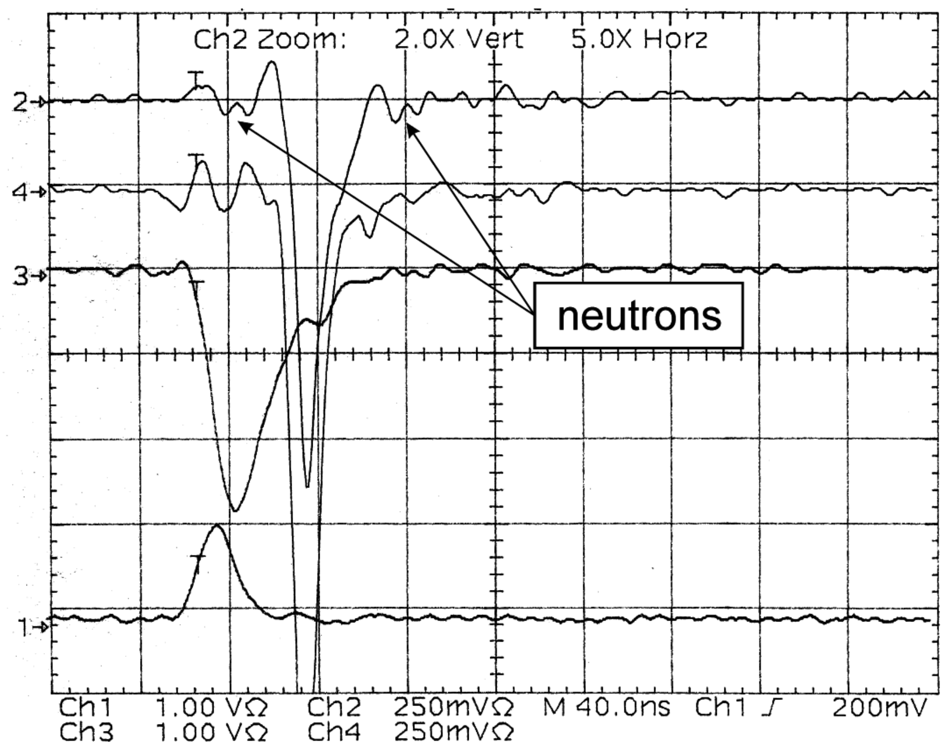

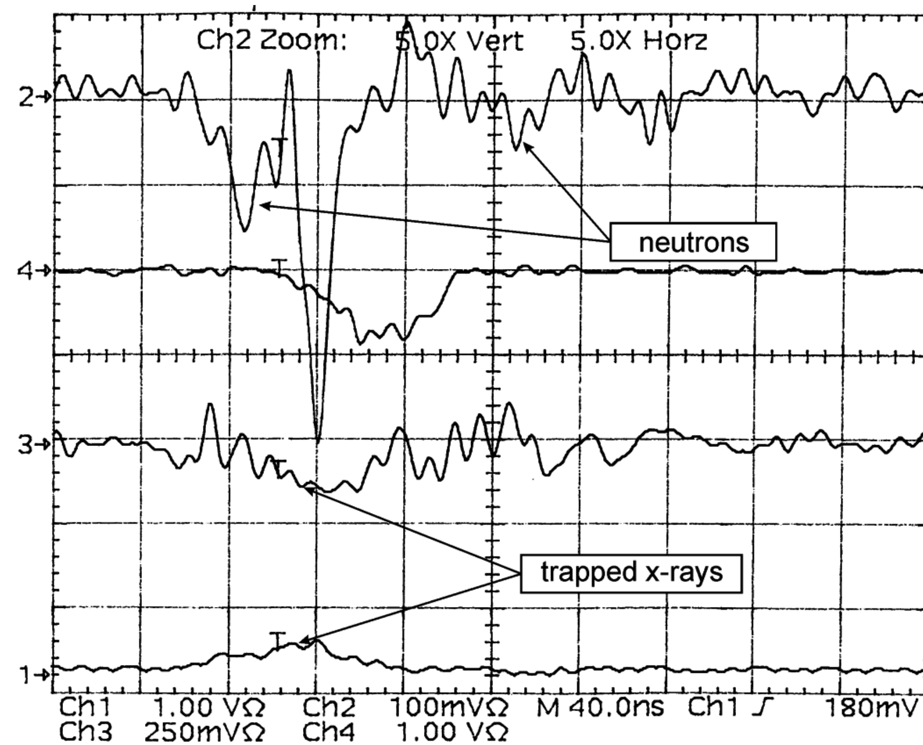

Oscillograms and CCD image of the shot with “coronal” anode (12 Pd tubes), where neutrons from initial stage do prevail also (0518D7).
(anode surface partially represented on CCD as well)

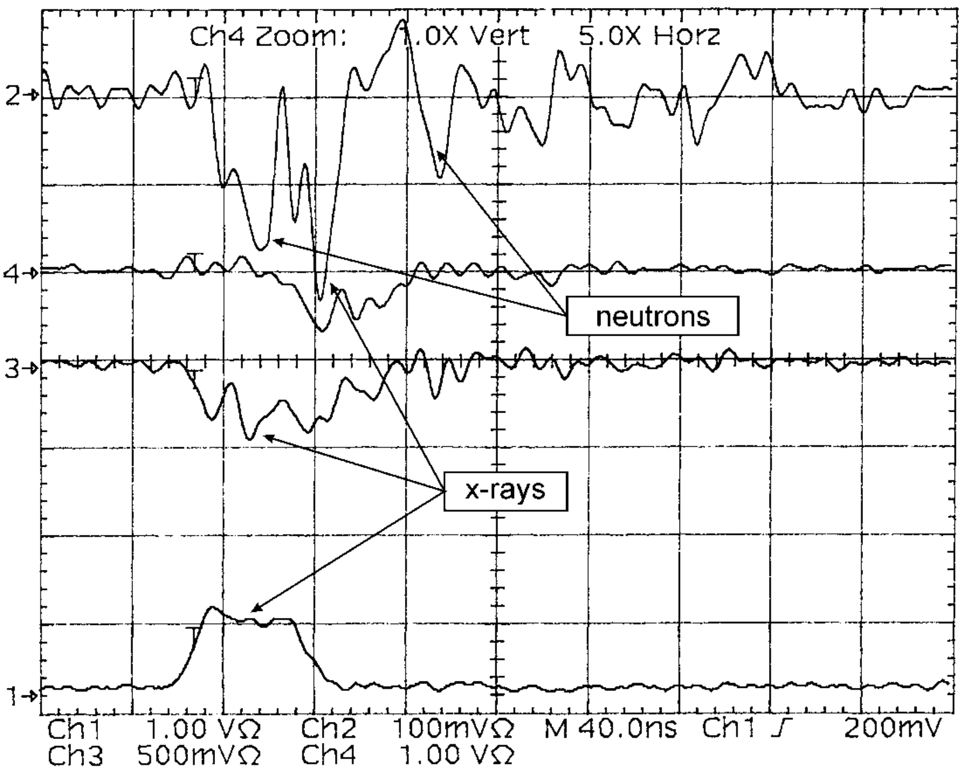

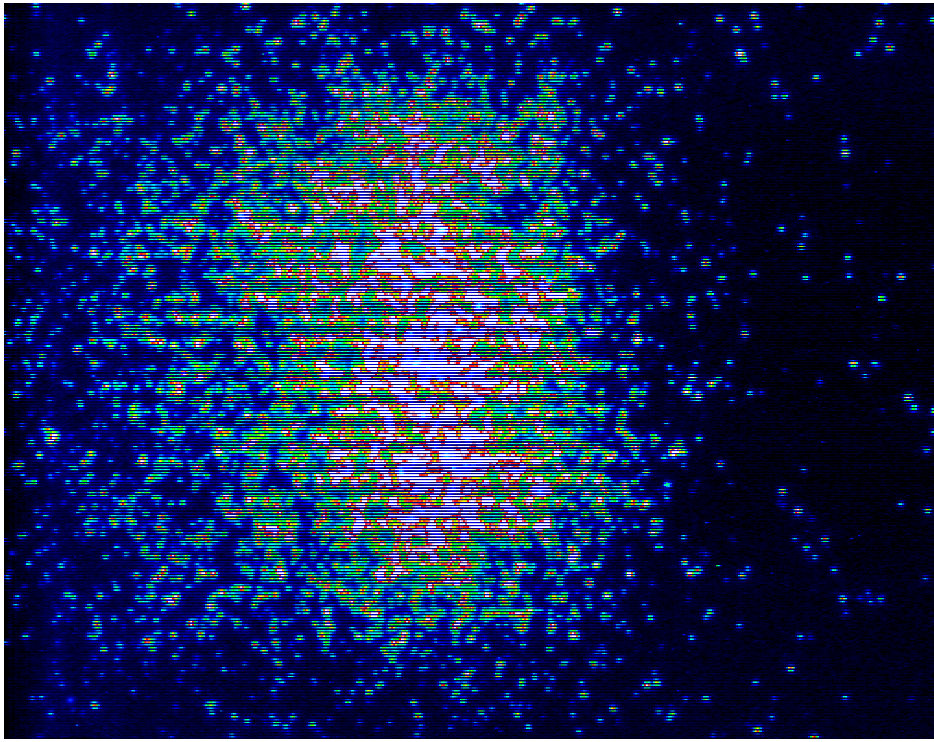

a) surface morphology of deuterium-loaded Pd anode (fragment 1, “coronal” anode; particular part of Pd tube, which is close to Cu head-end of anode); scale 15 *μm.*

b) Deuterium-loaded Pd anode surface morphology (fragment from “coronal” anode corresponds approximately to central part of bright area on previous CCD image; scale 15 *μm).*

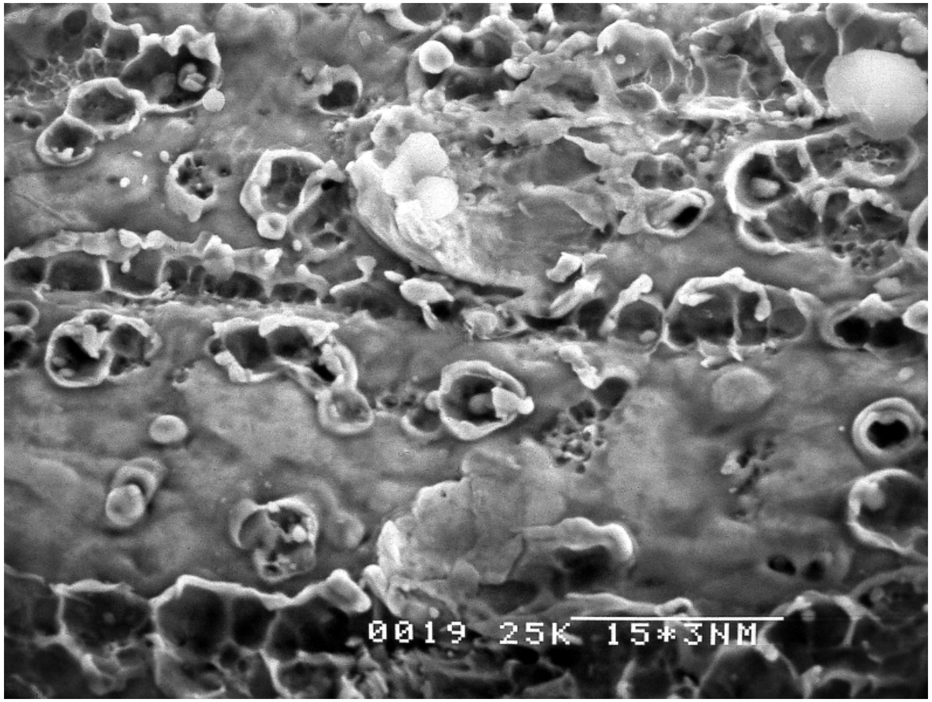

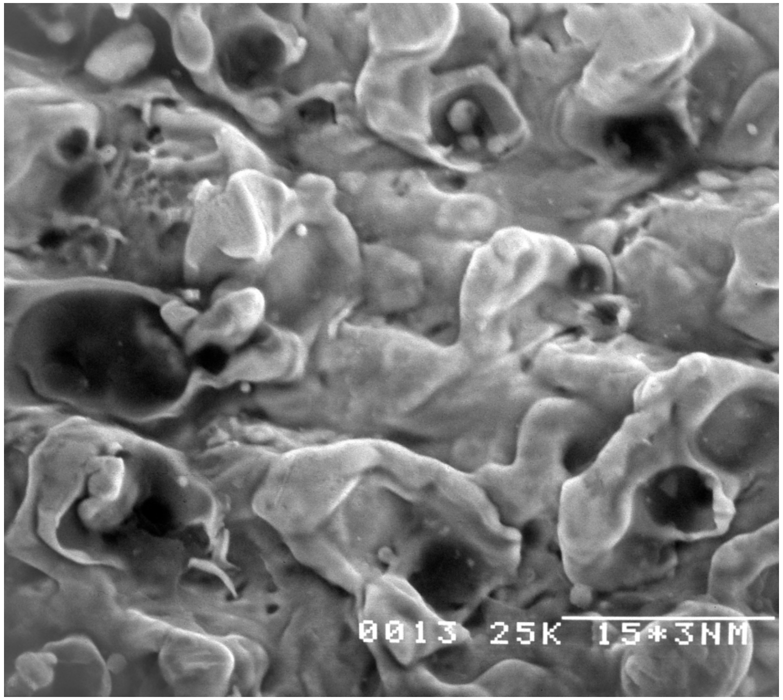

Deuterium-loaded Pd surface as *integrated multichannel microreactor* under e-beam action (?)

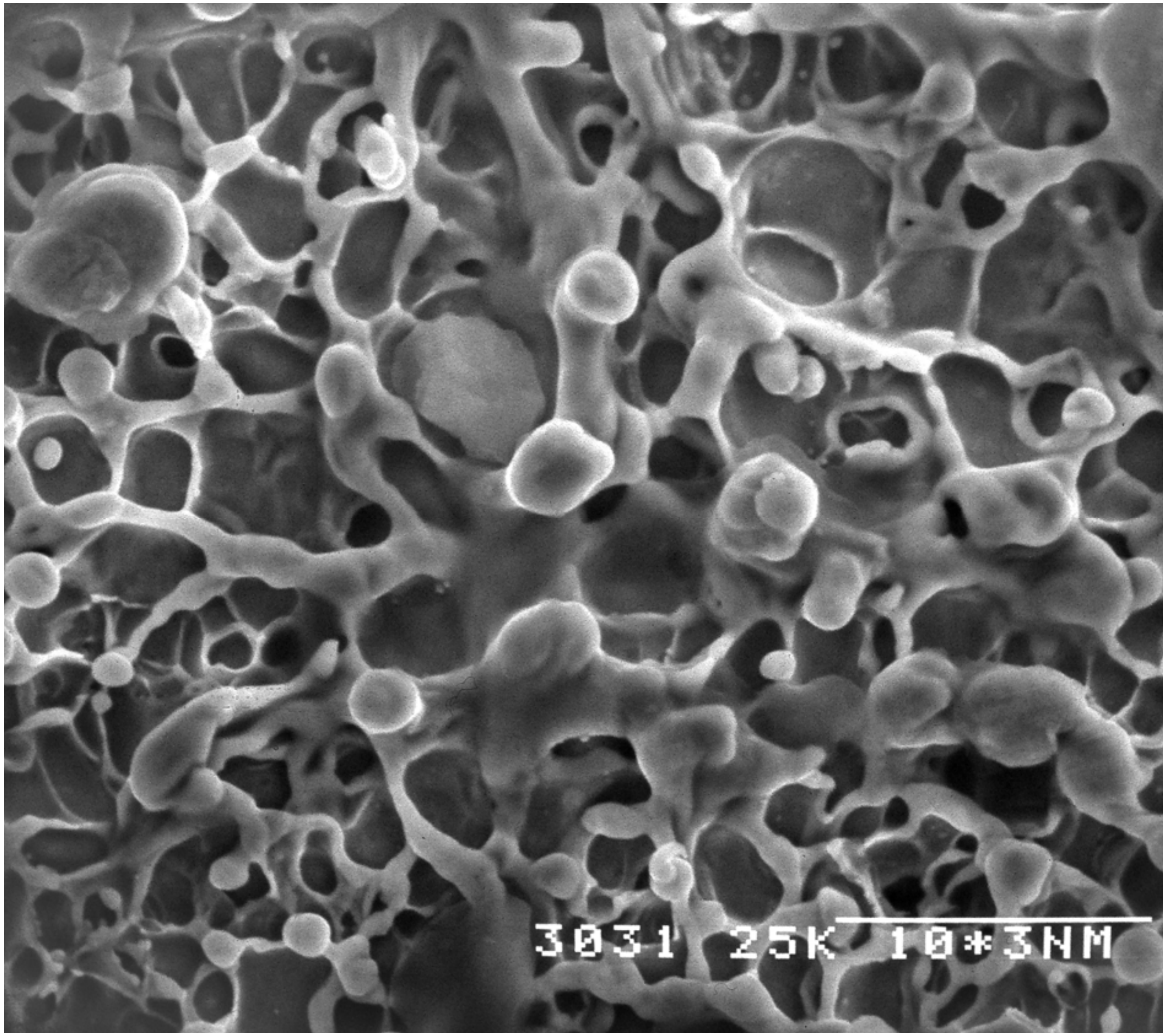

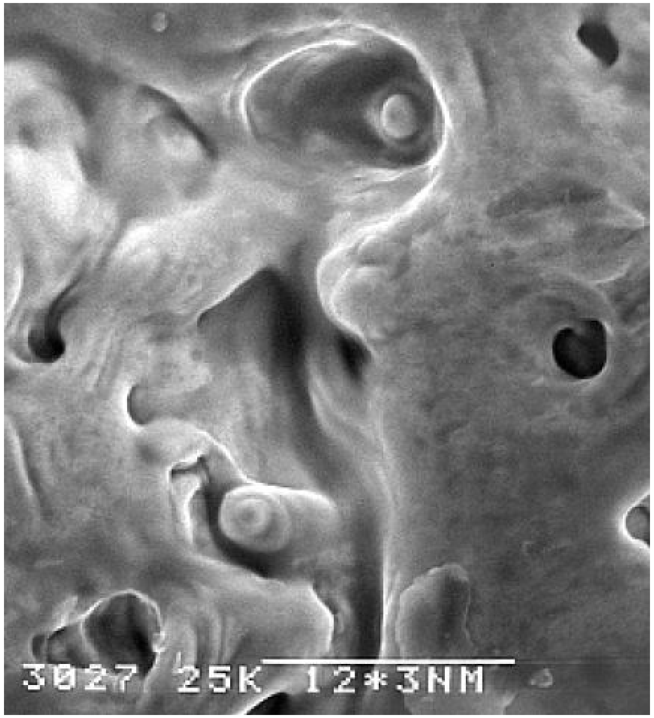
3027 25K 12*3NM

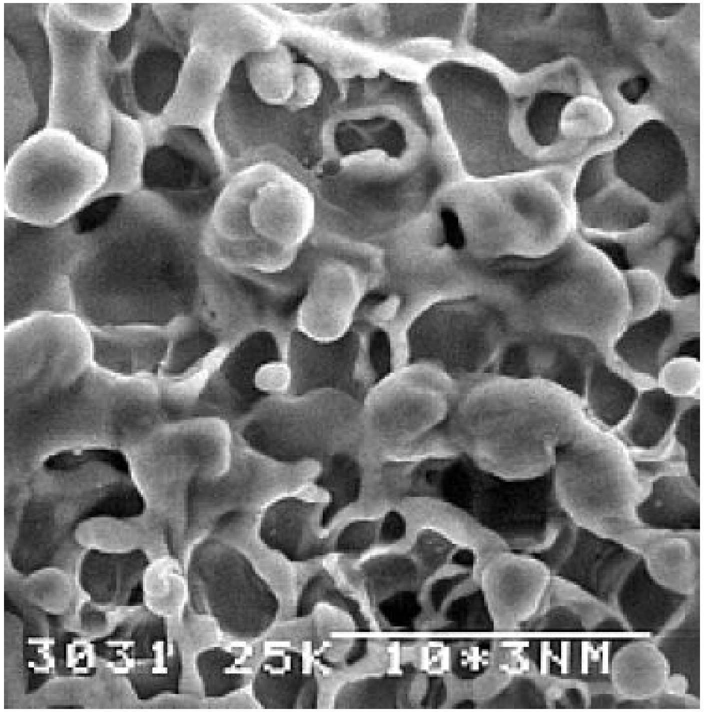
3031 25K 10*3NM

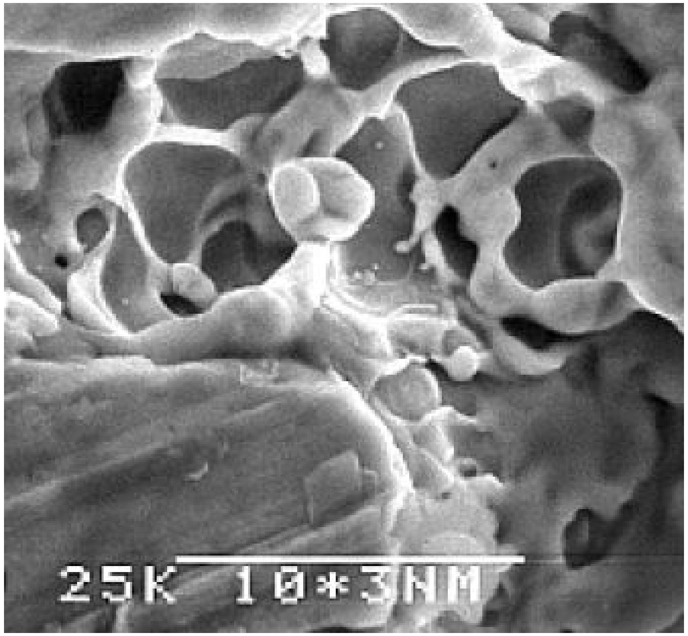
25K 10*3NM

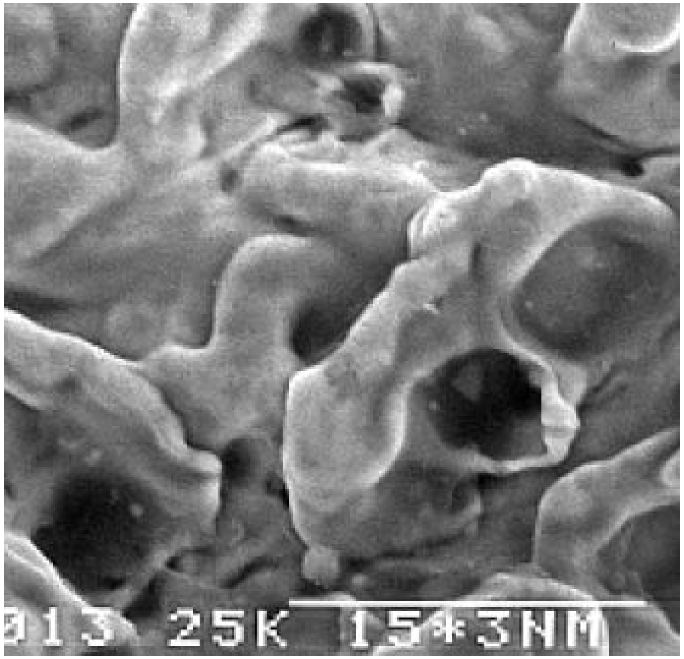
013 25K 15*3NM

PHYSICAL REVIEW B **72**, 212507 (2005)

Transport and magnetic anomalies below 70 K in a hydrogen-cycled Pd foil with a thermally grown oxide

Andrei Lipson,[1,2] Brent J. Heuser,[1,*] Carlos Castano,[1] George Miley,[1] Boris Lyakhov,[2] and Alexander Mitin[3]
[1]*University of Illinois, Department of Nuclear, Plasma, and Radiological Engineering, Urbana, Illinois, 61801 USA*
[2]*Institute of Physical Chemistry, Russian Academy of Sciences, Moscow, 119915 Russia*
[3]*P. L. Kapitza Institute for Physical Problems, Russian Academy of Sciences, Moscow, 119334 Russia*
(Received 27 May 2005; published 13 December 2005)

Electron transport and magnetic properties have been studied in a deformed 12.5-μm-thick Pd foil with a thermally-grown oxide and a low residual concentration of hydrogen. This foil was deformed by cycling across the Pd hydride miscibility gap and the residual hydrogen was trapped at dislocation cores. Anomalies of both resistance and magnetic susceptibility have been observed below 70 K, indicating the appearance of excess conductivity and a diamagnetic response that we interpret in terms of filamentary superconductivity. These anomalies are attributed to a condensed hydrogen-rich phase at dislocation cores near the Pd-Pd oxide interface.

DOI: 10.1103/PhysRevB.72.212507 PACS number(s): 74.10.+v, 72.15.−v, 61.72.Yx, 75.20.En

A.G. Lipson, B.J. Heuser, G.H. Miley et al. "Transport and Magnetic Anomalies in Hydrogen-Cycled Pd Foil with a Thermally-Grown Oxide Below 70 K", Phys. Rev. B 72, 082541 (2005)

Edge dislocation core in Pd with H_n-"metallic" hydrogen phase: Dislocation core is a nanotube with radius R_H = b (Burgers vector)

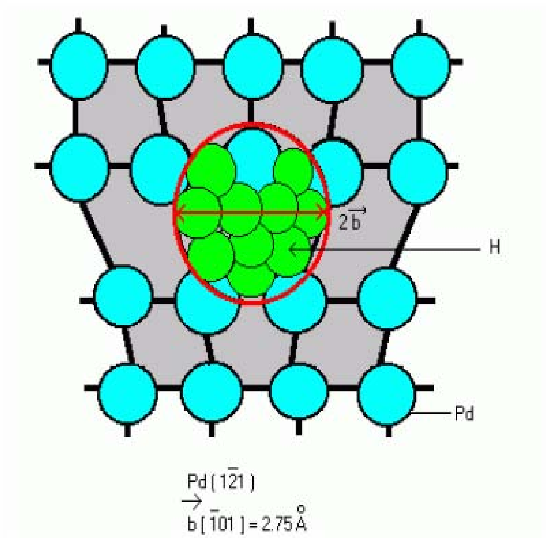

Lipson,I.Chernov et al 2009):

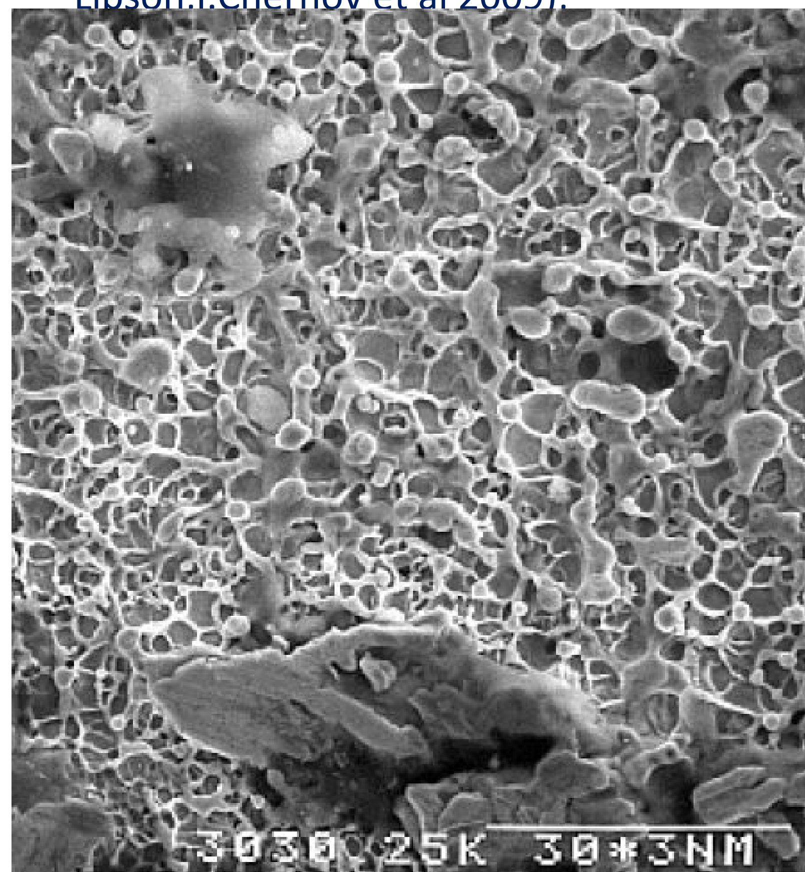

ЖЭТФ, 2011, том 139, вып. 6, стр. 1088–1097 © 2011

ЯДЕРНЫЕ РЕАКЦИИ В СИСТЕМАХ $Pd/PdO{:}D_x$ И $Ti/TiO_2{:}D_x$ ПРИ ИХ ВОЗБУЖДЕНИИ ИОНИЗИРУЮЩИМ ИЗЛУЧЕНИЕМ

И. П. Чернов[a], *А. С. Русецкий*[b*], *Д. Н. Краснов*[a], *В. В. Ларионов*[a], *Б. Ф. Ляхов*[c], *Е. И. Саунин*[c], *Ю. И. Тюрин*[a], *Ю. П. Черданцев*[a]

[a] *Национальный исследовательский Томский политехнический университет 634050, Томск, Россия*

[b] *Физический институт им. П. Н. Лебедева Российской академии наук 119991, Москва, Россия*

[c] *Институт физической химии и электрохимии им. А. Н. Фрумкина Российской академии наук 119991, Москва, Россия*

Поступила в редакцию 18 октября 2010 г.

Изучен выход продуктов ядерных реакций из палладия и титана, насыщенных дейтерием, в процессе воздействия электронного пучка и рентгеновских лучей. Детектирование заряженных частиц осуществлялось трековыми детекторами CR-39, не чувствительными к электронным помехам, электронам и рентгеновским квантам. Для идентификации типа и энергии частиц использовали одновременно три детектора, обернутые фольгами (Al и Cu) различной толщины. Статистически достоверно установлено, что воздействие электронов с энергией 30 кэВ и рентгеновских квантов инициирует в системах $Pd/PdO{:}D_x$ и $Ti/TiO_2{:}D_x$ синтез ядер дейтерия с выходом протонов с энергией 3 МэВ.

1. ВВЕДЕНИЕ

face Morphology 2009 Rome +++++.pdf - Adobe Reader
е Просмотр Документ Инструменты Окно Справка
15 / 22 81,5% Найти

Pore diameter distributions in Pd/PdO:Dx and Pd/PdO:Hx before and after electrolysis

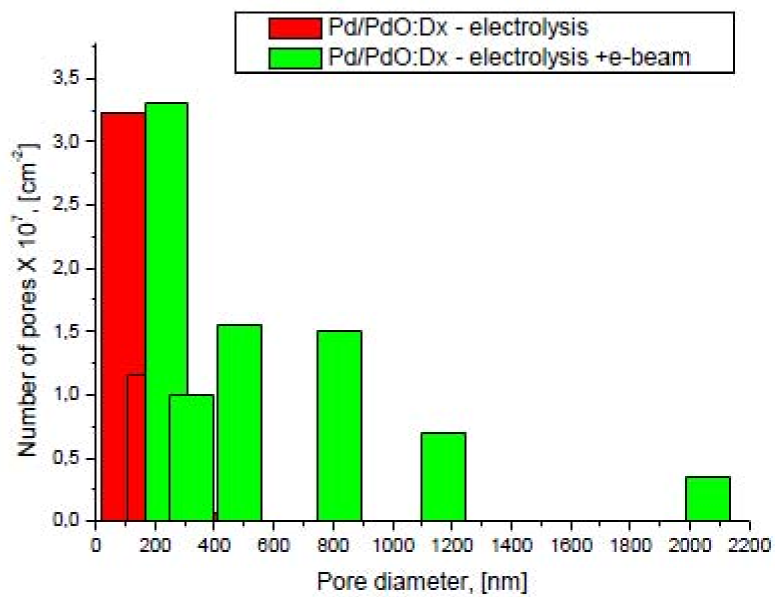

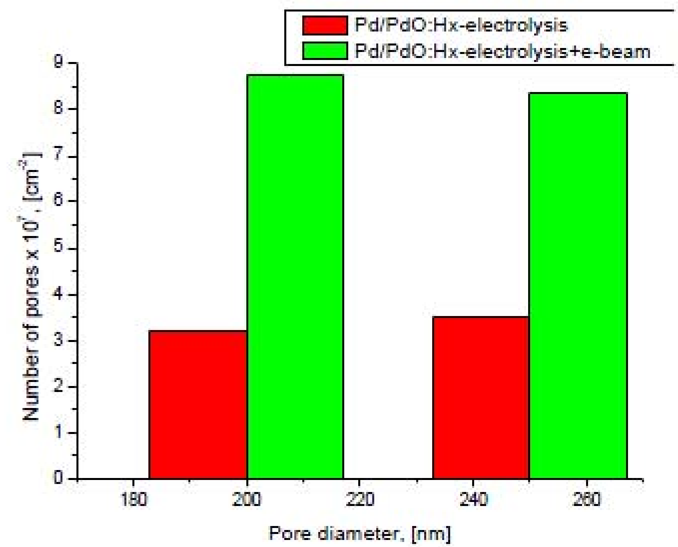

A. Lipson et al, ICCF-15, Rome 5-

19 / 22 81,5% Найти

Results for Pd/PdO:D_x target

- After 50 min of e-beam bombardment (J=0.6 µA/cm2 U = 30 kV) some moderate reduction of PdO and carbon layers is observed (from 40 to 25 nm). The residual D is located within the PdO layer.
- The mean D-desorption rate under e-beam in vacuum is compatible with that of D-desorption in air atmosphere (~ 2-3x 10^{15} D/s-cm^2).
- E-beam bombardment is accompanied by formation of numerical pores (from Pd through the PdO) with diameters in the range of 100 – 2000 nm. The larger ∅ pores (∅ > 350 nm) have not been found in the reference Pd/PdO:Hx samples after e-beam.
- Large craters with the ∅ ~ 10-12 µm are also presented at the Pd/PdO:Dx surface after e-beam treatment.

Formation of large craters at the surface indicates to high energy density at some specific sites of the Pd/PdO surface. These sites can show enhanced nuclear emission.

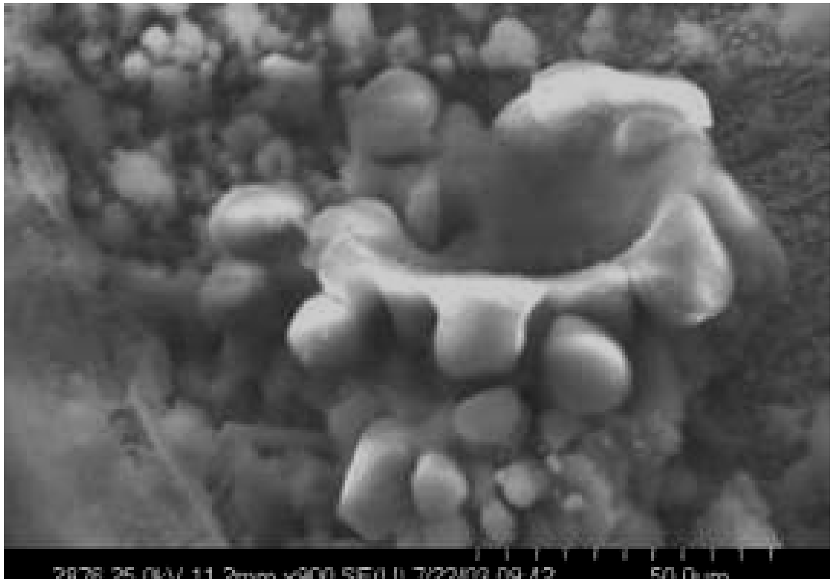

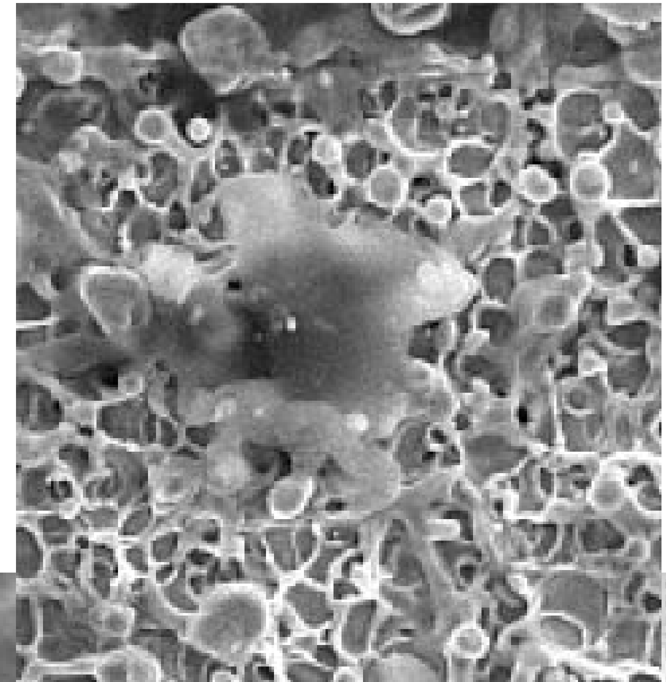

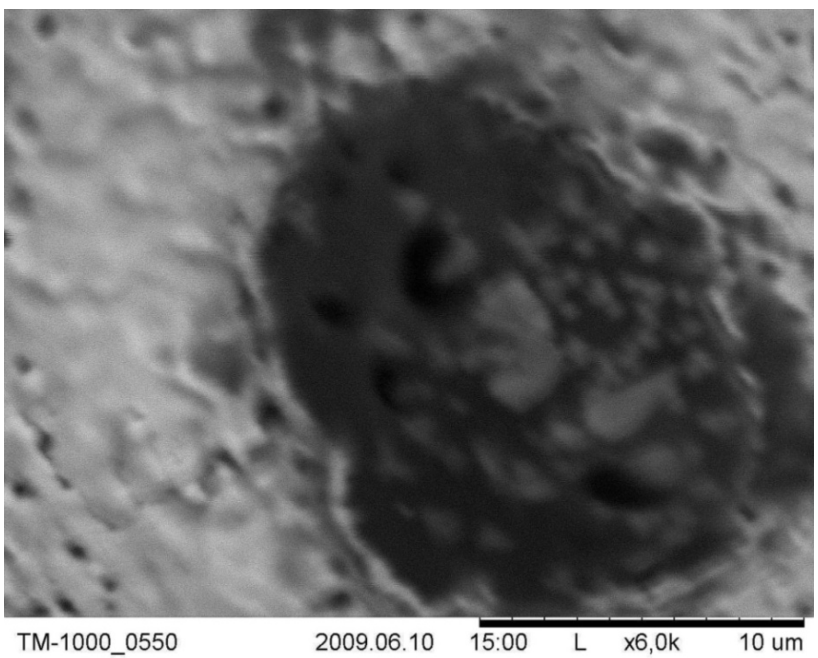
TM-1000_0550
2009.06.10
15:00
L
x6,0k
10 um

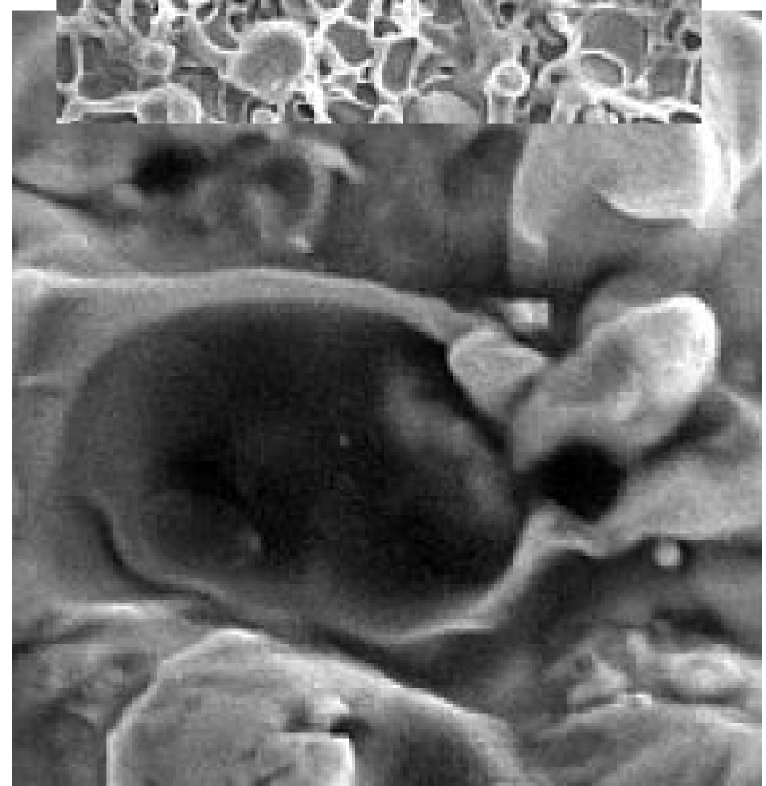

New experimental set-up for studying of nuclear syntheses processes at IEC-scheme based on nanosecond vacuum discharge (NVD)

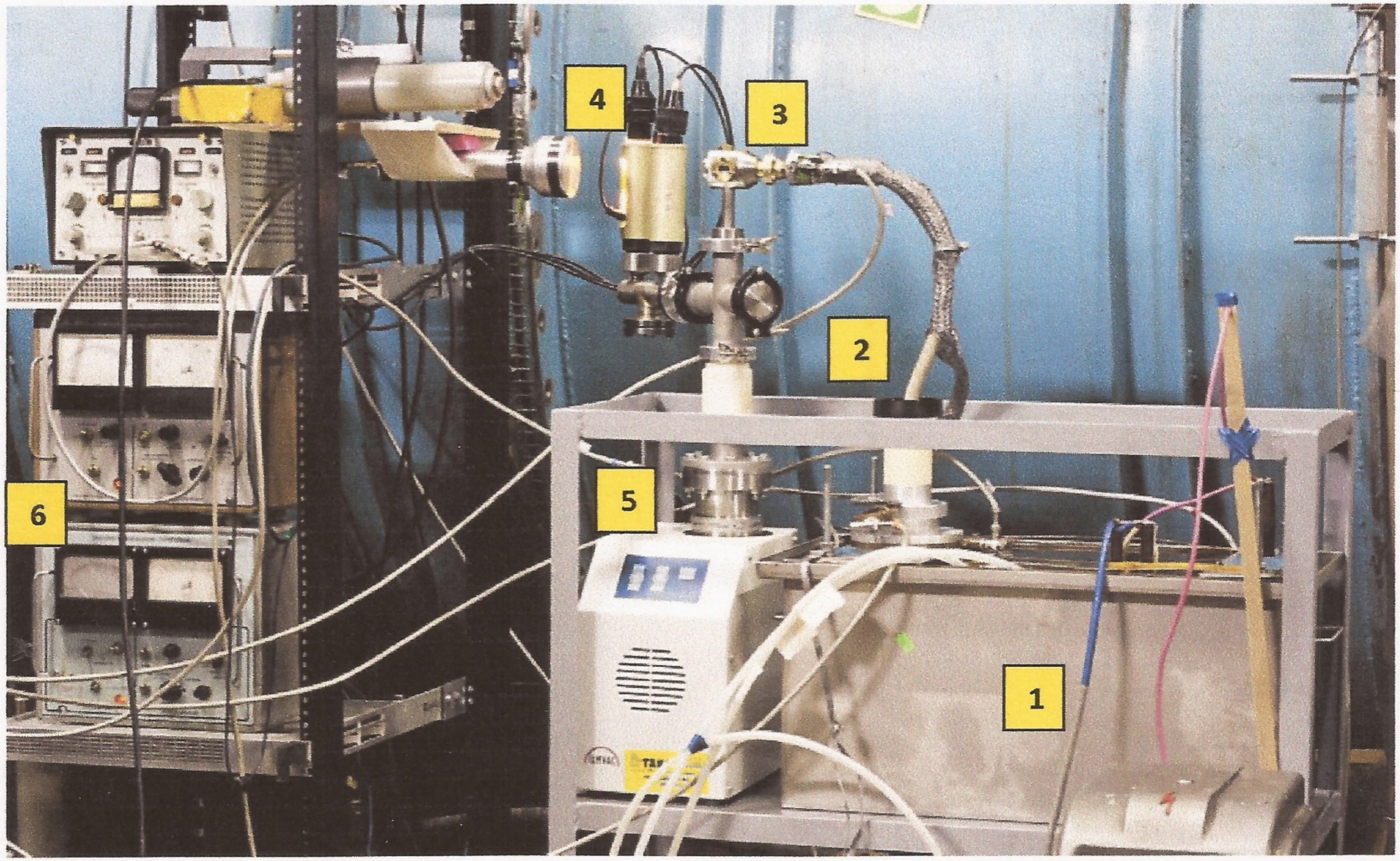

Рис. 1. Схема экспериментальной установки : 1– маслонаполненный ГИН Аркадьева-Маркса, 2 – высоковольтный вывод с разъемом в масляной ванне, 3 – вакуумная камера с анодным узлом, 4 – датчики вакуума, 5 – вакуумный пост, 6 – измерители вакуума.

Discharge camera and anode set-up

V-A characteristics and total energy and power loaded

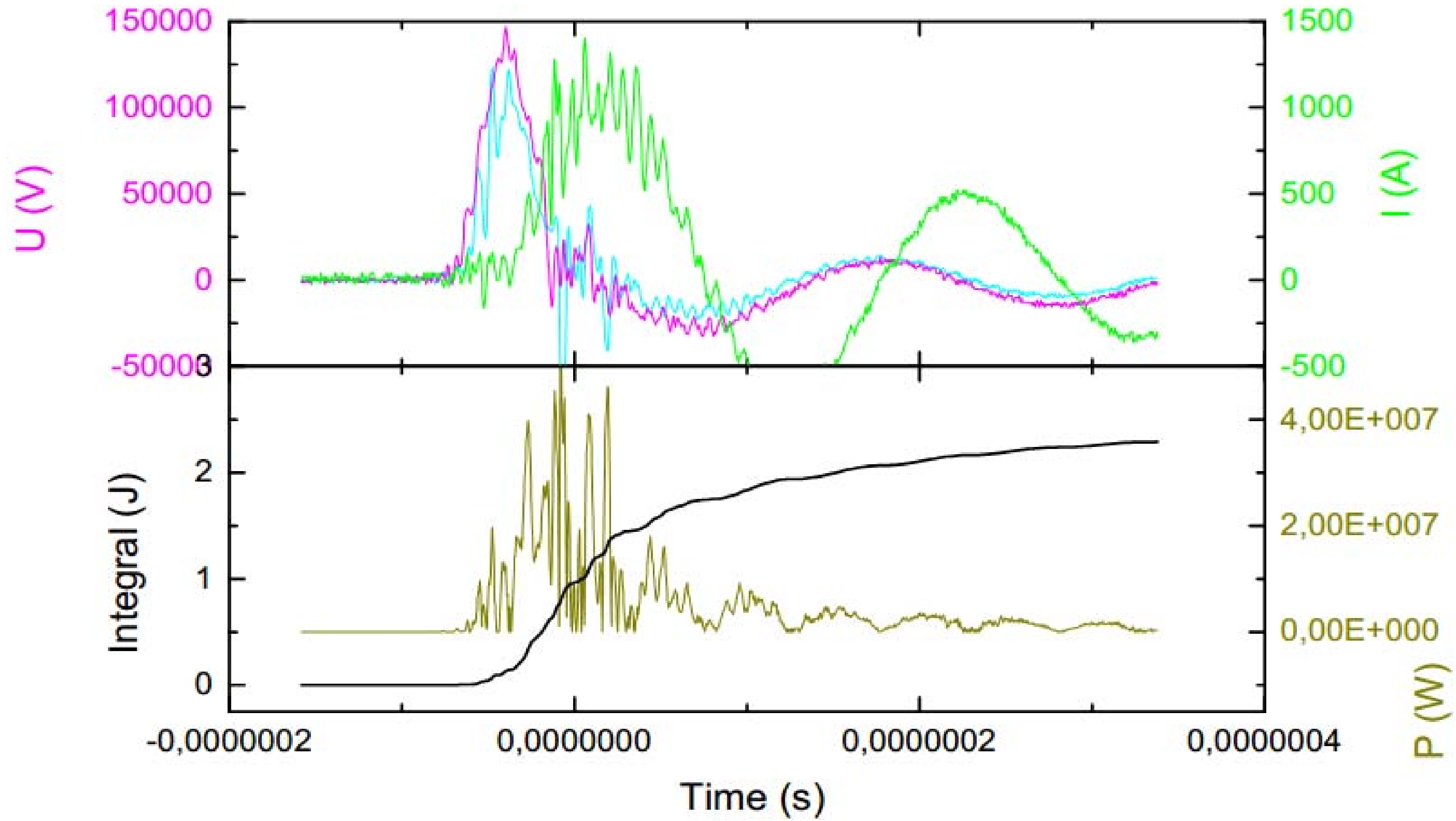

Working view of experimental set-up under first time-of-flight (TOF) study of DD neutrons yield at IEC-scheme based on NVD

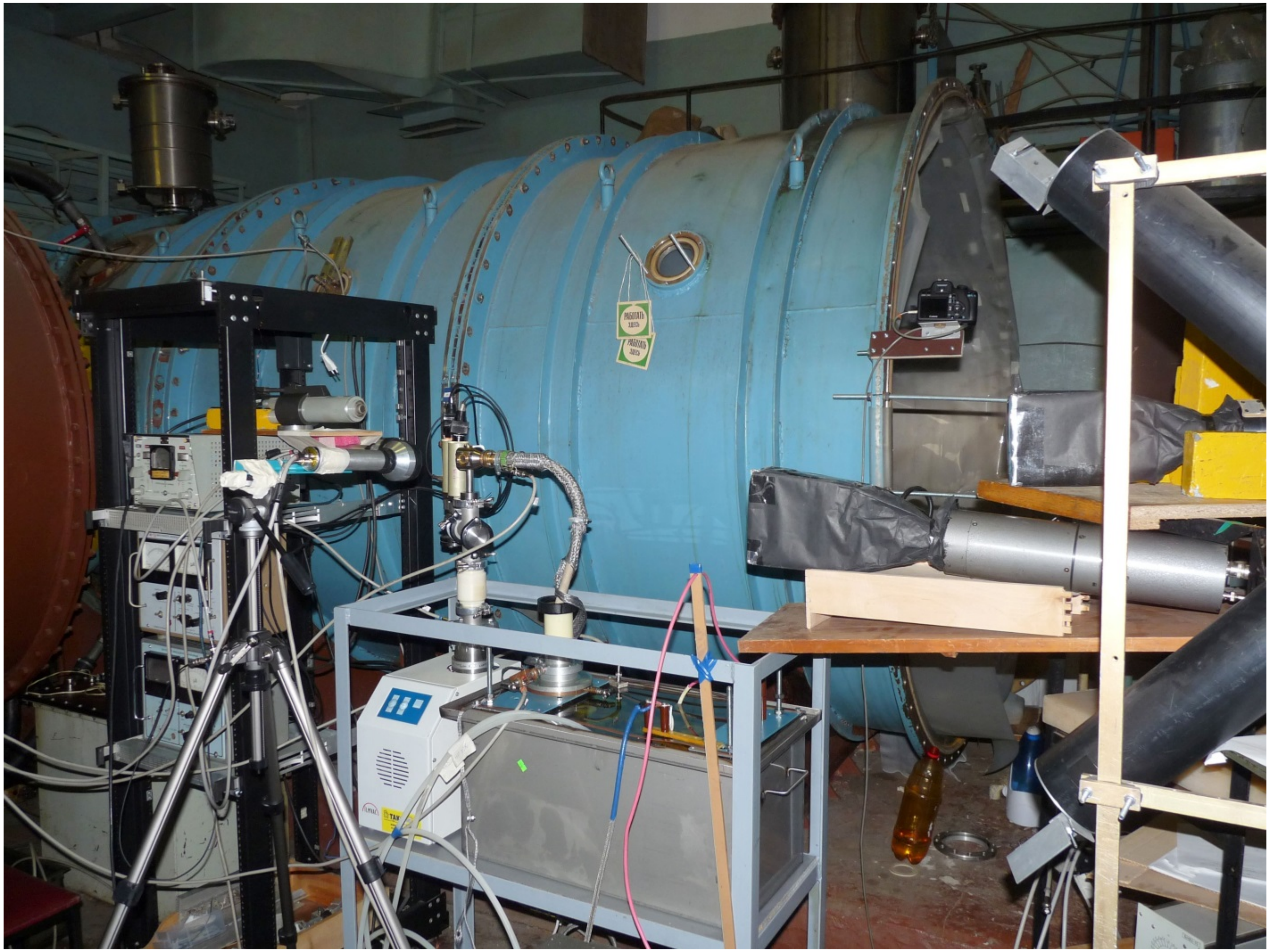

TOF registration of DD neutrons with energy 2,45 MeV

(delayed as ~ 46,6 ns/ m) (PM1 - 70 см, PM2 - 120 см)

Dynamics of x-rays and neutrons yields in the **regime 1** (tri 003)

.

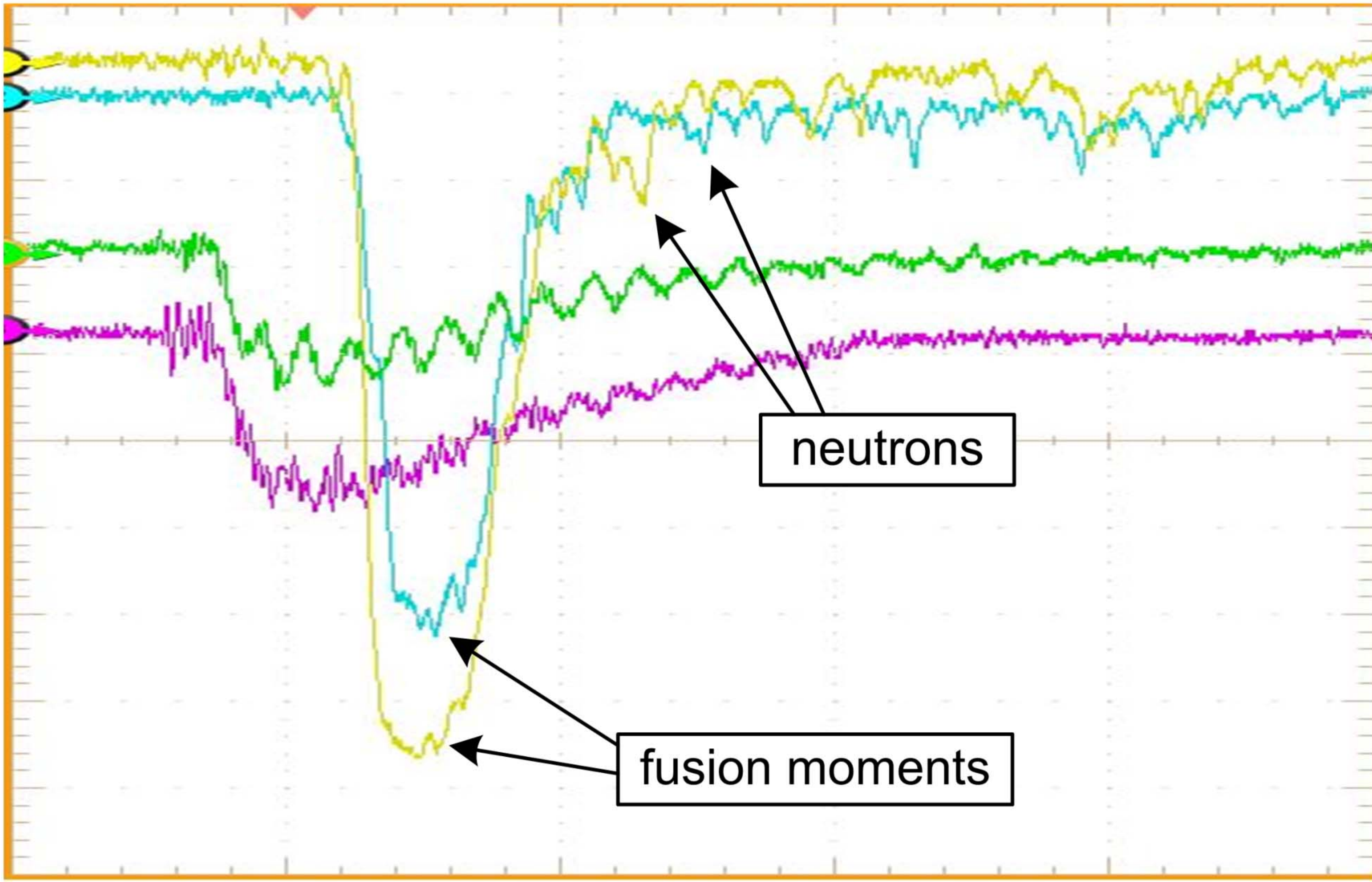

TOF registration of DD neutrons with energy 2,45 MeV

(delayed as ~ 46,6 ns/ m) (PM1 - 70 см, PM2 - 120 см)

Dynamics of x-rays and neutrons yields in the **regime 2**

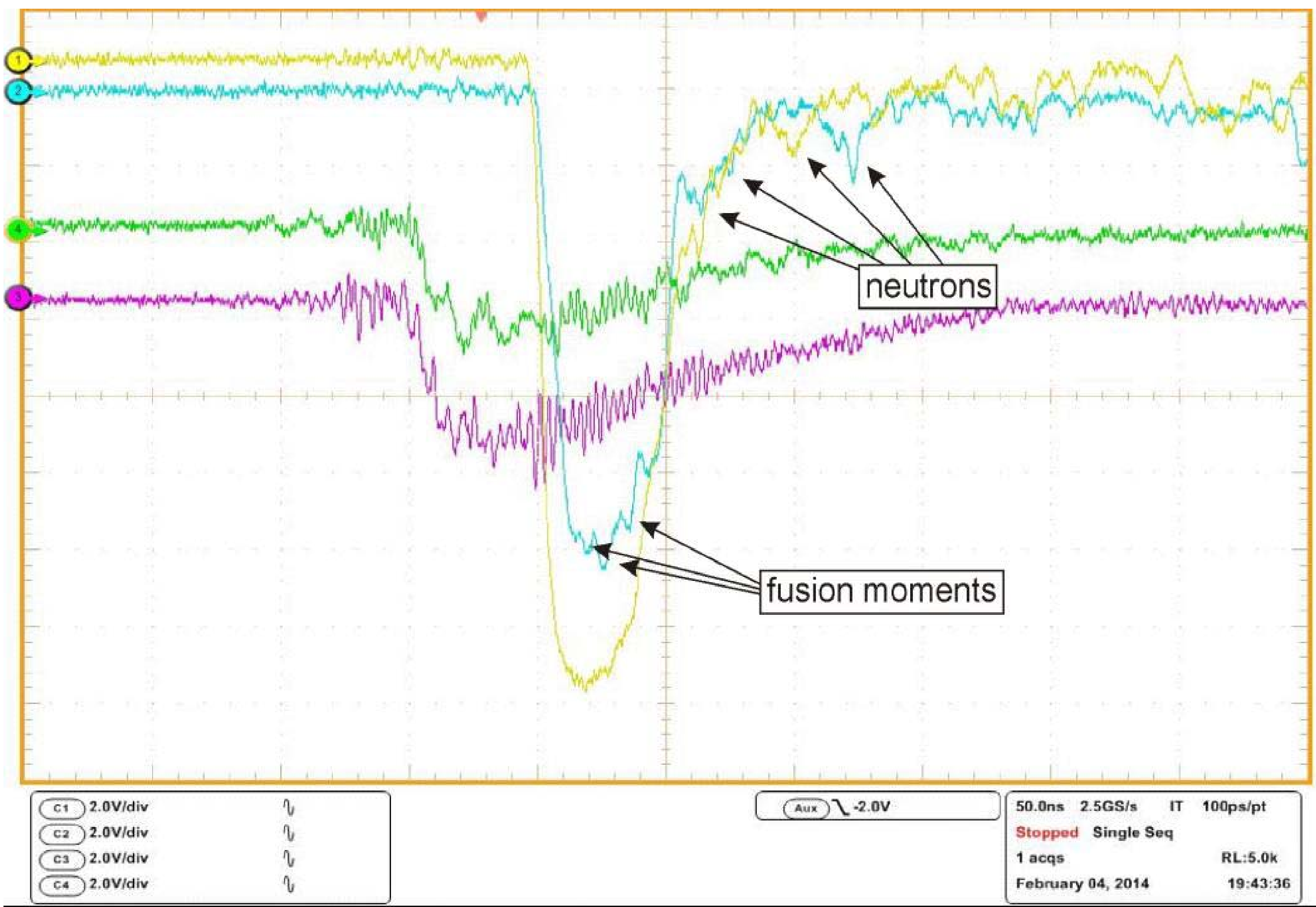

TOF registration of DD neutrons with energy 2,45 MeV

(delayed as ~ 46,6 ns/ m) (PM1 - 70 см, PM2 - 120 см)

Dynamics of x-rays and neutrons yields in the **regime 3** (tri 004).

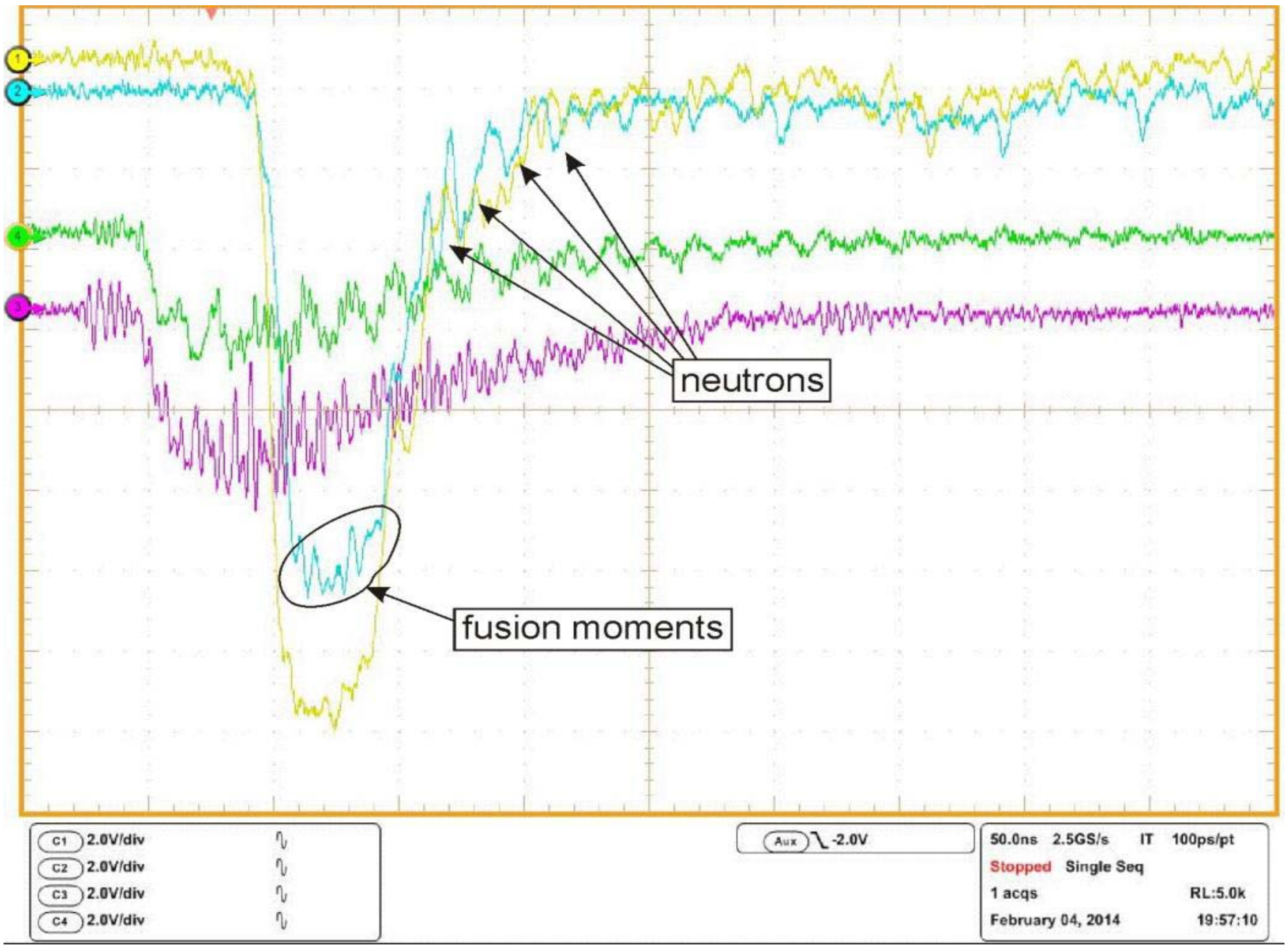

Modelled phenomena:

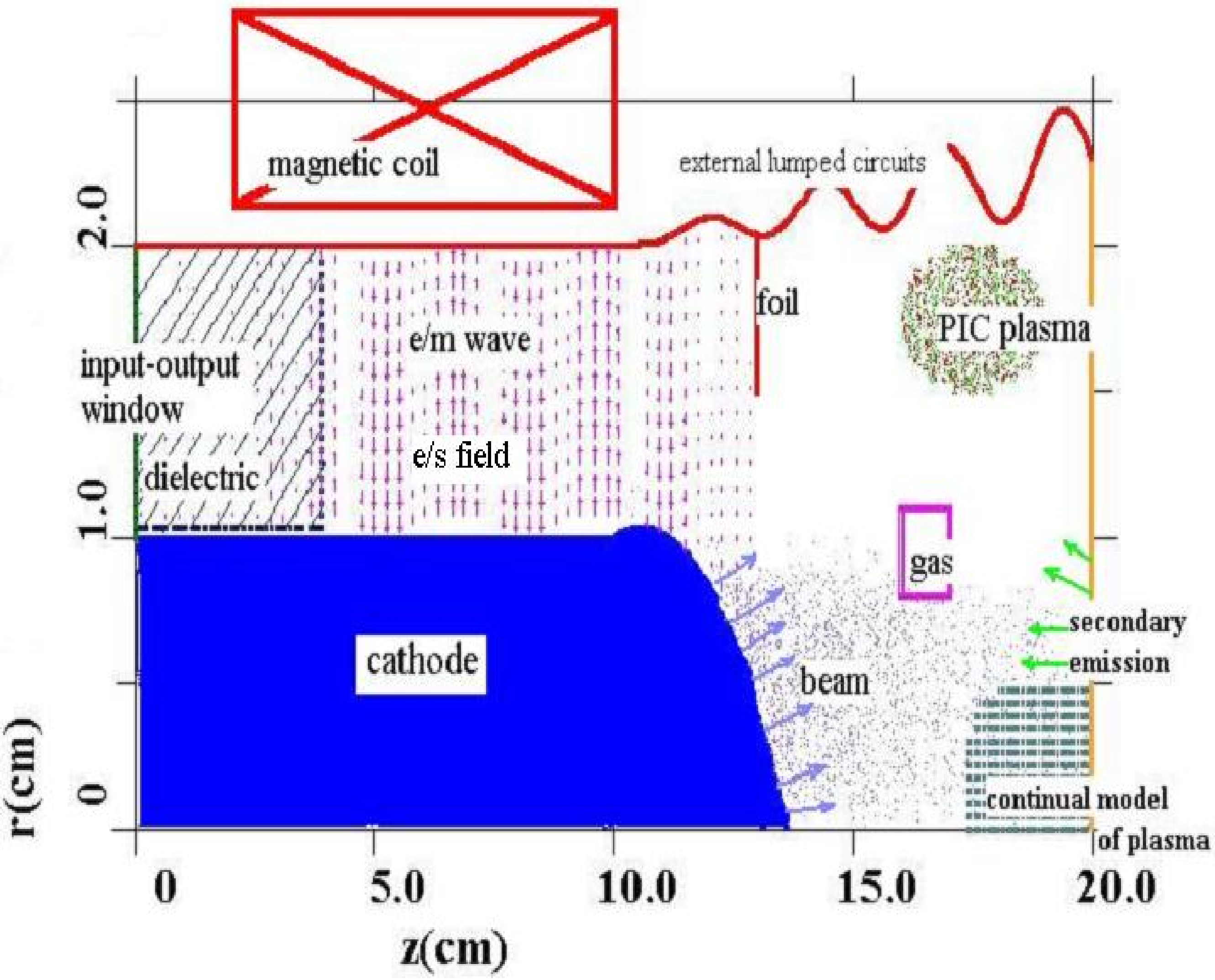

1. e/m waves
2. e – i -beams
3. plasmas (PIC & continual model)
4. dielectrics, dissipative zones, Lorentz medium
5. processes in gases (ionization, ...)
6. secondary emission
7. external lumped circuits
8. conducting foils
9. complicated geometry
10. calculation of external magnetic field
11. finite conductivity walls

Main restrictions:

$$\Delta t < \frac{\Delta x}{c}, \frac{1}{\omega_{p,b}}, \frac{1}{\nu}, \frac{1}{\Omega_B}$$

$$\Delta x < l, r_B, \lambda_D$$

KARAT simulations

Basic Equitations

Maxwell's eq.:

$$\begin{cases} \nabla \times \vec{B} = \dfrac{4\pi}{c}\vec{J} + \dfrac{1}{c}\dfrac{\partial \vec{E}}{\partial t} \\ \nabla \times \vec{E} = -\dfrac{1}{c}\dfrac{\partial \vec{B}}{\partial t} \end{cases}$$

$$\vec{J} = \overrightarrow{J_{PIC}} + \overrightarrow{J_{phen}}$$

$$\overrightarrow{J_{PIC}} = \frac{q}{\Delta v}\sum_m \left(\frac{q_m}{q}\right)\overrightarrow{V_m}$$

Equation of motion: $$\frac{d\overrightarrow{p_m}}{dt} = q_m\left(\vec{E} + \left[\frac{\overrightarrow{V_m}}{c} \times \vec{B}\right]\right)$$

Phenomenological currents: $$\overrightarrow{J_{phen}} = \overrightarrow{J_{pl}} + \overrightarrow{J_{\sigma}} + \overrightarrow{J_{\varepsilon}} + \vec{J}_{Lrntz}$$

$$\frac{d\overrightarrow{J_{pl}}}{dt} + \nu\overrightarrow{J_{pl}} = \frac{\omega_{pl}^2}{4\pi}\vec{E} + \frac{e}{mc}\left[\overrightarrow{J_{pl}}\vec{B}\right]$$

$$\overrightarrow{J_{\sigma}} = \sigma\vec{E}$$

$$\overrightarrow{J_{\varepsilon}} = \frac{\varepsilon - 1}{4\pi}\frac{\partial \vec{E}}{\partial t}$$

$$\left(\frac{\partial^2}{\partial t^2} + \Gamma_n \frac{\partial}{\partial t} + \omega_n^2\right)\vec{J}_{Lrntz} = \frac{\omega_{p,n}^2}{4\pi}\frac{\partial}{\partial t}\vec{E}$$

KARAT simulations

The finite difference scheme for Maxwell's equations with overstepping on the rectangular shearing grid :

$$\nabla \times \vec{B} = \frac{4\pi}{c}\vec{J} + \frac{1}{c}\frac{\partial \vec{E}}{\partial t}$$

(Ampere's law, for example)

$$\frac{\left(E_x\right)^{n+1}_{i-1/2,j,k} - \left(E_x\right)^{n}_{i-1/2,j,k}}{\tau} = \frac{\left(B_x\right)^{n+1/2}_{i-1/2,j+1/2,k} - \left(B_x\right)^{n+1/2}_{i-1/2,j-1/2,k}}{h_y} -$$

$$- \frac{\left(B_y\right)^{n+1/2}_{i-1/2,j,k+1/2} - \left(B_y\right)^{n+1/2}_{i-1/2,j,k-1/2}}{h_z} - 4\pi\left(J_x\right)^{n+1/2}_{i-1/2,j,k}$$

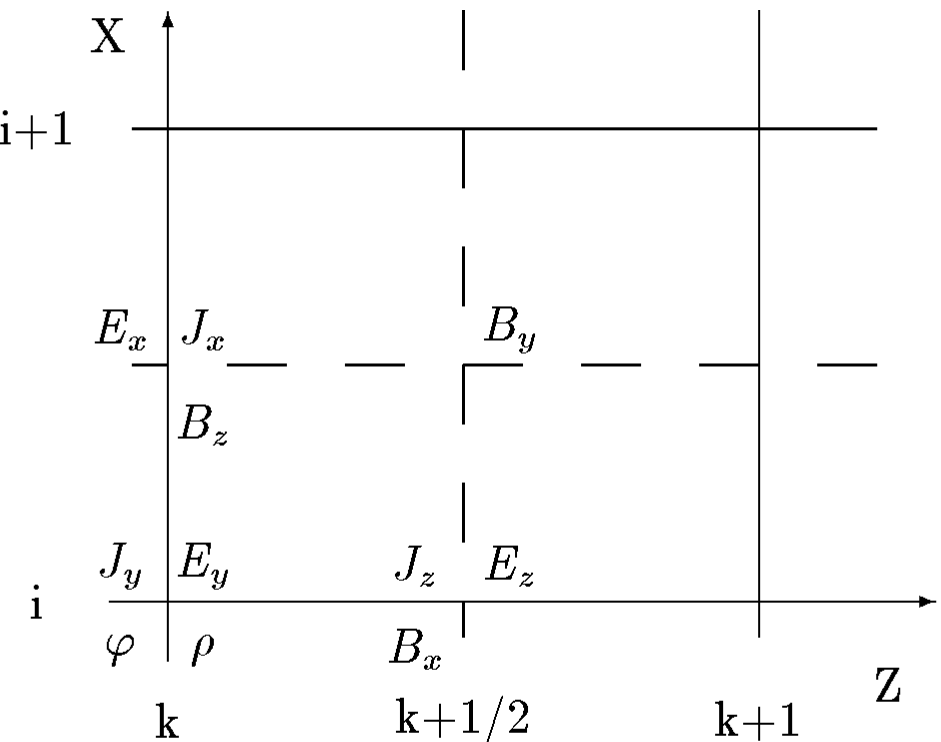

original approximation of 1987

KARAT simulations

Comparision with irradiated clusters:

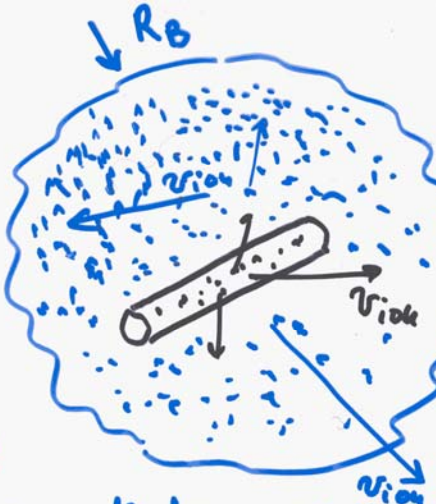

Ditmire et al ('99, '00)

$d = 200\ \mu m$

$\sim d/v_{ion} \simeq 0.2\ ns$

fusion burn time

coll. mean free path

$l_D \gg d$

neutron yield

$10^4\ n\ /\ 120\ mJ$

$\bar{E}_D \simeq 10\ keV$

($\Delta E = 83\ T_i^{1/2}$ keV, Maxwell)

Vacuum discharge used:

1) $l_D > R_B$

2) $l_D < R_B$

- final time of burn
- energy spread

$\Delta t = A\sqrt{T}\,d$ (ps, keV, m) A = 778 (DD)

$\Delta t \simeq 3\text{-}4\ ns$ $\bar{E}_D \simeq 20\text{-}30\ keV$

neutron peaks

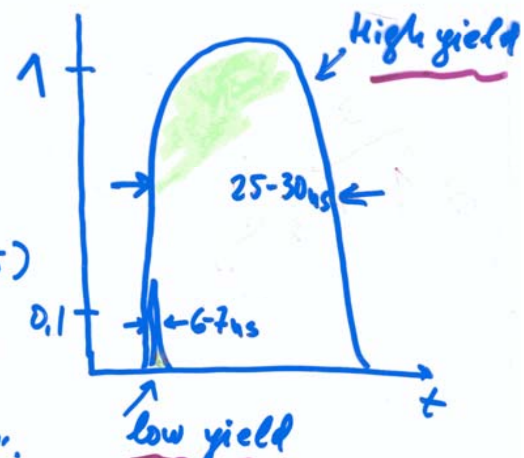

$E_{total} = 5\cdot10^{-13} N_{DD}$ (J)

neutron "sources":

- "tubes" of breakdown current $d \ll l_D$ (1)
- trapping and interaction with cold grains $R \gg l_D$ (2)
- interaction with the edge of Pd anode (3)

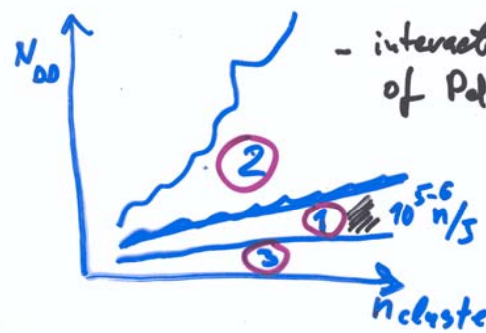

$$\left\{\begin{array}{l} N_{DD} = \frac{1}{4} n_D^2 \langle\sigma v\rangle \tau V \\ E = C_v T_{keV} \rho_{Pd} V \end{array}\right.$$

Basics of fusion

Some of the most important fusion reactions for energy production:

$D + T \rightarrow$

$He(3,52\ MeV) + \mathbf{n}(14,07\ MeV)$

$D + D \rightarrow$

$^3He(0,82\ MeV) + \mathbf{n}(2,45\ MeV)$, 50 %

$T(1,01\ MeV) + p(3,02\ MeV)$, 50 %

$D + {}^3He \rightarrow$

$He(3,67\ MeV) + p(14,68\ MeV)$

$p + {}^{11}B \rightarrow$

$3He(8,68\ MeV)$

$^3He + {}^3He \rightarrow$

$He(12,86\ MeV) + 2p$

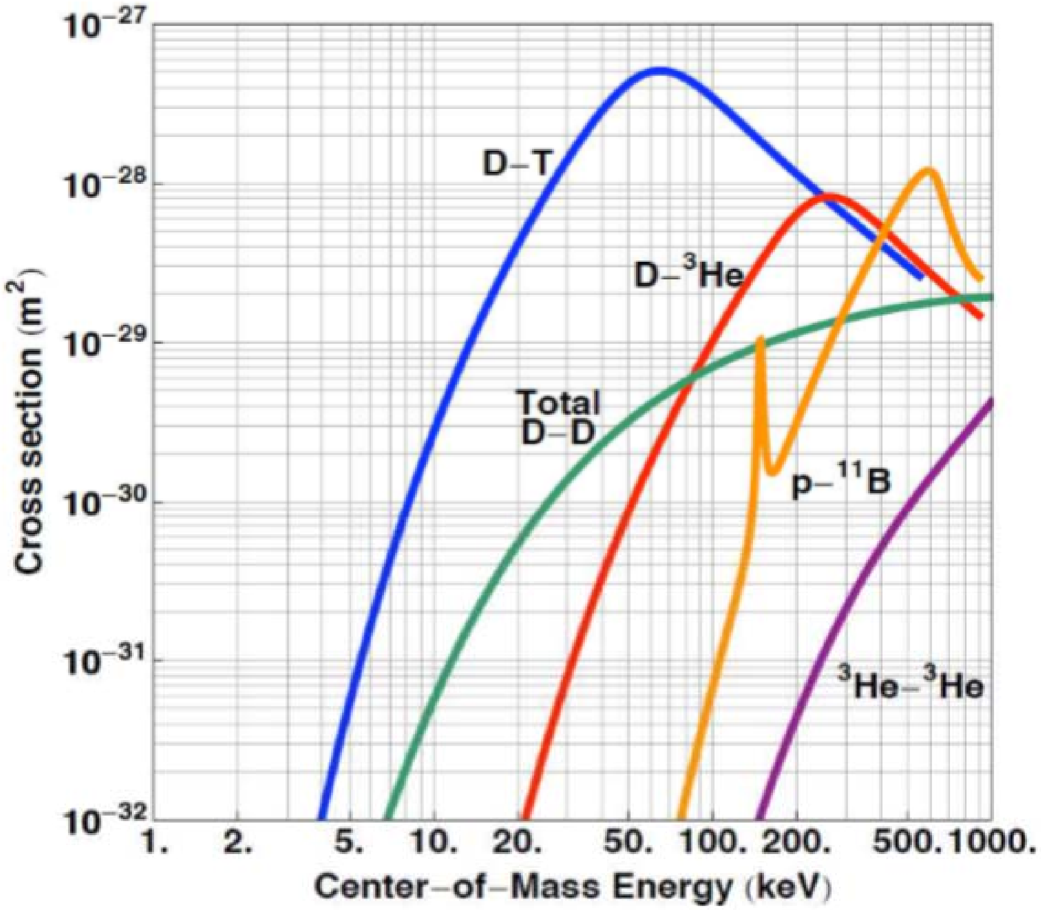

Figure: Cross sections as a function of center of mass energy for some of the most important fusion reactions [3]. (1 keV ≈ 8 MK)

WiffleBall confinement in a Polywell: magnetic field lines are expelled and cusps narrowed inside MaGrid due to the high-beta diamagnetic cloud of electrons in the center.

Polywell specifics

- A plot of the magnetic field generated by the MaGrid inside a Polywell. The null point is marked in red in the center.

- This is one model of the ion energy distribution inside a polywell.[31] This model assumes a maxwellian ion population, broken into different groups.